

**HYPERSPECTRAL VEGETATION INDICES FOR
ARECANUT CROP MONITORING**

Thesis

Submitted in partial fulfillment of the requirement for the degree of

DOCTOR OF PHILOSOPHY

by

BHOJARAJA B E



**DEPARTMENT OF APPLIED MECHANICS AND HYDRAULICS
NATIONAL INSTITUTE OF TECHNOLOGY KARNATAKA
SURATHKAL, MANGALURU-575 025**

December – 2016

HYPERSPECTRAL VEGETATION INDICES FOR ARECANUT CROP MONITORING

Thesis

Submitted in partial fulfillment of the requirement for the degree of

DOCTOR OF PHILOSOPHY

by

BHOJARAJA B E

121152AM12F02

Under the guidance of

Dr. AMBA SHETTY,

Associate Professor

&

Dr.M.K. NAGARAJ

Professor

Department of Applied Mechanics & Hydraulics
NITK Surathkal



**DEPARTMENT OF APPLIED MECHANICS AND HYDRAULICS
NATIONAL INSTITUTE OF TECHNOLOGY KARNATAKA
SURATHKAL, MANGALURU-575 025**

December – 2016

D E C L A R A T I O N

By the Ph.D. Research Scholar

I hereby *declare* that the Research Thesis entitled **“HYPER SPECTRAL VEGETATION INDICES FOR ARECANUT CROP MONITORING”**, Which is being submitted to the **National Institute of Technology Karnataka, Surathkal** in partial fulfilment of the requirements for the award of the Degree of **Doctor of Philosophy** in **Applied Mechanics and Hydraulics Department** is a *bonafide report of the research work* carried out by me. The material contained in this Research Thesis has not been submitted to any University or Institution for the award of any degree.

121152AM12F02, BHOJARAJA B.E.

(Register Number, Name & Signature of the Research Scholar)

Department of Applied Mechanics and Hydraulics
National Institute of Technology Karnataka, India

Place: NITK-Surathkal

Date:

C E R T I F I C A T E

This is to *certify* that the Research Thesis entitled “**HYPERSPECTRAL VEGETATION INDICES FOR ARECANUT CROP MONITORING**”, submitted by **BHOJARAJA B. E.** (Register Number: 121152AM12F02) as the record of the research work carried out by him, is *accepted as the Research Thesis submission* in partial fulfilment of the requirements for the award of degree of **Doctor of Philosophy**.

Dr. AMBA SHETTY
Associate Professor
Research Guide

(Name and Signature with Date and Seal)

Dr. M. K NAGARAJ
Professor
Research Guide

(Name and Signature with Date and Seal)

Chairman - DRPC
(Signature with Date and Seal)

Department of Applied Mechanics and Hydraulics
National Institute of Technology Karnataka, India

ACKNOWLEDGEMENT

I would like to express my sincere gratitude to my research supervisors Dr. Amba Shetty and Dr. M. K Nagaraj for their motivation and invaluable guidance throughout my research work. I am grateful to them for the keen interest in preparation of this thesis and encouragement. The interaction, guidance, discussions, invaluable suggestions and moral support were made me so confident. It has been my great pleasure to work with them. Only with their moral support and guidance, this research work could be completed and I could publish my research work in reputed International journals.

I acknowledge my sincere thanks to Prof. S Shrihari, Dept. of Civil Engineering and Prof. H.D. Shashikala, Dept. of Physics for being the members of Research Progress Assessment Committee and giving valuable suggestions and the encouragement provided at various stages of this work.

I wish to thank Prof. Subba Rao, former Head of the Applied Mechanics and Hydraulics Department and Prof. G.S Dwarakish Head of the Applied Mechanics and Hydraulics Department for permitting me to use the departmental computing and laboratory facilities and their support throughout my stay at the NITK campus. I also extend my heartfelt gratitude to Prof. Lakshman Nandagiri and all the faculty members of Applied Mechanics and Hydraulics. My special thanks to Dr. Pruthviraj for indeed help in procuring data and laboratory facilities.

I sincerely thank Mr. Manohar, Mr, Sadanand, and Mr. Yogesh Dept. of Civil Engineering for their guidance and help during laboratory experiments. I wish to thank former and present H.O.D's of Civil Engineering Dept. for permitting me to work in their Department Laboratories.

I acknowledge the help received by the NITK library staffs. I grateful for the co-operation and help rendered by the staff of laboratories and office of the Applied Mechanics and Hydraulics Department.

My special thanks to Mr. Balakrishna and Mr. B. Jagadish, Asst. Executive Engineer (Rtd.), Applied Mechanics and Hydraulics Department for their help in completing my experimental work.

I gratefully acknowledge the support and all the help rendered by Mrs. Megha, Mrs. Manju, Mr. Chittaranjan, Mr. Gaurav, Mr. Prashanth Mr. Aneesh whose contributions during field, data collection and laboratory analysis.

The informal support and encouragement of many friends has been indispensable. I also acknowledge the good company and help received by each and every research scholar of NITK.

I express my heartfelt gratitude to the authors research articles which have been refereed in preparing this thesis. I also express my gratitude to reviewers of my research articles for their invaluable suggestions in improving this work.

I thank Dr. Kumar Swamy, Dr. Dinesh, Dr. Nataraj University of Agricultural and Horticultural Sciences Shivamogga. I also thank CPCRI Vittala staff, APMC and The Campco Ltd Shivamogga staff for the help and support. Specially I thank all the farmers who helped during field visits.

I am especially grateful to my father Sri. Eshwarappa and mother Smt. Pankaja who provided me the best available education and encouraged in all my endeavors. I am grateful to my wife Dr. (Mrs.) Sudha for her cooperation and moral support, and I lovingly acknowledge the support and help extended from my family members during this research work. They have always been a source of inspiration for me.

Finally I am grateful to everybody who helped and encouraged me during this research work.

NITK Surathkal

BHOJARAJA B E

Date:

Dedication

Every challenging work needs self-efforts as well as guidance of elders especially one
who motivates to work

My Humble effort I dedicate to my respected Teachers
“Jai Guru Dev” (Victory to the Greatness in you) Sri Sri.....

Along with those who were very close to my heart
Father & Mother, loving wife, caring family members and amazing friends

ABSTRACT

Arecanut (*Areca catechu* L.) is one of the major profitable plantation crop grown in few regions of the World. Karnataka state in India produces almost half of the world's total production, in that contribution from Shivamogga district and Coastal Karnataka is significant. The production per unit area in Karnataka is considerably less. The major reasons may be improper irrigation practices, poor soil maintenance, lack of technical knowledge on irrigation water quality, quantity, fertilizers used and frequent occurrence of diseases, small size and spatially scattered farms. These reasons were very typical in Chennagiri region of Karnataka. Farmers' practice adding tank silt lifted from nearby tanks to their farms followed by drip irrigation in the form of flooding. In this region a typical disorder called crown choke harmed an adult plant's life. The objective of this research is: to explore the potential of advanced tools for Arecanut crop monitoring and to demonstrate it on portion of Chennagiri region of Karnataka.

Advanced technological tools used include GPS, Hyperspectral remote sensing data and GIS. Hyperspectral remote sensing is one of the fastest growing techniques in the field of remote sensing due to its vast applications with improved accuracy over conventional method. Spectral library was built separately for different age group and stressed crops using spectroradiometer. Care was taken to match field data with the Hyperion data acquisition time. Hyperion hyperspectral data was classified into stressed versus healthy and different age group crops using developed spectral library. Stressed versus healthy crop classification revealed 10% crops were under stress in patches. To find a scientific reason for crown choke disease affected crops inflated in study area, grid wise soil and water samples were collected, and subjected to standard physico-chemical analysis.

Potential evapotranspiration (ET_o) was computed using Normalized Difference Vegetation Index (NDVI) based crop coefficient (K_c) method due to non-availability of weather parameters. ET_o , Integrated with Hargreaves Samani method was adopted to compute the crop water requirement of different age crops.

Narrow bands in hyperspectral data facilitate computation of several spectral indices and can facilitate improved classification accuracy. Indices developed being Disease Index (DI) to identify disease severity in Arecanut crop, Age Index (AI) to segregate the Arecanut crops into different age groups and Arecanut Crop Water Requirement Index (ACWRI) was built to compute age based crop water requirement.

Important wavelengths were identified among the hundreds of bands to compute the crop water requirement using statistical techniques. Stepwise Multi Linear Regression (SMLR), Partial Least Square Regression (PLSR), and Variable Importance for Projection (VIP) were the techniques of choice. These techniques also facilitated construction of simple models to predict the Arecanut crop water requirement.

On the basis of diseased v/s healthy crop classification, it was inferred that more than 10% of plantation under study was affected by crown choke disease. The physico-chemical analysis revealed that improper soil management is the main cause for crown choke disorder. Soil characterization and water quality analysis infers soil is poorly graded (82% of silt content) with very low hydraulic conductivity of 3.2×10^{-7} cm/sec, and high bulk density of 2.12 g/cm^3 . This impervious nature caused water logging and lead to salinity.

Age based classification results revealed Arecanut crop can be classified into different age groups; below 3 years, 5 to 7 years, 8 to 15 years and above 25 years. And within class classification accuracy of 72% was observed for Support Vector Machine (SVM) classification with linear kernel.

Age based Arecanut crop water requirement map reveals that crop water requirement varies with age of the crop, below 7 years of crop it is 19 and for above 15 years it is 25 liter/day/plant. The derived ACWRI, DI, AI indices to monitor Arecanut crop ranges from 0 to 1 to indicate the age based crop water requirement, disease severity, and age of crop respectively. From the hyperspectral data significant wavelengths were identified: (i) to map the stressed Arecanut crops (750, 550 and 675nm), (ii) Arecanut crop age predication (540, 680 and 780nm). (iii) And to predict the age wise crop water requirement using statistical models: SMLR revealed that 681 and 721nm are significant. PLSR also in agreement with SMLR i.e 681,721 and 548nm are important. Whereas a VIP technique revealed wavelengths 1043, 1053, 1033, 1083, 1023, 1013, 1104, and 854nm are important.

This study concludes that, hyperspectral remote sensing data processed with standard procedures with appropriate atmospheric corrections algorithms and integrated with field studies along with statistical models can be effectively used for Arecanut crop monitoring. This study also demonstrates that, how advanced technological tools can be used to address societal problems say crop monitoring. The output of the research is useful to the farming community to actively plan their agriculture water requirement, and also improves water use efficiency.

Keywords: Age based classification, Arecanut crop monitoring, Hyperion, Indices, PLSR, SMLR, VIP.

TABLE OF CONTENTS

Sl.No.	TITLE	Page. No.
	ACKNOWLEDGEMENT	
	ABSTRACT	i
	TABLE OF CONTENTS	iii
	LIST OF FIGURES	ix
	LIST OF TABLES	xiii
	LIST OF ABBREVIATIONS	xiv
	 CHAPTER 1	
	INTRODUCTION	
1.1	Arecanut Plantation and Its Geographical Distribution	1
1.2	Areca Plant Description	3
1.3	Problems in Arecanut crop Monitoring	4
1.4	An Integrated Approach in Plantation Crop Monitoring	5
1.5	Spectral Signatures of Vegetation	6
1.6	Hyperspectral Remote Sensing Applications in Crop Monitoring	8
1.7	Hyperspectral Vegetation Indices	9
1.8	Statement of the problem	10
1.9	Objectives of the Study	11
1.10	Need and Benefits of the Study	11
1.11	Format of Thesis Presentation	12
	 CHAPTER 2	
	LITERATURE REVIEW	
2.1	Introduction	13
2.11	Hyperspectral Data Pre-Processing	14

2.12	Hyperspectral Remote Sensing for Identification of Stressed Crops	15
2.13	Hyperspectral data Classification	19
2.14	Hyperspectral Prominence Wavelengths for Crop Monitoring	21
2.15	Hyperspectral Vegetation Indices	23
2.16	Crop Water Requirement	27
2.17	Statistical Techniques for Hyperspectral Data processing	28
2.2	Summary of Literature	29
2.3	Literature Gap	30

CHAPTER 3

RESEARCH METHODOLOGY

3.1	Introduction	33
3.2	Location and Characteristics of the Study Area	33
3.2.1	Selection of Study Area	35
3.3	Overview of Methodology	39
3.4	Data Collection	39
3.4.1	Spectral analysis using ASD data	39
3.4.2.1	Spectral library	42
3.4.2	Temperature data	42
3.4.3	GPS data	42
3.4.4	Soil and Water Samples Data	43
3.4.5	Hyperion Satellite Data	43
3.4.5.1	Hyperspectral Image Pre-Processing and Image Classification	44
3.4.6	Radiometric Correction	45
3.4.7	Spectral Resize	46
3.4.8	Geometric Correction	46
3.4.9	Minimum Noise Fraction Transformation	47
3.4.10	Spectral sub set	48

3.5	Application Software	51
3.6	Image Classification	51
3.6.1	Spectral Angle Mapper (SAM) Classification	51
3.6.2	Support Vector Machine Classification	53
3.6.3	Minimum distance classification	54
3.7	Vegetation Indices	54
3.7.1	Hyperspectral Vegetation Indices	55
3.8	Crop Water Requirement through NDVI based Crop Coefficient	56
3.9	Arecanut Crop Water Requirement Index (ACWRI)	57
3.10	Correlation Analysis	58
3.11	Stepwise Multi Linear Regression (SMLR)	58
3.12	Partial Least Square Regression (PLSR)	59
3.13	Identification of significant wavelengths	61
3.13.1	VIP scores and β coefficients	61

CHAPTER 4

HYPERSPECTRAL DATA: A TOOL FOR MONITORING STRESSED ARECANUT CROPS

4.1	Introduction	63
4.2	Spectral library of healthy Vs diseased Arecanut crops	65
4.3	Physicochemical analyses	67
4.4	Water quality analysis	74
4.5	Physical properties of the soil	77
4.6	Summary	81

CHAPTER 5

HYPERSPECTRAL DATA :A TOOL FOR AGE BASED CLASSIFICATION OF ARECANUT CROP

5.1	Introduction	83
-----	--------------	----

5.2	Classification	83
5.2.1	Spectral Angle Mapper (SAM) Classification	83
5.2.1.1	Spectral library of different age group Arecanut crops	84
5.2.2	Minimum distance classification	86
5.2.3	Support Vector Machine Classification	86
5.3.1	Classification results	86
5.3.1	Classification of Hyperion imagery	86
5.3.2	Minimum distance classification results	88
5.3.3	Support Vector Machine Classification	89
5.4	Optimum Band Selection and Model Building	92
5.5	Summary	94

CHAPTER 6

HYPERSPECTRAL VEGETATION INDICES FOR ARECANUT CROP MONITORING

6.1	Introduction	97
6.1.1	First Order Derivative Reflectance	99
6.2	Arecanut Disease Index	101
6.2.1	Normalization of an Index	104
6.3	Age Index	106
6.4	Summary	109

CHAPTER 7

HYPERSPECTRAL VEGETATION INDEX FOR AGE BASED ARECANUT CROP WATER REQUIREMENT

7.1	Introduction	111
7.2	Crop Water Requirement through NDVI based Crop Coefficient	113
7.3	Arecanut Crop Water Requirement Index (ACWRI)	115
7.4	Correlation Analysis	115
7.5	Image classification using Spectroradiometer based reflectance spectra	115
7.6	Arecanut Crop Water Requirement Index	123
7.7	Assessment of arecanut crop water requirement using PLSR model	126
7.8	Arecanut Crop Water Requirement Model (ACWR)	127
7.9	Selection of Important Variables	128
7.10	Stepwise Multi Linear Regression (SMLR)	130
7.10.1	SMLR Results	130
7.11	Summary	133

CHAPTER 8

CONCLUSIONS

8.1	Introduction	135
8.2	Summary	135
8.2.1	Hyperspectral Data: A Tool for Monitoring Stressed Arecanut Crops	135
8.2.2	Hyperspectral Data: A Tool for Age Based Classification of Arecanut Crop	136
8.2.3	Hyperspectral Vegetation Indices for Arecanut Crop Monitoring	137
8.2.4	Hyperspectral Vegetation Index for Age Based Arecanut Crop Water Requirement	137
8.2.5	Important Wavelengths and Model Building	137
8.3	Specific Conclusions	138

8.7	Contributions from This Research	141
8.8	Recommendations	141
	Limitations	141
	Future scope	142
9	REFERENCES	143
10	APPENDIX	159
11	PUBLICATIONS	169
12	Bio-data	171

LIST OF FIGURES

Figure No.	Figure Caption	Page. No.
1.1	Geographical distribution of Areca species (Furtado, 1933)	02
1.2	Multispectral vs. Hyperspectral Remote Sensing	06
1.3	Typical Reflectance Curve of Vegetation	08
3.1	Location map of the study area showing Arecanut plantation region on Hyperion image	34
3.2	Continuously irrigated water stagnated plot	36
3.3	Water stressed Arecanut plot	37
3.4	Pre-plan of the field visit map	37
3.5	Overall methodology adopted for the study	38
3.6	Field data collection using spectroradiometer	40
3.7	Laboratory data collection setup	40
3.8	Field data collection	41
3.9	GPS vector layers	43
3.10	Sample of field spectra obtained from Spectroradiometer	49
3.11	Extracted endmember from Hyperion image	49
3.12a	Scatter plot between image spectra corresponds to field spectra	50
3.12b	Spectral matching	50
3.13	Principle of Spectral Angle Mapper Classifier	52
3.6	Vegetation Spectrum in Detail	51
3.7	Electromagnetic spectrum	
4.1	(a)Healthy and (b)crown choke disease affected Arecanut plant	64
4.2	Methodology adopted for classifying the diseased vs healthy Arecanut crop	65
4.3	Spectral library plots of healthy Vs diseased arecanut crops	66
4.4	SAM classified image	66
4.5	Soil and water sampling locations on the Hyperion image	69
4.6	Soil sampling	70

4.7	Soil and Water Samples	70
4.8	Spatial variation of Soil pH	71
4.9	Spatial variation of Soil electrical conductivity	71
4.10	Spatial variation of Soil organic content	72
4.11	Spatial variation of available surface Soil nutrients	73
4.12	soils micro nutrients Fe, Mn, Zn, Cu	74
4.13	Irrigation water pH	74
4.14	Irrigation water electrical conductivity	75
4.15	Irrigation water Ca, Mg, Ca+Mg	76
4.16	Irrigation water HCO ₃	76
4.17	Field soil sampling picture under the crown choke affected plant	77
4.18	Excavated soil sampling duct	78
4.19	Field soil sample collection to analyse physical properties	78
4.20	Bulk density and soil moisture measurements at field.	79
4.21	Hydrometer analyses in the laboratory	79
4.22	Test plots	83
5.1	Spectral library plots of different age group Arecanut crops	84
5.2a&b	Enlarged Spectral library for Arecanut crops of different age groups.	85
5.3	SAM classifications using spectral library	87
5.4	Minimum distance classification	88
5.5	SVM classification using training sites with different Kernel Functions	90
6.1	Diseased Arecanut crop Spectra	98
6.2	Healthy Arecanut crop spectra	99
6.3	Stressed and healthy vegetation reflectance spectra	99
6.4	First order reflectance curves.	100
6.5	Correlation coefficient vs. wavelength.	101
6.6	Index points for healthy Arecanut crop spectral signature	102
6.7	Index points for stressed Arecanut crop spectral signature	102
6.8	A, B, C Index points those form a triangle to derive DI	103

6.9	Normalized Disease Index map	105
6.10	Spectral library of different age group Arecanut crops	106
6.11	Index points A, B and C those form a triangle to derive AI	107
6.12	Results of Age Index validation	108
7.1	Spectral reflectance discrimination of crop	116
7.2	SAM classified Arecanut crop map	118
7.3	Arecanut crop NDVI map	119
7.4	Arecanut crop Kc map	120
7.5	Age Arecanut wise Crop Water Requirement	122
7.6	Reflectance plots of data used for correlation analysis	123
7.7	Coefficient of correlation plot for all band combinations of equation 7.8	124
7.8	ACWRI map of the study area	125
7.9(a)	PLSR for calibration	127
7.9(b)	PLSR for validation of ACWR	127
7.10	Results of Model validation	128
7.11	VIP scores corresponding to wavelengths	129
7.12	β coefficients corresponding to wavelengths for ACWR	129
7.13	Results of SMLR performance for ACWR in MATLAB	131
7.14	Results of SMLR performance for ACWR in MATLAB	131
7.15	Model validation results of SMLR	132
7.16	Age wise ACWR map by SMLR	133

LIST OF TABLES

Table No.	Table Caption	Page No.
3.1	Important parameters used for radiometric correction using FLAASH	45
4.1	Confusion matrix of SAM classification	67
4.2	Statistics of available surface soil nutrients status of Arecanut farms	72
4.3	Statistics of available surface soil micro nutrients status of Arecanut farms	73
4.4	Soil Physical properties	80
5.1	Confusion matrixes of SAM and Minimum distance classification	89
5.2	Confusion matrix of SVM classification	91
5.3	Observed Vs predicted age in years	92
5.4	Overall classification accuracy comparisons	
5.5	Statistics of various age group classes area under Arecanut crop and SVM individual class classification accuracy	93
6.1	Age wise Arecanut Crop Water Requirement	108
7.1	Age wise Crop Water Requirement	121

LIST OF ABBREVIATIONS

Abbreviation	Description
CWRI	Areca nut Crop Water Requirement Index
AI	Age Index
ALI	Advanced Land Imager
ArcGIS	Aeronautical Reconnaissance Coverage Geographic Information System
ACWR	Areca nut Crop Water Requirement
ASCII	American Standard Code for Information Interchange
ASD	Analytical Spectral Devices
CFSR	Climate Forecast System Reanalysis
CWR	Crop Water Requirement
DARs	Data Acquisition Requests
DI	Disease Index
ENVI 5 [®]	Environment for Visualizing Images 5
EO-1	Earth Observing-1
ERDAS IMAGINE	Earth Resource Development Assessment System
ET	Evapotranspiration
ET ₀	Reference Evapotranspiration
ET _a / ET _c	Actual Evapotranspiration
ET _o	Reference Evapotranspiration
FAO	Food and Agricultural Organization
FLAASH	Fast Line-of-sight Atmosphere Analysis of Spectral Hypercube
GIS	Geographic Information System
GPS	Global Positioning System
HI	Hydrocarbon Index
K	Hydraulic conductivity
k	Kappa Coefficient
K _c	Crop Coefficient
L1R	Level 1R

L1T	Level 1T
LEISA	Atmospheric Corrector Linear Etalon Imaging Spectral Array
MATLAB	MATrix LABoratory
mid-IR	mid-infrared
MLR	Multiple Linear Regressions
MNF	Minimum Noise Fraction
MODTRAN4	MODerate resolution atmospheric TRANsmission4
MSL	Mean Sea Level
NASA	National Aeronautics and Space Administration
NDVI	Normalized Difference Vegetation Index
NF	Noise Fraction
NIPALS	Non-linear Iterative Partial Least Squares
NIRS	Near-infrared spectroscopy
OA	Overall accuracy
PAR	Photosynthetically Active Region/Radiation
PCA	Principal Component Analysis
PET	Potential Evapotranspiration
PLSR	Partial Least Square Regression
PPI	Pixel Purity Index
R^2	Coefficient of determination
RMSE	Root-Mean-Square Error
ROI	Region of Interest
RS	Remote Sensing
SAM	Spectral Angle Mapper
SIMPLS	Statistically Inspired Modification of PLS
SMLR	Stepwise Multi Linear Regression
SNR	Signal to Noise Ratio
SVM	Support Vector Machine
SWIR	shortwave-infrared
TIFF	Tag Image File Format

USGS	United States Geological Survey
UTM	Universal Transverse Mercator
UV	Ultraviolet
VIP	Variable Importance for Projection
VI _s	Vegetation Indices
VNIR	Visible and Near-Infrared
WGS84	World Geodetic System 1984

CHAPTER 1

INTRODUCTION

1.1 Arecanut Plantation and Its Geographical Distribution

Plantation crops are known as commercial crops, ensure a better return to growers, higher revenue to the Government, and improved income to workers. These are cultivated on an extensive scale in a contiguous area, owned and managed by an individual or a company. Arecanut (*Areca catechu* L.) is one of the major plantation crops in the world, predominantly grown in India by small and medium farm holders. Commercial crop of greater economic importance and plays a vital role in improving Indian economy, especially in view of its export potential, employment generation and poverty alleviation, particularly in rural sector. It is also an important cash crop in the Western Ghats, East Coast and North Eastern regions of India. Over seven million farmer families are directly dependent on Arecanut farming and more than 60 million people indirectly depend on Arecanut for their livelihood as labor in Arecanut gardens.

It is grown in India, Philippines, Bangladesh, Indonesia, Malaysia, Srilanka and in some parts of Pacific Islands. Among all other countries, India is the largest producer and consumer of Arecanut in the world, accounts for about 57 percent of the world's production; followed by China; Bangladesh and Myanmar. In India though the production of Arecanut is localized in few states, the commercial product is widely distributed all over the country. Particularly in South India, small and medium land holding farmers practice Arecanut as a plantation crop and these plantations are scattered in sizes varying from one to hundreds of acres. The crop serves many livelihoods because of its high commercial value.

In different regions of the world Arecanut is called by different local names; in India it is Arecanut or betel nut, whereas in Indonesia it is called as Pinang. Figure 1.1 shows geographical distribution of areca species. Yellow colour portion of the figure shows abundant distribution of Arecanut crop across the countries.

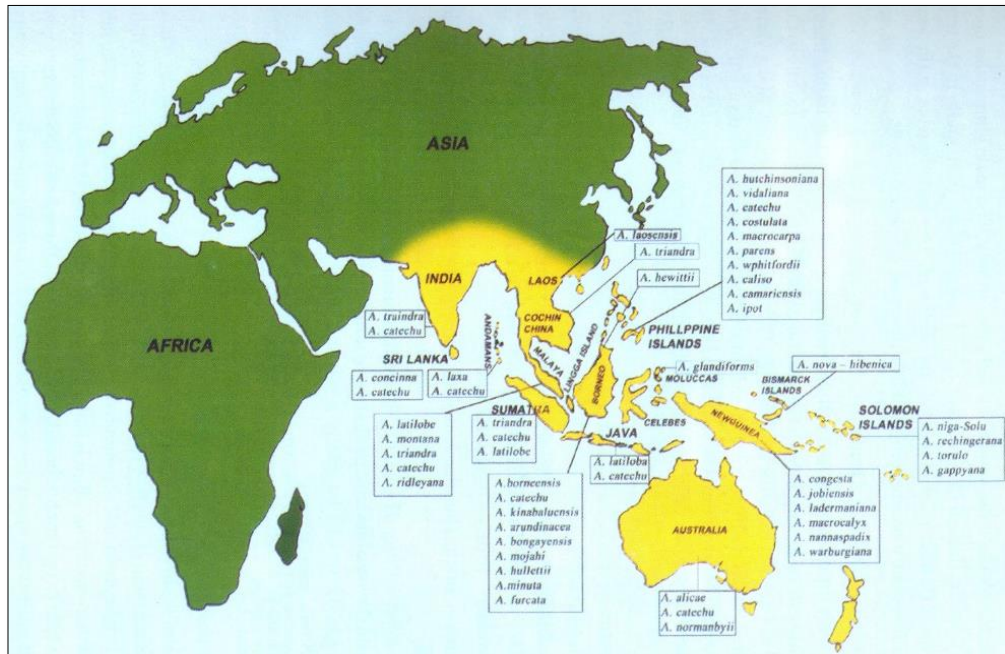


Figure 1.1 Geographical distributions of Areca species (Furtado, 1933)

As per Jain Irrigation Systems Ltd. A pioneering micro irrigation industry of India's report, (2000), India is the largest producer of Arecanut in the world. It occupies a prominent place among the cultivated crops in the states of Kerala, Karnataka, Assam, Meghalaya, Tamilnadu and West Bengal. India is also the largest consumer of Arecanut. The area under Arecanut is estimated to be 2.6 lakh ha yielding about 3.13 lakh tones of processed nuts. Karnataka accounts for nearly 40% of the total Arecanut production; Kerala 25% and Assam 20% and rest of the area is distributed in other states. It is estimated that about 85% of the area under Arecanut are owned by small and marginal farmers. Ramappa (2013) summarized that, India leads the league with over 5.5 lakh tonnes of Arecanut produce per year. Karnataka is the largest producer as well as major Arecanut growing state in India followed by Kerala and Assam accounting for about 39% of the world's production.

1.2 Areca Plant Description

Arecanut is a tropical plantation crop cultivated primarily for its kernel. This kernel is obtained from its fruit. The habit of chewing Arecanut is typical of the Indian subcontinent and its neighbourhood. Areca plant comes under the species of palm having scientific name of 'areca catechu'. It is a tall stemmed erect palm, reaching varied heights, depending upon the environmental conditions. It is an important component of religious, social and cultural celebrations and economic life of people in India. Arecanut is also used in medicines. This crop is essentially grown in clay loamy soils. It flourishes well in regions with very high rainfall of 4500 mm, such as Malnad region of Karnataka as well as the low rainfall of 750 mm areas like the Maidan region of Karnataka.

The crop starts yielding after 5 years and sustains for about 50 years. There are more than 20 diseases which affect growth of the crop and decrease the yield of the crop. Even though the favourable temperature range for Arecanut crop is 25 to 35⁰ C and range of humidity is from 70 to 95%., Arecanut grows in areas with a wide range of temperature, from a minimum of 4°C (West Bengal) to a maximum of 40°C (Karnataka). In northeastern regions it is grown on the plains because at higher elevation the winter temperature will have adverse effect on plant growth. Areca palm is sensitive to drought; therefore, irrigation is essential in long dry spell areas. The palm does not withstand either drought or water stagnation. The traditional irrigation method follows weekly irrigation system; approximately 175 litres/palm was applied (Mahesha et al. 1989). Though Arecanut crop is having commercial value, there is no proper monitoring and management techniques. The general problems faced by farmers in Arecanut crop monitoring, is discussed in section 1.3.

1.3 Problems in Arecanut crop Monitoring

- 1. Improper irrigation:** Arecanut crop is sensitive to drought. Poor monsoon and improper irrigation facilities generally decrease the yield of Arecanut crop. Also due to lack of technical knowledge on age based crop water requirement either excessive or deficient supplements of water takes place which adversely affect plant's growth. Improving farmers' knowledge on accurate crop water needs also help in optimizing crop productivity as well as water usage. Hence there is a need to study the exact quantity of water required for Arecanut crop based on its age.
- 2. Diseases and nutritional disorders:** The productivity of Arecanut palms is affected by number of diseases and nutritional disorders depending upon the climatic conditions prevailing. Of late due to a number of reasons, the yield of the crop has been reducing. For remedial measures and to estimate pesticides, fertilizer requirements knowing the stressed crop area is essential. But there are no proper mapping techniques to estimate these stressed crop areas over a large area.
- 3. Non-scientific soil management:** Non-scientific soil management not only decreases yield of crop but also affect the plant's life. Improperly managed soil Arecanut fields leads to poor development of roots, brittle and crinkled. Studies (Bhat, 1978) have shown, under well drained deep soil conditions, Arecanut roots traverse down to about three meters and the roots confine to only about 1.40 meters under shallow soil condition. So soil management is an important aspect in Arecanut crop monitoring but there are limited studies on Arecanut crop soil management.
- 4. Limited Age-Based information:** The yield of the Arecanut crop is mainly depends upon its age, which starts yielding from 5-7 years and continues up to 50 years. Age information of the crop is crucial for rough estimation of yield. Small scale marketing agencies, one which controls the stabilization of rates and export are always interested in knowing the Arecanut crop health, age and thereby it helps in appropriate yield estimation. Computing and mapping age wise discrimination of Arecanut crop is an essential part of crop monitoring to know

spatial distribution of yielding crops and to know areas of high and low water requirements. But there are no such studies based on crop age.

5. In India, most Arecanut plantations are scattered, small in size and have varying agricultural methods of farming. Added to this, there is lack of technical knowledge on Arecanut crop monitoring. Traditional methods of monitoring involve visual examination and are limited by the ability of the human eye to discriminate the health status. These methods are often complex, costly, time consuming and they cannot be applicable for large scale.

Plantation crop monitoring with advanced techniques and an integrated approach may be the best option to address some of the problems faced in Arecanut crop monitoring.

1.4 An Integrated Approach in Plantation Crop Monitoring

An integrated approach in crop management system incorporates several technologies. They are; Global Positioning System (GPS), Geographical Information System (GIS), yield monitor, variable rate technology and remote sensing.

Understanding crop phenology through analysis of spectral reflectance can help in discriminating crops on the basis of health, age and also water needs at different ages. Though multispectral imagery is useful to discriminate land surface features and landscape patterns, hyperspectral imagery allows identification and characterization of materials. Hyperspectral imaging, also known as imaging spectroscopy, collects information across the electromagnetic spectrum in contiguous, narrow bandwidths and helps in measuring surface behavior throughout the electro-magnetic spectrum. The recent developments in remote sensing namely, Hyperspectral remote sensing can play a definite role in understanding crop science there by helps in optimization in crop monitoring. Figure 1.2 shows the difference between multispectral remote sensing vs hyperspectral remote sensing.

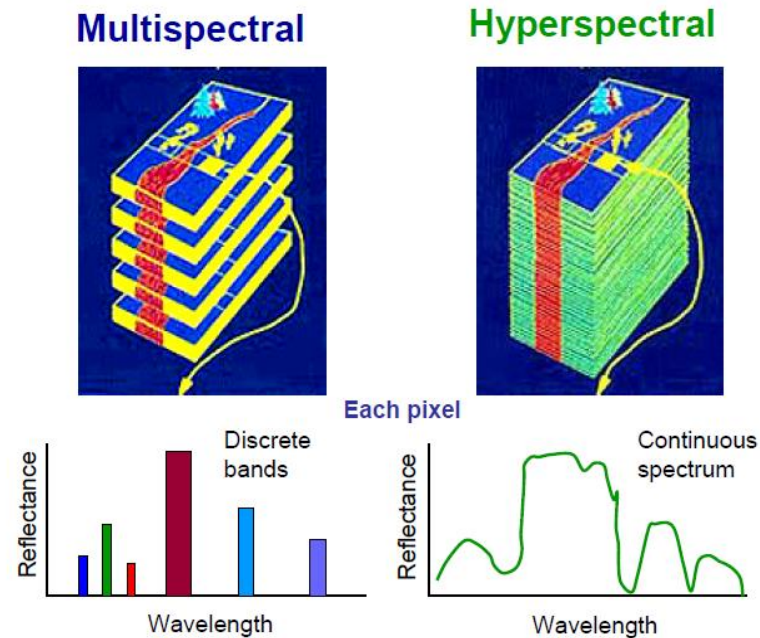


Figure 1.2 Multispectral vs. Hyperspectral Remote Sensing

(Source: <http://slideplayer.com/>)

Figure 1.2 illustrates that multispectral remote sensing (MSS) wavelengths are discrete in nature with a wider bandwidth represent coarse spectral signature. From MSS not able to discern small difference between reflectance spectra has smaller data volumes with limited number of spectral bands. In case of Hyperspectral, due to continuous bands, with no gaps and narrowness, complete record of spectral responses of materials over the wavelengths is possible. Has a large data volume which covers visible-NIR-Thermal range which carries spectral information to identify and to distinguish spectrally unique materials.

1.5 Spectral Signatures of Vegetation

Crop leaves represent the main surfaces of plant canopies, where energy and gas are exchanged. Hence, knowledge of their optical properties is essential to understand the transport of photons within vegetation. The general shape of reflectance and transmittance curves for green leaves is almost similar for all species. It is controlled by absorption features of specific molecules and the cellular structure of the leaf tissue.

In the visible domain (400 - 700 nm) absorption by leaf pigments is the most important process leading to low reflectance and transmittance values. The main light absorbing pigments are chlorophyll a and b (C_{ab}), carotenoids, xanthophylls, and polyphenols. Chlorophyll a is the major pigment of higher plants and together with chlorophyll b account for 65 percent of the total pigments. Figure 1.3 shows typical reflectance of vegetation curve and chlorophyll absorption.

Chlorophyll a and b have absorption bands in the blue at around 430/450 nm and in the red domain at around 660/640 nm. These strong absorption bands induce a reflectance peak in the green domain at about 550 nm.

In the mid-infrared domain (mid-IR: 1300-2500 nm), also called shortwave-infrared (SWIR), leaf optical properties are mainly affected by water and other foliar constituents. The major water absorption bands occur at 1450, 1940, and 2700 nm and secondary features at 960, 1120, 1540, 1670, and 2200 nm. Water largely influences the overall reflectance in the mid-IR domain and also has an indirect effect on the visible and near-IR reflectance.

Protein, cellulose, lignin, and starch also influence leaf reflectance in the mid-IR. In fresh leaves, spectral features related to organic substances are masked by the leaf water, so that estimation of leaf constituents is difficult. The spectral properties of live foliage set up the radiation field in a canopy, and these spectral properties express the presence and abundance of both the inputs and products of photosynthesis.

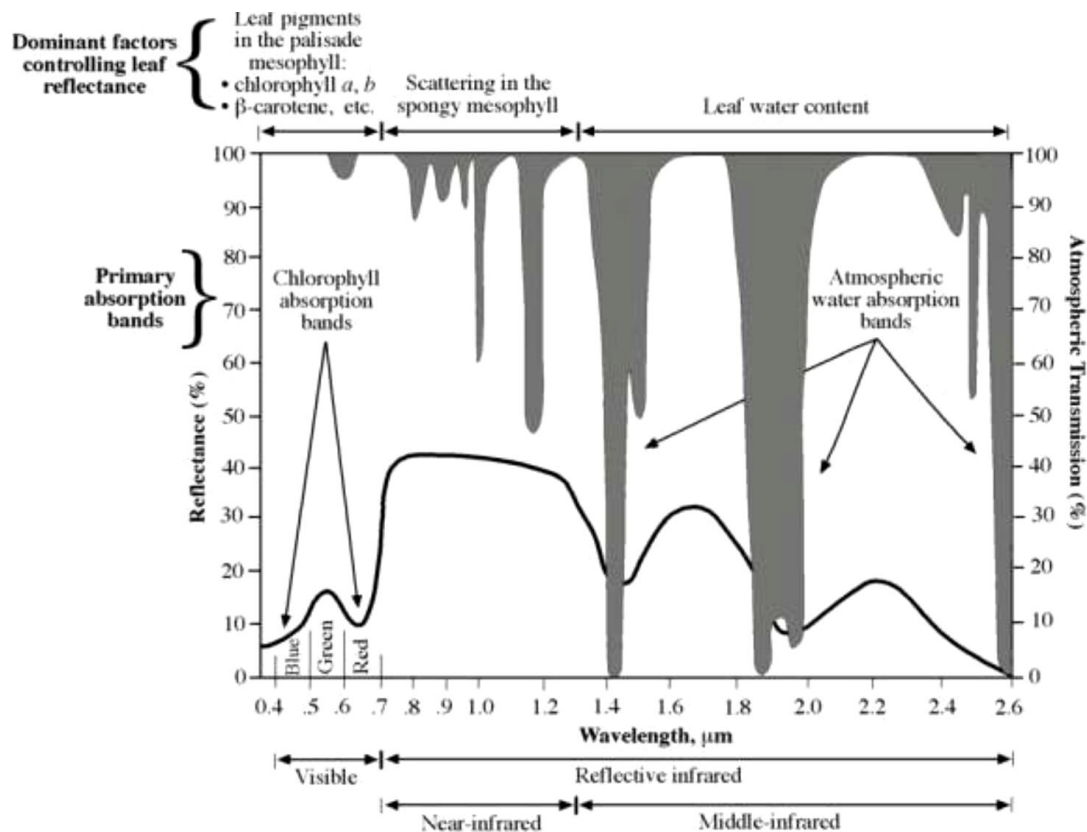


Figure 1.3 Typical Reflectance Curve of Vegetation (Jensen, 2009)

To utilize these behaviors of plant foliage in order to monitor crop, hyperspectral remote sensing becomes an essential tool. It aids in classification between Arecanut crops of various age groups and to identify stressed crops with accuracy.

1.6 Hyperspectral Remote Sensing Applications in Crop Monitoring

The Earth Observing-1 (EO-1) satellite, launched in November, 2000 by National Aeronautics and Space Administration (NASA), carries on board hyperspectral sensors (Hyperion) and is one of the freely available data source.

Hyperspectral images have potential applications in crop monitoring which includes types, health, moisture status and maturity of crops. It is also used in detection and identification of minerals, vegetation, artificial materials and soil background. Hyperspectral narrow-band spectral data are emerging as practical solutions in modeling and mapping vegetation. Recent research has demonstrated the advances in hyperspectral data in a range of applications including quantifying agricultural crops (*Sahoo et al., 2015*), modeling forest canopy biochemical properties (*Hansen et al., 2003*), detecting

crop stress and disease (*Krishna et al.*,2015), mapping leaf chlorophyll content (*Panigada et al.*, 2010), identifying plants affected by contaminants such as arsenic, demonstrating sensitivity to plant nitrogen content, classifying vegetation species and type, characterizing wetlands, and mapping invasive species as it influences crop production. The need for significant improvements in quantifying, modeling, and mapping plant chemical, physical, and water properties is more critical than ever before to reduce uncertainties in the understanding of vegetation and to sustain it.

Further for more accurate results and customized applications, vegetation indices are useful. The advantages of indices over classification are clear distinguished between soil and vegetation, by reducing atmospheric and topographic effects.

1.7 Hyperspectral Vegetation Indices

Vegetation indices are combinations of surface reflectance at two or more wavelengths designed to highlight a particular property of vegetation. These can be used for monitoring crop health and to assess change in plant vigor by classification.

Satellite image classification is the technique of transforming a digital image of a geographic area into land-use land-cover maps of fewer broad classes. This employs image processing technique and spectrum based pixel classifying algorithms which assign every pixel in an image to a certain class depending on the majority features present in the pixel. Satellite image classification is the widely used technique for temporal change detection.

1.8 Statement of the Problem

Realising the importance of Arecanut plantations for small and marginal farmers, few research issues to be addressed are listed below

- ✓ For planning and designing of irrigation and scheduling, total area of plantations crop coverage.
- ✓ To estimate yield of the crop, age based crop area estimation,
- ✓ Nutrients deficient plantation crops area to estimate fertilizer needs.
- ✓ New Indices for mapping and monitoring Arecanut crops.

And few facts to be known are;

- 1) The exact estimation of yield is depending upon the health of the crop and also in case of Arecanut crop the yield of the crop is depending upon its age.
- 2) Finding out the cause for the disease, is also an important task for remedial measures.
- 3) In sustainable agriculture for planning and scheduling of the irrigation, knowledge on the exact amount of crop water requirement is essential.
- 4) To map the different ages of crop and stressed crop distribution also crop water requirement, vegetation indices plays vital role in a simplified manner.

1.9 Objectives of the Study

The primary objective of research is to demonstrate an integrated approach for Arecanut crop monitoring using hyperspectral data and other advanced tools. As part of analysis framed sub objectives are;

- 1) Investigate the feasibility of hyperspectral data for mapping (Classification) different age group and stressed versus healthy Arecanut crops.
- 2) Mapping the age based Arecanut crop water requirement.
- 3) Development of hyperspectral vegetation indices for stressed, different age groups and age based Arecanut crop water requirement

1.10 Need and Benefits of the Study

For agriculture dependent farmers in India, efficiency in farming is a serious issue. Crop monitoring offer several substantive benefits to get most out of available resources. It is particularly important for Arecanut which is more prone to variety of stress and has high irrigation water requirement. Using maps, farmers can pursue strategies to enhance farming, and the benefits include,

- Judicial usage of available water resource – sustaining surface and ground water.
- Age wise classification and disease identification allows better planning.
- Increase yields by finding potentially yield limiting problems in a timely fashion.
- Satellite based monitoring is fast, easy and accurate.
- GIS mapping.

Applying the right amount of inputs at the right place, at the right time benefits crops, soils, ground water, and thus benefits the entire crop cycle. Thus boosting sustainability of resources and supporting country's growth.

1.11 Format of Thesis Presentation

Chapter One presents introduction about the Arecanut plantation crop and its geographical distribution. Problems related to crop monitoring and feasible advanced solution namely hyperspectral remote sensing. Formulations of problem and study objectives are listed.

Chapter Two reviews literature related to crop monitoring using hyperspectral remote sensing and its applications. A brief summary of literature followed by identified research gaps are presented.

Chapter Three provides detailed methodology framed to solve the research objectives. The data sources, data processing tools and techniques used in study were discussed in detail.

Chapter Four presents the description about segregation of stressed vs healthy Arecanut crops using an integrated approach. And also provides details of cause identification for a particular disorder in Arecanut crops.

Chapter Five discusses classification of Arecanut crops into different age groups, by comparing popular classifying algorithms to check the feasibility in age based classification.

Chapter Six presents the concepts in development of new narrow bands combination indices, to improve classification accuracy. For age based and healthy vs stressed crops.

Chapter Seven focuses on computing age based crop water requirement for Arecanut crops in the form of an index. Also to identify the prominence wavelengths to develop simple predictive models to estimate age based crop water requirement.

Chapter Eight is devoted to presentation of the conclusions drawn from the research. Important recommendations based on findings are listed. With limitations of the study and future scope are presented.

In order to arrive at the objective of research, literatures were focused on selected themes and are presented in the following chapter.

CHAPTER 2

LITERATURE REVIEW

2.1 INTRODUCTION

This chapter presents a review of relevant literature to bring out the background of the study undertaken in the area of applications of hyperspectral remote sensing in crop monitoring.

Remote sensing data capturing platforms include ground, airborne and Space borne (satellite). Since airborne data acquisitions techniques are costly, the study is carried out using freely available satellite data integrated with reflectance data captured in both field and laboratory. Ground based data capturing generally accomplished by spectroradiometers.

Spectroradiometer enables to acquire the hyperspectral data either from the field measurements or in laboratory, whereas the Hyperion is an example of Space borne hyperspectral data. Several studies have been carried out using these technologies.

Wide ranges of articles dating from 1989 to 2016 were reviewed during the course of work to frame a methodology. Works related to hyperspectral image processing, age based classification of crops, segregation of crops based on health status, correlation analysis, vegetation indices and crop water needs related articles were reviewed.

In order to arrive at the objective of research, literatures reviewed were classified into following themes.

- Hyperspectral Data Pre-Processing
- Hyperspectral Remote Sensing for Identification of Stressed Crops
- Hyperspectral Prominence Wavelengths for Crop Monitoring
- Hyperspectral Vegetation Indices
- Classification of crops for monitoring and management
- Hyperspectral remote sensing for Crop water requirement
- Statistical Techniques for Hyperspectral Data processing

Thenkabail et al., (2000) recommends a 12 narrow band sensor, in the 350 to 1050 nm range of spectrum is optimum for estimation of agricultural crop biophysical information. Gazala et al., (2013) analyzed spectral reflectance pattern to assess soybean yellow mosaic disease. Parsanna kumar et al., (2013) utilized hyperspectral remote sensing to detect stress in rice crop due to plant hopper. Thenkabail et al., (2013) identified redundant bands to overcome the high data dimensionality for particular application such as agricultural crop characterization, classification, monitoring, modelling, and mapping. Bandyopadhyay et al., (2014) derived regression model to predict the grain and biomass yield of wheat in advance using spectral indices. Krishna et al., (2014) developed a model, to trace yellow rust disease in winter wheat. VNIR and SWIR regions are used to assess yellow rust severity detection in winter wheat crop. PLS regression, ANOVA and MLR, combinations were tried to developed a robust model and identified significant wavelengths as (428nm, 672nm and 1399nm). Sahoo et al., (2015) presented comprehensive applications of hyperspectral remote sensing related to agriculture based on broad range of the literature. Applications are not limited to crop's discrimination, moisture, stress, parameter retrieval, pest and diseases assessment and selection of optimum wavebands, to study different agricultural applications. Marshall et al., (2016) demonstrated the strengths of hyperspectral narrow bands and hyperspectral ratio-based indices in modelling crop evapotranspiration and two its primary components.

2.11 Hyperspectral Data Pre-Processing

Khurshid et al., (2006) described the procedure for de-stripping of bands, MODTRAN based radiometric correction to obtain surface reflectance from at-sensor reflectance were briefed. Removal of stripes and pixel (column) dropouts and noise reduction explained by the authors is followed during image processing of Hyperion image.

Miglani et al., (2008) evaluated the satellite-based hyperspectral data available from Hyperion onboard EO-1 of NASA for agricultural application. Principal component analysis was carried out for selecting appropriate bands. The first 5 principal components (PCs) explained 98 percent of variability. The next five PCs only added a very small fraction of additional variability. The dimensionality of Hyperion data was found to be of the order of four. ATCOR 2 was used for the atmospheric correction. It has lowered the reflectance of the image in the blue and red region whereas it

enhanced the same in the NIR and SWIR regions, when compared with apparent reflectance. Atmospheric correction also increased the correlation with the observed reflectance.

Singh and Dowerah (2010) briefed various hyperspectral imagery pre-processing methods such as radiometric correction, dimensionality reduction etc., along with various image classification techniques. Broad areas of application of hyperspectral remote sensing are also being discussed in the article. Basics of image processing methodology were derived from this article.

Chakravorty et al., (2011) explained the method of data processing, removal of the absorption bands and bands having no information. Methods of atmospheric and geometric correction were explained in detail including various interpolations and resampling techniques. They concluded FLAASH and QUAC models for atmospheric correction certainly reduced haziness in the image but FLAASH correction showed better correction than QUAC as it incorporates more knowledge of the atmospheric conditions of the study area at the time of acquisition. They also mentioned geometric correction using Nearest Neighborhood resampling method is preferable as it does not alter pixel brightness value during resampling even though the pixels were jagged relative to original un-rectified data.

Nielsen (2011) explained the algorithm behind MNF transformation. Noise Fraction, Signal to Noise ratio was explained with mathematical relationship.

2.12 Hyperspectral Remote Sensing for Identification of Stressed Crops

A study by Laudien et al., (2004) evaluates the comparison of classification results from two different multi and Hyperspectral sensors and discusses the possibility of detecting sugar beet disease.

To identify the stress in plants Moshou et al., (2006) used trained neural networks for different parameters. By QDA (Quadratic Discriminant Analysis) technique the type of stress in plant was identified. Where, Larsolle et al., (2007) extracted spectral signatures to identify the disease severity and plant density.

Jing et al., (2007) observed that foliar *Chl a* (Chlorophyll-a) concentrations were strongly correlated with canopy spectrum in the visible region and the first-order

derivative spectrum in blue edge, green edge and red edge. And derivative of spectra in red edge and green edge have strong predication power for foliar *Chl a* concentrations of diseased winter wheat.

Thorsten et al., (2008) studied band selection techniques for Hyperspectral data to identify relevant and redundant information in spectra regarding a detection of plant stress caused by pathogens. Anshu et al., (2008) studied the important bands for monitoring the agricultural crops.

Franke et al., (2008) focused on remotely sensed detection of the fungal disease powdery mildew (*Blumeriagraminis*) in wheat. They tested the potential of hyperspectral data for an early detection of stress symptoms. A sophisticated endmember selection procedure was also used and, additionally, a linear spectral mixture model was applied to a pixel spectrum with known characteristics, in order to derive an endmember representing 100% powdery mildew-infected wheat. Regression analyses of matched fraction estimates of this endmember and in-field-observed powdery mildew severities showed promising results.

Shafri et al., (2009) concluded from their study that the red edge based techniques were more effective than vegetation indices in detecting infected oil palm trees plantation.

Baariegul et al., (2010) evaluated different wavelength ranges and found 400 and 1000nm reliably detects head blight on wheat ears. P.C.A method identified four distinct wavelengths which ranges (500-533nm, 560-675nm, 682-733nm and 927-931nm) respectively to differentiate between spectra of diseased and health of wheat.

Jones et al., (2010) determined the disease severity of tomato using ultraviolet, visible, and near-infrared reflectance spectroscopy. They used chemometric methods to identify significant wavelengths and created spectral-based prediction models. They identified significant wavelengths through analysis of the B-matrix from partial least squares (PLS) regression, analysis of a correlation coefficient spectrum, and through the use of a stepwise multiple linear regression (SMLR) procedure. These analysis methods revealed several significant regions wavelengths and produced predictive models of disease severity based on absorbance spectra.

Sankaran et al., (2010) recognized the need for developing a rapid, cost-effective, and reliable health monitoring sensor that would facilitate advancements in agriculture. They described the currently used technologies that can be used for developing a ground-based sensor system to assist in monitoring health and diseases in plants under field conditions. These technologies include spectroscopic and imaging based and volatile profiling-based plant disease detection methods. The work compared the benefits and limitations of these potential methods.

Ray et al., (2010) using ASD hand held spectroradiometer data determined the most optimum narrow bands and Hyperspectral indices to discriminate between different levels of stress in potato crop.

Shalei et al., (2011) conducted studies to select the most sensitive hyperspectral wavelengths for discrimination of imperceptible spectral variations of paddy rice under different cultivation conditions. They cultivated paddy rice under four different nitrogen cultivation levels and three irrigation levels. Principal component analysis and band to band correlation were used to select significant wavelengths. Results indicated that good discrimination was achieved. They concluded that the narrow bands based on hyperspectral reflectance data appear to have great potential for discriminating rice of differing cultivation conditions and for detecting stress in rice vegetation.

Hyperspectral data has been shown to be highly suitable for detection and discrimination of agricultural crops. However, the entire spectrum covered by Hyperspectral data is probably not needed for discrimination between healthy and stressed plants (Thorseten et al., 2011). They concluded that few phenomenon-specific spectral features are sufficient to detect wheat stands infected with powdery mildew.

Ray et al., (2011) investigated the utility of hyperspectral reflectance data for potato late blight disease detection. They have collected the hyperspectral data for potato crop at different level of disease infestation using hand-held spectroradiometer over the spectral range of 325–1075 nm. The data was averaged into 10-nm wide wavebands, resulting in 75 narrow bands. They partitioned the reflectance curve into five regions, viz. 400–500 nm, 520–590 nm, 620–680 nm, 770–860 nm and 920–1050 nm and a notable difference in healthy and diseased potato plants were noticed in

770–860 nm and 920–1050 nm range. Shalei et al., (2011) conducted studies to select the most sensitive hyperspectral wavelengths for discrimination of imperceptible spectral variations of paddy rice under different cultivation conditions. They cultivated paddy rice under four different nitrogen cultivation levels and three irrigation levels. Principal component analysis and band to band correlation were used to select significant wavelengths. Results indicated that good discrimination was achieved. They concluded that the narrow bands based on hyperspectral reflectance data appear to have great potential for discriminating rice of differing cultivation conditions and for detecting stress in rice vegetation.

Ray et al., (2011) investigated the utility of hyperspectral reflectance data for potato late blight disease detection. They have collected the hyperspectral data for potato crop at different level of disease infestation using hand-held spectroradiometer over the spectral range of 325–1075 nm. The data was averaged into 10-nm wide wavebands, resulting in 75 narrow bands. They partitioned the reflectance curve into five regions, viz. 400–500 nm, 520–590 nm, 620–680 nm, 770–860 nm and 920–1050 nm and a notable difference in healthy and diseased potato plants were noticed in 770–860 nm and 920–1050 nm range.

Also various vegetation indices, namely NDVI, SR, SAVI and red edge were calculated using reflectance values. The differences between the vegetation indices for plants at different levels of disease infestation were found to be highly significant. They have determined the optimal hyperspectral wavebands to discriminate the healthy plants from disease infested plants to be 540, 610, 620, 700, 710, 730, 780 and 1040 nm although up to 25% infestation could be discriminated using reflectance at 710, 720 and 750 nm.

Kumar et al., (2012) reported that the most significant spectral bands for the aphid infestation in mustard are in visible (550-560nm) and near infrared regions (700-1250nm and 1950-2450nm) respectively.

Wang et al., (2012) Analyzed leaf spectrum of tobacco infected with disease and insect pests at different severity levels measured using ASD-handheld spectroradiometer, the wave lengths between 631nm and 328nm and 733nm as well as 864nm were selected out as sensitive bands region to the severity levels.

Studies conducted by Huang et al., (2016) determines early detection of soybean injury from dicamba using hyperspectral data.

2.13 Hyperspectral data Classification

Various classification methods are available for classifying the hyperspectral data. Depending upon the application and accuracy some classification methods may out perform for particular studies. The following literature discusses about the different classification methods employed for agricultural crops.

Gualtieri et al., (1998) described the algorithm behind SVM binary classification technique along with optimal margin method for separable data. They demonstrated the application over an agricultural scene and explained the optimization problem. The classification is accurate (with 96%, and 87% accuracy for a 4 class problem, and a 16 class problem respectively) but needs the signatures of all the possible classes in the study area, hence making it suitable only for broad categories and not for within class separation.

Gomez et al., (2003) Evaluated unsupervised and semi-supervised methods for classification. The semi-supervised method yielded higher accuracy of classification.

Galvao et al., (2005) conducted studies for discrimination of five Brazilian sugarcane varieties. These varieties were discriminated with EO-1 Hyperion data by Multiple Discriminant Analysis (MDA) method using reflectance values, ratios of reflectance and several spectral indices sensitive to changes in chlorophyll content, leaf water and lignin-cellulose. Results showed that sugarcane varieties can be discriminated using EO-1 Hyperion data.

Rao et al., (2007) used space borne hyperspectral imagery for the development of a crop specific spectral library and automatic identification and classification of rice, chilli, sugarcane and cotton. In their study they developed the spectral library from Hyperion image and in- situ hyperspectral measurements and tested the potential of the developed spectral library for identification and classification of crops. It was concluded that the integration of in-situ hyperspectral measurements with space borne hyperspectral imagery can provide improvement in the discrimination of various classes of interest.

Ashoori et al., (2008) examined Hyperion data of an agricultural area located in Tehran for discrimination of wheat and barley fields. They also studied the usefulness of texture quantization methods for improving the discrimination of crop types. Different methods like First order statistics of the Grey Level Co-occurrence Matrix, Geostatistics and Fourier transform were used for texture feature generation. Maximum likelihood classifier was then used to classify the outputs. Results showed that the use of texture features lead to higher accuracies and better discrimination of similar classes.

Fahimnejad et al., (2008) studied the capabilities of Hyperion hyperspectral imagery for discrimination of wheat and barley. Atmospheric correction and other pre-processing operations were performed on the imagery. They used two supervised classification approaches including Spectral Angle Mapper classification and Linear Spectral Unmixing and found that linear spectral unmixing algorithm gives higher accuracy compared to Spectral Angle Mapper classification. They also concluded that Hyperion data have promising capabilities for discrimination of wheat and barley.

Govender et al., (2008) compared the classification of vegetation types using both hyperspectral and multispectral data. Several statistical classifiers including maximum likelihood, minimum distance, mahalanobis distance, spectral angle mapper and parallelepiped methods were used. Classification using mahalanobis distance and maximum likelihood produced the maximum accuracy. They also concluded that the use of hyperspectral data can improve the classification accuracy.

Xing-Ping et al., (2009) described the methodology of end member extraction along with SAM classification method and Mixture Tuned Match Filtering (MTMF) soft classification method. They also explained a classification methodology involving multiple classifiers with soft classification followed by hard classification which had increased classification accuracy.

Joevivek et al., (2009) have carried out research work on finding the best suitable learning algorithm and the best kernel for hyperspectral image classification. They have carried out classification of the image with different methods and found that support vector machine outperforms other supervised algorithms and also found that linear kernel performs better than all other kernels.

Satpathy et al., (2010) described the procedure for mapping various land covers using Hyperion images using Spectral Angle Mapper (SAM) and Matched filtering mapping techniques. They also mentioned the top 10 bands in MNF contain most of the spectral information and they were used to determine the pure pixels in the Hyperion image using PPI procedure.

Shwetank et al., (2010) reviewed that there is no spectral library for classification and discrimination of rice crop.

Skowronek et al., (2016) by utilizing hyperspectral remote sensing data in combination with field data derived a distribution map of an invasive bryophyte species.

2.14 Hyperspectral Prominence Wavelengths for Crop Monitoring

Hamed et al., (2003) studied the contribution of different parts of the spectrum in describing disease severity of wheat using Independent Component Analysis (ICA) and Principal Component Analysis (PCA). NIR & Visible region between 550 and 750 nm were found sensitive for discrimination and quantification of fungal disease severity in wheat.

Laudien et al., (2004) concluded from their studies that red (630nm to 690nm) and near infrared portions of the spectra (760 to 900nm) are important for agricultural applications. Spectroradiometer field data was used to train the supervised classification. From this information, images were classified into several vitality classes.

Vigier et al., (2004) used canopy reflectance of soybeans measured with a narrowband spectrometer. The mean reflectance in the broad band region (R_{675} - R_{685}) contributed the most for soybean plant damage estimation.

Mozaffar et al., (2008) applied Endmember Extraction Algorithms (EEAs) on a Hyperion image of southern of Tehran, IRAN. They have suggested a large number of endmembers to enhance the classification accuracy while the seasonal variation in the spectral response was also taken into account in vegetation classification. They compared the results of Geometrical approach in vegetation endmember extraction assistance with vegetation indices. The objective of their study was to select optimal

bands in hyperspectral images those are most useful in vegetation classification, then to identify optimal endmember, signature spectrum that represents a certain class, for vegetation classification, and to test effective Endmember Extraction Algorithms for classification of vegetation type. Their study proved that Endmember extraction provides a powerful tool for analysis of highly redundant, pixel spectra and channel images of hyperspectral data sets.

Yang et al., (2009) found that the wavelength from 757 to 1039nm were most sensitive region of the spectrum for assessing the severity of bacterial leaf blight in rice.

Song et al., (2011) selected the most sensitive wavelengths for discrimination of the imperceptible spectral variations of paddy rice under different cultivation conditions. A comprehensive comparison was made to select the most influential narrow-band combination (552, 675, 705 and 776 nm) to discriminate rice leaves from four kinds of nitrogen cultivation conditions and also a 3-wavelength combination (1158, 1378 and 1965 nm) was established this facilitates spectral discrimination of rice leaves grown in three kinds of irrigation conditions by using several parametric and nonparametric methods. The narrow bands based on hyperspectral reflectance data appeared to have great potential for discriminating rice of differing cultivation conditions and for detecting stress in rice vegetation and these selected wavelengths also had great potential use for the design of future sensors.

Arafat et al., (2013) concluded NIR spectral zone was the best discriminate between maize and rice. Linear discrimination analysis showed to specific wavebands to isolate each crop from the other one. They found that wavebands (350:712, 1451:1562, 1951:2349nm) were best to isolate wheat and waveband (730:1299nm) was the best to isolate maize while three wavebands could be used to isolate rice (350:713, 1451:1532, 1951:2344nm)

Wilson et al., (2014) summarized, that hyperspectral reflectance data collected using a handheld portable spectroradiometer, with a spectral range of 400–900 nm, is well suited for crop discrimination. They found classification accuracies were relatively high throughout the entire growing season using a set of wavebands identified as significant for crop discrimination through stepwise discriminant analysis. The study

resulted in recommending a total of 23 optimal bands in the 400–900 nm range to discriminate soybean, canola, wheat, oat and barley in Northeastern Ontario, Canada.

Age

Chemura et al., (2014) concluded that there is potential in using object based image analysis and an empirical model to determine the age of oil palm at field scale from high resolution satellite imagery. They found linear function relating age to crown diameters to crown projection area (CPA) was useful to predict the age of oil palm per field with accuracy of ± 1 year up to 13 years. The method uses spectral information to obtain spatial information that can be used for determining characteristics of target features.

2.15 Hyperspectral Vegetation Indices

Sometimes there may be overlapping between the different classes in case of classification due to over sighting of training sites or in reference spectral signatures to overcome these types of problems and to improve the classification accuracy deriving different indices may helpful.

Hansen et al., (2003) studied the spectral behavior of various crops with respect to the laboratory measured biophysical parameters to model a narrow band equation to predict several plant characteristics based on its reflectance. They also explained a novel statistical based method to develop narrow band indices. Authors explained correlation analysis based method to identify peculiar bands suitable to form specific vegetation index. One may adopt this technique of band correlation to develop crop specific indices.

Apan et al., (2003) developed different spectral vegetation Indices (SVIs) by selecting the sample pixels of diseased and non-diseased areas by multiple discriminant function analysis and they observed 96.9% classification accuracy.

Apan et al., (2004a) evaluated several narrow band indices from EO-1 Hyperion imagery to discriminate sugarcane areas affected by ‘orange rust’ disease. It was found that 1660nm yielded increased separability of rust-affected areas.

Apan et al., (2004b), evaluated several narrow-band indices from EO-1 Hyperion imagery in discriminating sugarcane areas affected by ‘orange rust’ (Pucciniaakuehnii) disease.

They generated forty spectral vegetation indices (SVIs), focusing on bands related to leaf pigments, leaf internal structure, and leaf water content, from an image acquired over Mackay, Queensland, Australia. An optimum set of indices were selected using Discriminant function analysis based on their correlations with the discriminant function. The predictive ability of each index was also assessed based on the accuracy of classification. Their results demonstrated that Hyperion imagery can be used to detect orange rust disease in sugarcane crops. 'Disease–Water Stress Indices' (DWSI-1~R800/R1660; DWSI-2~R1660/R550; DWSI-5~ (R800zR550)/ (R1660zR680)) formulated by them produced the largest correlations, indicating their superior ability to discriminate sugarcane areas affected by orange rust disease.

Zhang et al., (2005) analyzed five different indices to detect late blight disease in field tomatoes and concluded that there is a significant enhancement capability of multispectral remote sensing for disease discrimination at the field level.

Steddom et al., (2005) compared the precision, reproducibility and sensitivity of a multispectral radiometer to visual disease assessments using individual wavebands from radiometer as well as Vegetative Indices calculated from the individual wavebands and there has been an improved accuracy.

Dutta et al., (2006) demonstrated a simple approach for disease detection on mustard crop. They used five diseased water stress indices for the identification of diseased crop. From the ground truth data GPS locations of the diseased fields were obtained and marked in LISS IV data and overlaid on the Hyperion data. The spectral response of the diseased crop obtained from hyperspectral data were then compared to the disease scores obtained through ground truth. Significance tests were also carried out for separability of the spectral curves between healthy and diseased crops.

Stephanie et al., (2007) extracted indices from spectral profiles by means of band reduction techniques. They concluded from leaf level measurements decrease in leaf chlorophyll concentration resulted due to iron deficiency. Studies suggested that spectral bands and narrow waveband ratio vegetation indices selected via multivariate logistic regression classification were able to distinguish iron untreated and iron treated trees. The visible part of the spectrum mostly dominated by the amount of pigments (e.g Chlorophyll, Carotenoids) provided the most discriminative spectral region (505-740nm) in their study.

Chavez et al., (2009) prepared a visual assessment of disease symptoms in both virus-infected and virus free plants and compared it with spectroradiometry and multispectral photographic images of the plants recorded during their growth and development. Results showed that changes in reflectance in certain regions of the electromagnetic spectrum indicative of disturbances in light reflection by vascular tissues in infected plants measured with a spectroradiometer as well as derived spectral vegetation indices such as NDVI, SAVI and IPVI provided early detection of viral infection. They concluded remotely sensed spectroradiometry and multispectral imagery proved to be an effective method for an early detection of PVV infection in potato plants grown under controlled conditions. They observed that inoculated plants presented differential reflectance from healthy ones in the blue and red regions of the electromagnetic spectrum are encouraging.

Rumpf et al., (2009) attained reliable results by combining vegetation indices, which are usually called features in classification for the early detection of plant diseases. In order to identify optimal subsets of features for the different pathogens already at an early stage of infestation, they have found that entropy and mutual information are adequate concepts. Accordingly, they used the minimum redundancy – maximum relevance (mRMR) criterion to evaluate the features and they have found that they need different indices and feature subsets of different sizes for different diseases. They have found that by using the optimal subset of features the classification accuracy for *Uromycesbetae* was even better than using all features.

Rumpf et al., (2010) obtainable a procedure for the early detection and differentiation of sugar beet diseases based on Support Vector Machines and spectral vegetation indices. Hyperspectral data were recorded from healthy leaves and leaves inoculated with the pathogens for a period of 21 days after inoculation. Nine spectral vegetation indices, related to physiological parameters were used as features for an automatic classification. They have found that early differentiation between healthy and inoculated plants as well as among specific diseases can be achieved by a Support Vector Machine with a radial basis function as kernel. Their study has shown that combined VIs, together with SVMs using an appropriate radial basic function are able to discriminate between the foliar diseases *Cercospora* leaf spot, sugar beet rust, powdery mildew and healthy plants and as well as between the plant diseases themselves.

Shankar et al., (2010) found the most optimum narrow bands and hyperspectral indices to discriminate between different levels of stresses including nutrient stress, water stress and disease stress of potato crop. They also included discrimination of varieties considering it as a genetic stress. They have used band-band R^2 , principal component analysis and discriminant analysis respectively for the selection of optimum bands. It was found that the red edge indices performed the best for separating variety, disease intensity and nitrogen application rate.

Prabhakar et al., (2011) characterized leafhopper stress on cotton, identified the sensitive bands, and derived hyperspectral vegetation indices specific to this pest. Broad band comparison of mean reflectance spectra between healthy and leafhopper infested plants showed significant decrease in blue (450 to 520 nm), red (630 to 690 nm) regions, while reflectance significantly increased in the NIR region (760 to 900 nm). Their analysis of hyperspectral data revealed narrow bands at 376 and 496 nm (blue), 691 and 715 nm (red), 761 nm (NIR) and 1124 nm (SWIR-1) as sensitive to leafhopper damage.

Mirik et al., (2012) examined the spectral reflectance characteristics and changes in selected spectral vegetation indices to discern infested and healthy wheat. They have quantified the relationship between spectral vegetation indices and Russian wheat aphid feeding damage (hot spots). Linear regression analyses were carried out which showed that there were varying relationships between Russian wheat aphid density and spectral vegetation indices, with coefficients of determination (r^2) ranging from 0.91 to 0.01. These results indicated that remote sensing data have the potential to distinguish damage by Russian wheat aphid and quantify its abundance in wheat.

Mahlein et al., (2013) developed specific spectral disease indices (SDIs) for the detection of diseases in crops. Sugar beet plants and the three leaf diseases *Cercospora* leaf spot, sugar beet rust and powdery mildew were used as model system. With a non-imaging spectroradiometer, hyperspectral signatures of healthy and diseased sugar beet leaves were assessed at different developing stages and disease severities of pathogens. Significant and most relevant wavelengths and two band normalized differences from 450 to 950 nm, describing the impact of a disease on sugar beet leaves were extracted from the data-set using the RELIEF-F algorithm.

They have exhaustively searched the best weighted combination of a single wavelength and a normalized wavelength difference by testing all possible combinations to develop hyperspectral indices for the detection of sugar beet diseases. The optimized disease indices were then tested for their ability to detect and to classify healthy and diseased sugar beet leaves.

Lin et al., (2015) identified spectral bands of established narrow band index to detect soil phosphorous concentration. They used several indices to determine the best combination to predict chemical concentration.

In addition to these, articles pertaining to estimation of crop water requirement were reviewed to gain more insights on the topic. Studies carried out with limited meteorological data were reviewed meticulously. Various reviewed articles, including Arecanut crop water requirement are summarized and criticized in the next section.

2.16 Crop Water Requirement

Mahesha et al., (1989) have worked on Arecanut crops, and determined the crop water requirement for Arecanut crops of age 12-15 years based on the evaporative demand of the crop. The crop water demand was evaluated using the crop coefficient and the potential evapotranspiration values (computed by the modified Penman method using monthly and weekly climatic data from 1971-85) and Balasimha et al., (1996) have presented age wise crop water requirement of Arecanut crops. Study was carried using traditional methods which were time consuming; moreover, age wise discrimination and spatial mapping of crop water requirement were not carried out.

Allen et al., (1998) presented guidelines for estimating crop water needs using crop coefficient and reference crop evapotranspiration calculations. The manuscript explains the concepts of crop coefficient along with influencing factors. It also describes the calculations of various constants like temperature coefficients and extraterrestrial radiation. Even though this is an exemplary literature on crop water requirement, crop coefficients of many crops is not investigated by the authors, especially the plantation crops. In addition, the presented FAO- 56 methodology to calculate PET demands many measured meteorological data hindering its use in remote locations.

Jabloun and Sahli (2008) estimated reference crop evapotranspiration using Hargreaves and Samani equation for a location with limited meteorological data. They concluded Hargreaves method is a substitute to FAO methodology to determine Crop water requirement in the absence of elaborate meteorological data in remote locations. This literature served as the guideline to choose Hargreaves and Samani method as an alternative to FAO – 56 procedures.

Casa et al., (2008) worked on assessing crop water demand using remote sensing for various crops. Hargreaves method was used to calculate potential evapotranspiration and spatial distribution of monthly crop coefficients was prepared by assigning K_c values to crop map prepared using Landsat ETM+ images. K_c values used in the article were obtained from FAO- 56 guideline, making this methodology only suitable to the crops with established K_c . Hence a remote sensing based calculation was necessary for other crops.

Kamble et al., (2013) derived an equation to compute crop coefficient using remotely sensed data. They built relationship between NDVI and Crop coefficient based on study conducted on various crops and location using regression analysis. The relationship presented by the authors is utilized in this work to determine the crop coefficient which is compatible with Hargreaves and Samani equation. One can use the proposed equations to determine NDVI based spatial map of K_c which replaces traditional methods.

2.17 Statistical Techniques for Hyperspectral Data processing

Wang et al., (2008) used both hand held spectroradiometer and airborne hyperspectral image to map sericea and its invasiveness in a public grass field in Mid-Missouri. The maximal 1st-order derivative in red-near infrared region (650–800nm) was derived to separate sericea from fescue, the dominant grass in pastures in Missouri. They have applied a 1st-order derivative analysis to calculate maximal derivatives that maximized the spectral difference between sericea and fescue, the dominant grass in pastures. Then, a threshold approach was applied to identify sericea patches of various sizes in the study area. Finally, by developing an empirical regression model, the biophysical distribution of sericea in these patches was finally extracted from the hyperspectral imagery.

Zhang et al., (2012) analyzed disease severity using two regression models PLSR and MLR among this they found PLSR as the best.

Krishna et al., (2014) studied spectral behavior of stressed wheat crop to build a narrow band index to assess wheat yellow rust disease. They developed an index based on correlation analysis. They also modeled an equation using Partial Least Square Regression technique to predict intensity of disease using few key spectral bands. This study inspires to derive the methodology for building vegetation index.

2.2 Summary of Literature

From review of literature it can be observed that the hyperspectral remote sensing applications in the field of agriculture is applied to only certain annual crops namely, Sugarcane, Soybean, Mustard, Wheat, Rice, Potato, Paddy rice, and Tobacco. Studies were mainly concentrated on either identification of crop health or discrimination of crops. This includes Chilly, Sugar cane and Cotton with Maize, wheat with rice and barley. Most of the studies have been carried out using hyperspectral data acquired by spectroradiometer and Hyperion satellite data. Spectroradiometer data was used for building the spectral libraries. Hyperion data is used to extract the endmembers for classification and deriving indices. The extracted endmembers were used for discrimination and to map crop health status. Most of the researchers found that red edge position is best for stress detection. Different statistical methods used for discrimination and identification of sensitive wave lengths include, PCA & ICA and MLR, LD, PLS, PLSR methods.

Improved accuracy was observed with derivative of reflectance spectra using different atmospheric corrections methods. Supervised classification method yielded better accuracy in most of the cases compare to unsupervised classification. The classification methods used in most of the cases are Maximum likelihood, SAM and SVM.

Few band combinations come out as significant for particular types of disease affected plants. By identifying these particular bands and using this information for deriving indices using algorithms leads to improved accuracy namely NDVI, SR, and SAVI.

Concept and calculation of crop water requirement was analyzed from various articles, in addition to which a suitable method to determine reference crop evapotranspiration was identified. On the other hand, works with regard to remote sensing based crop coefficient were reviewed.

In addition to these, literatures concerning vegetation monitoring through indices were assessed to understand the concepts of vegetation indices and methodology to derive crop specific index from hyperspectral data.

Literatures from various researchers working on hyperspectral remote sensing on vegetation were adapted to implement correlation analysis based methodology to derive the index.

2.3 Literature Gap

The review of literature witnesses that there are a few studies on Arecanut crop. The commercial crop which sustains for a long year where there is variation in reflectance with its age.

There are no particular wavelengths related studies those are sensitive to age of the crop. There is no particular model to predict either the age of the crop or to identify the disease affected crop. There is no spectral library for this commercial crop.

Where there is a variation in reflectance with respect to its age and with respect to healthy verses diseased affected one. The Arecanut yield increases gradually with age until the palms reach full maturity at 10-15 years and then continue until the palms stop bearing at 40-60 years of age. Also there is a decrease in yield due to crop subjected to number of diseases. Hence the crop age and yield are interdependent, and due to number of diseases the crop yield decreases, for yield estimation and better crop management it is necessary to know the age of the crop and the diseased affected crops. To fill these gaps following objectives were taken for the proposed study.

Since traditional methods to determine crop water requirement is laborious and time consuming, there is a need to employ remote sensing technology. Literature review revealed that, number of studies is carried out on crop water requirement of various seasonal crops, but rarely on plantation crops such as Arecanut, leaving Arecanut farmers with lack of knowledge on age wise crop water requirement.

Age wise classification of Arecanut plantations to discriminate water requirement is not attempted in previous studies. Despite the advancements in remote sensing, few studies are carried out on Arecanut crops and on understanding variation in its crop coefficients or on developing a narrow band index in this regard.

Remote sensing based crop water requirement monitoring of Arecanut is one area where research is essential.

Based on the observed research gap, objectives of this work are formed to understand the variation of Arecanut crop water needs with crop age. Age based classification and segregation of diseased v/s healthy Arecanut crops. Integration of remote sensing and crop water needs and crop type classification are combined to derive the methodology of the work. Developed methodology is outlined in next chapter along with study area and data.

RESEARCH METHODOLOGY

3.1 INTRODUCTION

This chapter includes the description of;

- Geographical location and characteristics of the study area,
- Overall methodology adopted to monitor Arecanut plantation crop using remote sensing,
- Data products, data pre-processing methods, statistical approaches implemented for the study,
- Concepts in deriving algorithms for developing hyperspectral vegetation indices.

3.2 Location and Characteristics of the Study Area

The Chennagiri taluk in Davangere district of Karnataka is locally known as the 'land of arecanut' owing to the abundance of arecanut plantations is chosen for the study. The study area lies between geographical extents of 13° 57 ' 00 " and 14° 01 ' 45 " N latitude and 75° 57 ' 15 " and 75° 59 '15 " E longitude spread over an area covering 3,175.2 hectares (31.752 sq. km). Several major villages such as Vaddanahal, Pandomatti and Honnebagi are rapidly developing in this region. It consists of 279 Villages and 62 Panchayats and is at a distance of 60 km from Chitradurga district, 60 km from Davanagere district, 44 km from Shivamogga district and 32 km from Bhadravathi Taluk. Figure 3.1 shows location map of the acquired Hyperion imagery corresponding to January month of 2014; it can be observed that the continued existences of only irrigated plantation crops are predominant on the image.

The average elevation of Chennagiri is 662 m above MSL with markedly flat terrain. The temperature ranges between 17 to about 40° C and is a relatively dry with humidity of around 18%. The region is considered as semi-arid though it receives an average annual rainfall of 808 mm. The population of the Channagiri Taluk is around 3 lakhs with majority of population earning their livelihood from Arecanut plantation. Ground water is the major source of irrigation and drip irrigation is practiced throughout the study area.

The study area is covered by either black or red sandy soil. The Arecanut crop farming in this region currently involves addition of tank silt dredged from ponds followed by drip irrigation is practiced generally in the form of flooding.

Arecanut variety grown here is called “Chennagiri local”, which is a tall variety with medium yield. Plants are spaced at an average distance of 8 ft. and in some plots; to prevent from bright sun during summer intercropping method was practiced where banana plants were grown in between juvenile Arecanut plants. Majority of the crop is harvested tender, before the fruits are ripened for production of red supari.

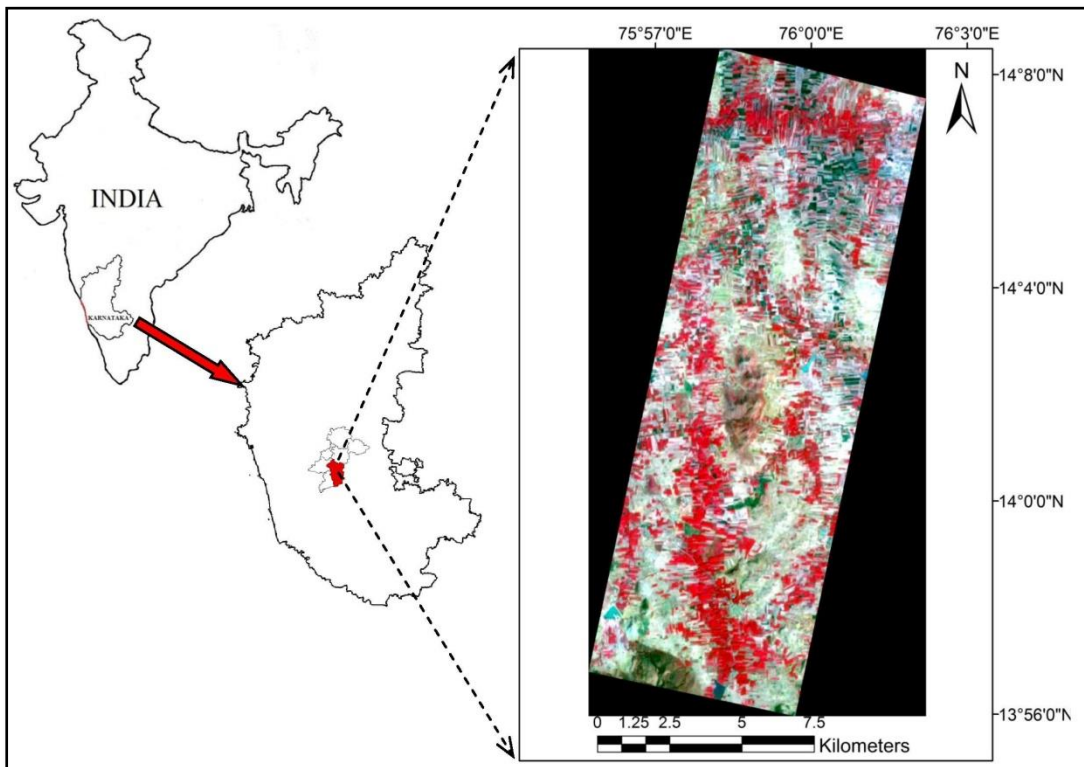


Figure 3.1 Location map of the study area showing Arecanut plantation region on Hyperion image

3.2.1 Selection of Study Area

India is both highest producers as well consumer of Arecanut, Karnataka State alone contributes about 50% of total India's Arecanut production. In Karnataka majority of Arecanut is produced from Shivamogga district, Davanagere district and some parts of coastal zone. The coastal zone of Karnataka is locally known as traditional belt of Arecanut (Kundapura, Udupi and Mangaluru). Due to high commercial value farmers started growing this crop in Chikkamangulu and some part of Shivamogga districts, gradually this crop spreads to Davanagere district and also in major portions of Karnataka. The Chennagiri Taluk of Davanagere district is locally known as 'Land of Arecanut' because of abundance of spread out of this commercial crop. Though Chennagiri taluk receives less rainfall, this cash crop is grown under irrigation. Major portion of irrigation is from 'Shanthisagar' known as world's second largest pond. Hence there is no strict rule for cropping pattern; due to high commercial value almost every farmer is growing this crop for their livelihood.

Most of the farmers are small farm holders with less than 10 acres of land generally holding sizes vary from 1 to 100s of acre and each individual planter practices different farming practices. Farmers were adding tank silt lifted from nearby ponds followed by drip irrigation. There are no proper drainage systems to drain off extra irrigated water. The soil type is sandy or red loamy on top of this added tank silt which gradually settles down and forms an impermeable layer thereby reducing the air voids. This blocks the entry of air and also reduction in hydraulic conductivity which ceases the root development. In summer due to shortage of water the added tank slit gets dry, which damages the plant's root. To overcome this problem, farmers continuously irrigate their farm fields; this cause's water stagnation which increases pH value thus soil salinity takes place which causes damage to the plants. Figure 3.2 show the continuously irrigated water stagnated Arecanut farm.



Figure 3.2 Continuously irrigated water stagnated plot

In coastal Karnataka, in spite of soil being lateritic with high K value they practice drainage in between two rows of Arecanut plantations. This acts as drainage gallery in rainy season to drain off excess rain water and the same act as drowning gallery in summer. The fallen Arecanut leaves were cut in to small pieces and dumped in this gallery which acts as organic manure also prevents water loss from the soil. This practice has not followed in the Chennagiri region and even there is no cultivation practices followed inside the Arecanut plantations. Consolidation of silt spread in the farms causes 'reduction of hydraulic conductivity. Figure 3.3 shows the non-cultivated, water stressed Arecanut plot. Due to these reasons number of diseases playing an adverse effect on yield of the crops.



Figure 3.3 Water stressed Arecanut plot

Though Chennagiri taluk is known as land of arecanut for its large spread of Arecanut gardens, the productivity is not up to the mark. If there is a proper maintenance and management of this crop, definitely there will be an increase in yield and good economic growth. It also indirectly reduces the huge amount of ground water exploitation.

For monitoring Arecanut crop with advanced techniques definite methodology was formulated. Analyzing the abundance of cropping pattern, sampling locations were fixed. These samples were unique in nature, consists large quantity of Arecanut crops only. This Includes crop with varying age groups, diseases affected plots. Figure 3.4 shows the field visit navigation plan map prepared using google earth. The overall methodology adopted is explained in the following section.

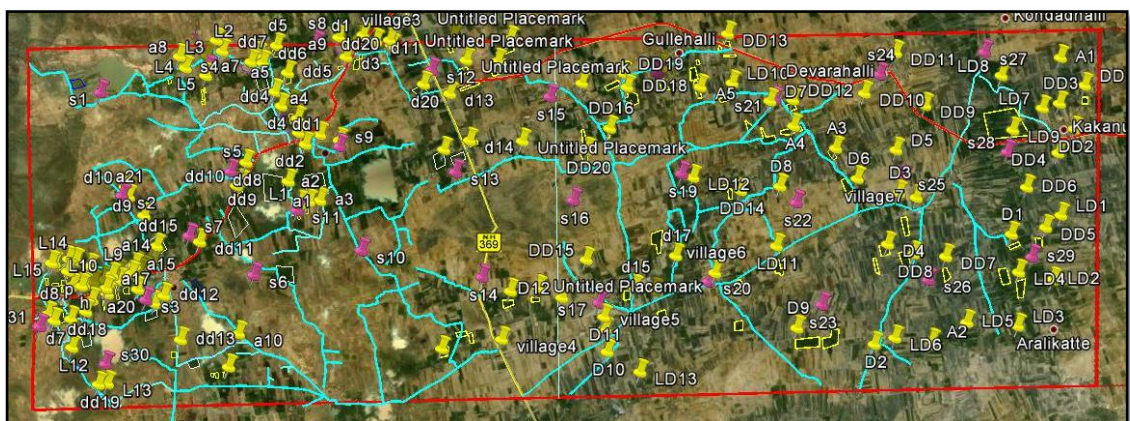


Figure 3.4 Preplan of the field visit map

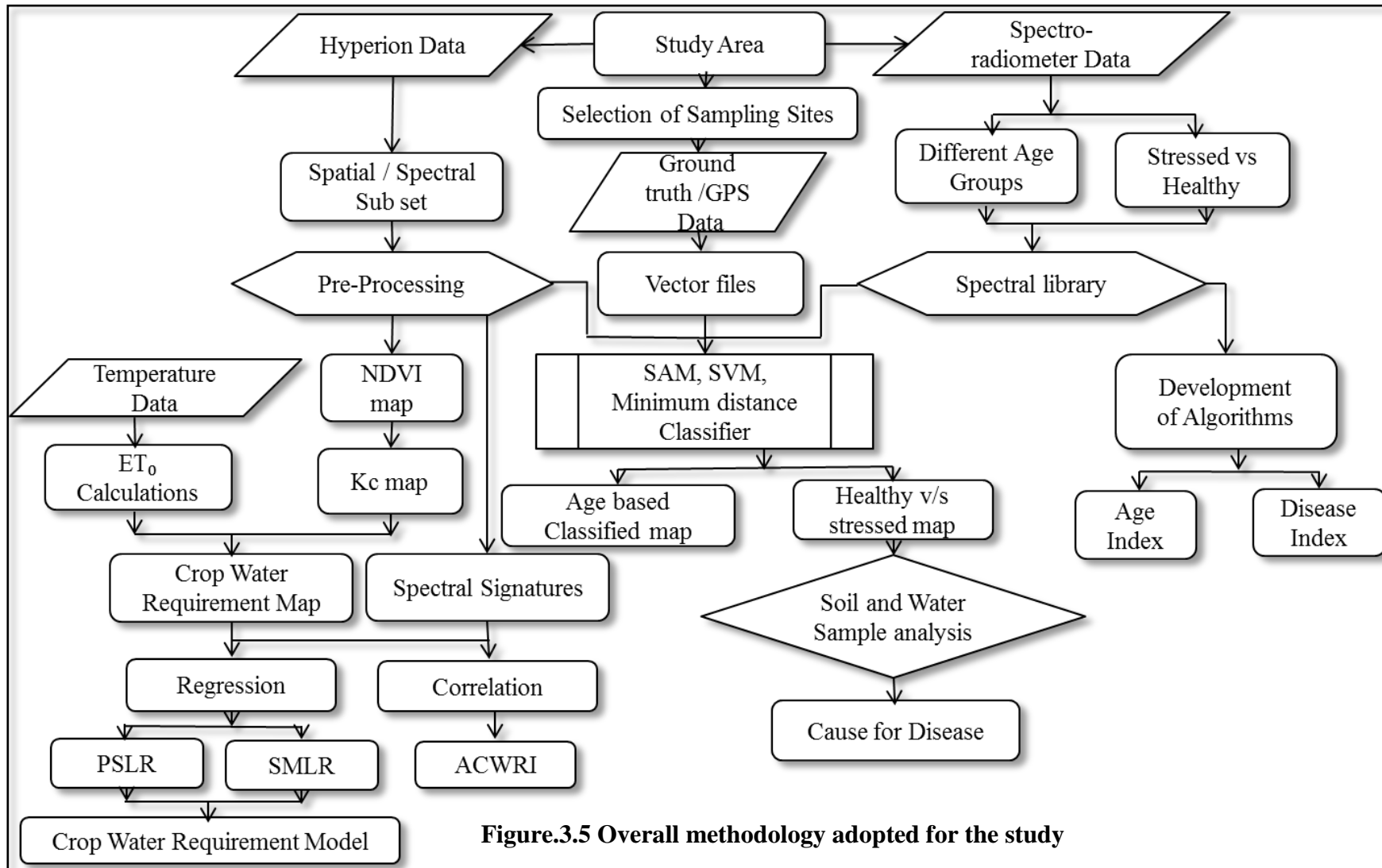


Figure.3.5 Overall methodology adopted for the study

3.3 Overview of Methodology

Figure 3.5 shows the overall methodology adopted for the study to achieve the formulated research objectives. It describes the step wise procedures of different data sets collection for the study, data pre-processing techniques, image classification methods, statistical techniques and analysis of obtained results followed by conclusions.

3.4 Data Collection

To accomplish the present work, primarily remotely sensed satellite imagery is obtained from USGS website on request. For the classification of Hyperion imagery ground truth, data is required; this was collected during the field visit. Field data collection includes ASD field spectroradiometer data and Global Positioning System (GPS) data.

3.4.1 Spectral analysis using ASD data

Spectroradiometer is a device designed to measure the spectral power distribution of a source. From the spectral power distribution, the radiometric, photometric, and colorimetric quantities of light can be determined in order to measure, characterize, and calibrate light sources for various applications such as mineral or vegetation studies.

For the selection of study area several preliminary field visits were carried out to ensure the presence of all age groups of Arecanut crop. After selecting the study area, Arecanut foliage reflectance data of varying age-groups were collected during 10th to 14th February 2014, close in time to the acquisition of Hyperion imagery to build spectral library. Grid-wise data collection method was adopted. The study area was divided into number of grids with a minimum grid size of 1000 m² and a representative spectrum was collected from each grid. Tree top reflectance measurements were carried out for representative plots refer Figure.3.6. Leaf samples were collected from inaccessible farms and in situ reflectance was captured using ASD handheld Spectroradiometer Field Spec® with wavelength range of 325–1075nm at resolution of 1 nm refer Figure.3.7. To derive the representative spectral signatures, a set of 20 samples were compared and averaged.



Figure 3.6 Field data collection using spectroradiometer

In case of laboratory measurements, the instrument was mounted on a tripod with 15cm distance from leaf in the presence of an external halogen light source. It was optimized to the halogen light source and calibrated with white reference panel. Nine spectrometer readings were collected for each sample and it was then averaged to obtain the accurate spectroradiometer reading. The instrument operates with the software RS³. Figure 3.7 shows the laboratory data collection method.



Figure 3.7 Laboratory data collection setup

The spectroradiometer data was analyzed using view spec pro. View Spec™ application is a program used for post-processing spectra files that were saved using an ASD instrument. The spectral signatures for stressed and healthy Arecanut plants were analyzed and used to identify specific spectral channel that distinguishes both. The Red Edge region was keenly analyzed since it refers to the region of rapid change in reflectance of vegetation in the near infrared range of electromagnetic spectrum. The idea behind choosing of red edge wavelength region was its high correlation with chlorophyll content of vegetation.

NIR has longer wavelengths than visible light; it exhibits peculiar properties that can be exploited for remote sensing applications, especially in identifying the plant stress. Healthy vegetation always gives high NIR reflectance unlike stressed vegetation that result in low NIR reflectance. Collected data were grouped by observing the spectral seperability. To derive the representative spectral signatures a set of 20 samples were averaged and four different classes were noticed in the reflectance pattern, i) below 3, ii) 3-7, iii) 8-15 and iv) above 15 years' age. Figure 3.8 shows the different age group Arecanut crops and spectroradiometer setup.



Figure 3.8 Field data collection, i. Six months' crop, ii. Below 3 years' crop, iii. Above 5 years' crop iv. 15 to 20 years' crop. v&vi. Above 25 years' crop. viii. Spectroradiometer setup.

3.4.2.1 Spectral library

Spectral library includes collections of spectral reflectance curves obtained from field or laboratory spectroradiometer measurements. It is possible to differentiate among materials by their spectral reflectance signatures, whereas direct identification is usually not possible. Many researchers have measured the spectral reflectance of hundreds of materials in the lab, and have compiled a spectral library. The libraries are used as references for material identification in remote sensing images. From UV to mid-infrared 0.2-150-micrometer region contains over 1300 spectra including mid-infrared data as well as spectra from and additional visible and near-infrared spectra are some of the examples. The library includes many more minerals, organic and volatile compounds, vegetation, and man-made materials. But from the analysis it was found that there is no spectral library for Arecanut plantation crop.

In this study, age-based Arecanut crop and disease versus healthy Arecanut crop spectral library were built using different age group Arecanut plantation spectra and representative stressed spectra collected during field visit and it is used for the respective classifications.

3.4.2 Temperature data

Temperature data of the study area was collected from Climate Forecast System Reanalysis (CFSR) to calculate potential evapotranspiration (ET_0) of the day for calculating Arecanut age wise crop water requirement.

3.4.3 GPS data

Extensive field survey was carried out using GPS device to collect spatial data of Arecanut fields. Arecanut field of different age groups and crown choke affected fields were captured in the device as polygon shape files. Later differential correction was applied onto these shape files with 95% confidence level. Trimble Juno series GPS with 1m accuracy was used to collect field data of Arecanut plantations with respect to their age and health in the form of spatial polygons. About 180 farms were considered in GPS survey to generate vector layer of typical farms of various Arecanut crop age groups. These vector layer aids for the supervised classification using training site. Figure 3.9 shows the GPS vector layer of different age group Arecanut crops from the field visit.

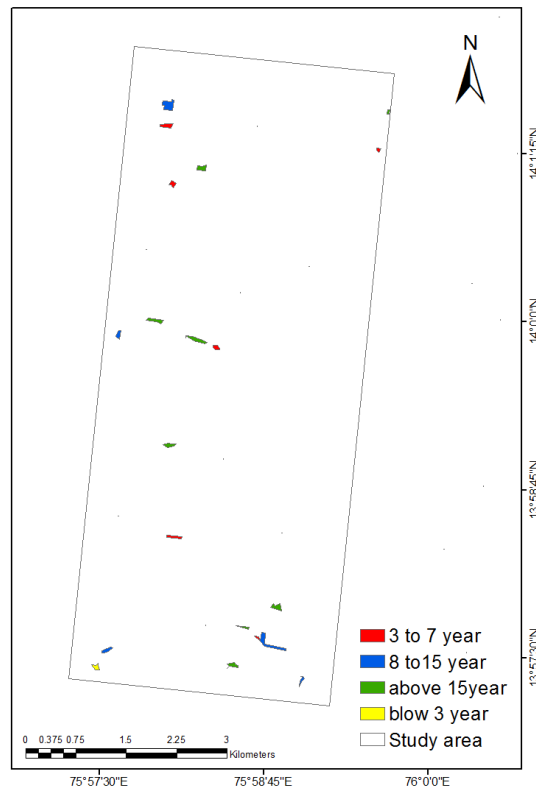


Figure 3.9 GPS vector layers

Ground truth information collected from the field visit is divided into four different age-wise classes along with one stressed and an additional class with mixed crops. The mixed crop class includes all plots where areca palm is grown along with other crops like banana, teak wood etc.

3.4.4 Soil and Water Samples Data

To identify the cause of diseases which spread across the farm, soil and water samples were collected randomly from the disease affected farm fields and samples were collected from healthy farm fields. Also soon after the collection, samples were tested for different laboratory analysis using standard testing procedures.

3.4.5 HyperionSatellite Data

Hyperion is the hyperspectral image spectroscope aboard Earth Observing 1 (EO-1): an earth orbiting satellite by National Aeronautics and Space Administration NASA launched on November 21, 2000. EO-1 satellite is the first hyperspectral imaging instrument deployed on a satellite platform. The push broom type EO-1 satellite has

three imaging sensors: Hyperion sensor, The LEISA (Linear Etalon Imaging Spectral Array) Atmospheric Corrector (LAC), and the multispectral Advanced Land Imager (ALI). Hyperion image has the dimensions of 256 x 6925 x 242 which is a high-spectral resolution imager which captures 242 spectral bands (from 400 nm to 2500 nm with 10 nm sampling interval) covers visible-near infrared (VNIR) to short-wave infrared (SWIR) regions, with a 30m spatial resolution. The instrument images a 7.5 km by 100 km land area per image. The EO-1 satellite has an orbital distance of 705 km, 98.7° inclination, and sun-synchronous orbit (Dutt and Jupp, 2004). To accomplish the present work, primarily remotely sensed satellite imagery is obtained from USGS website on request(<http://earthexplorer.usgs.gov/>) dated 21st January 2014.

3.4.5.1 Hyperspectral Image Pre-Processing and Image Classification

Hyperspectral image processing involves a series of techniques to obtain required information from satellite data. It includes dimensionality reduction and enhancement of signal to noise ratio.

Based on the review of literature on widely accepted and reliable methods for hyperspectral data processing was adopted for image processing and classification.

Hyperion scene consisted of 242 bands. First the image was converted into absolute radiance and initial bad bands were removed.

- Radiometric correction was performed to remove atmospheric attenuation.
- Registration of the image was carried out using another geo-referenced image (RMS error was less than 0.5 pixels).
- Minimum Noise Fraction (MNF) transformation was executed to determine the inherent dimensionality of image data, to segregate noise in the data and to reduce computational requirements for subsequent processing.
- Inverse MNF transformation was performed to include only the good bands.

3.4.6 Radiometric Correction

Radiometric correction refers to modification of reflectance values of every pixel in the image data to eliminate effects of atmosphere on the reflected radiation and also to incorporate sensor gain and offset to obtain and platform attenuations to get hold of surface reflectance. Therefore, atmospheric correction is very essential for quantitative analysis of surface reflectance. Such data of a hyperspectral image can be used to detect the presence of targets by means of a reference spectral library. Efficiency of atmospheric correction tools depends on number of atmospheric parameters while calculating surface reflectance.

The Fast Line-of-sight Atmosphere Analysis of Spectral Hypercube (FLAASH) method is a physics-based approach for atmospheric correction that utilizes various metadata with reference to time, location, and many other parameters to generate a radiative transfer model incorporating Moderate resolution atmospheric TRANsmision4(MODTRAN4).It can correct images collected both in nadir and off nadir geometries. FLAASH produces accurate surface reflectance results which in turn results in accurate classification. Table 3.1 shows the important parameters used for radiometric correction using FLAASH.

Equation for spectral radiance at a sensor pixel L that applies to the solar wavelength range is,

$$L = \left(\frac{A*r}{1-S*r_e} \right) + \left(\frac{B*r_e}{1-S*r_e} \right) + L_a \quad (3.1)$$

Where,

r is the pixel surface reflectance.

r_e is an average surface reflectance for the pixel and a surrounding region.

S is the spherical albedo of the atmosphere.

L_a is the radiance back scattered by the atmosphere.

A and B are coefficients that depend on atmospheric and geometric conditions

The values of A, B, S and L_a are determined from MODTRAN4 calculations that use the viewing ,solar angles and the mean surface elevation of the measurement, they assume certain model atmosphere, aerosol type, and visible range.

Table 3.1 Important parameters used for radiometric correction using FLAASH

Parameter	Value	Parameter	Value
Sensor Altitude (km):	705	Ground Elevation (km):	0.66
Pixel size (m):	30	Flight Date:	21 st Jan 2104
Number of bands:	242	Water Absorption Feature:	1390 nm
Atmospheric Model:	MODTRAN-4	Aerosol Retrieval:	Rural
Aerosol Model:	2K-T	Initial Visibility (km):	40

3.4.7 Spectral Resize

Spectral resizing is a procedure for removing bands with no data and known unstable band. Spectral subset of radiometrically corrected image was performed to exclude bad bands. 145 Stable bands (10-57, 83-97, 101-119, 134-164, 183-184, and 188-220) were retained after spectral resizing for further processing. This is carried out to exclude water absorption bands mainly in the region between 1336 nm and 1488 nm, 1790 nm and 1972 nm. Major advantages of resizing are to improve classification accuracy and to reduce processing time.

3.4.8 Geometric Correction

The images acquired by Earth observation systems cannot be transferred to maps because, they are geometrically distorted. These distortions are due to errors in the satellite's positioning on its orbit, the fact that the Earth is rotating on its axis as the image is being recorded, the effects of relief, etc. They are amplified even more by the fact that some satellites take oblique images. Geometric correction is necessary to pre-process remotely sensed data and to remove geometric distortion so that individual picture elements (pixels) are in their proper planimetric (x, y) map locations.

This facilitates remote sensing-derived information to relate it to other thematic information in GIS. Geometrically corrected imagery can be used to extract accurate distance, polygon area, and direction (bearing) information. Internal geometric errors are introduced by the remote sensing system itself or in combination with Earth rotation or curvature characteristics.

These distortions are often systematic (predictable), may be identified and corrected using pre-launch or in-flight platform ephemeris (i.e., information about the geometric characteristics of sensor and the Earth at data acquisition).

Image geometric correction was carried out by image to image registration using another georeferenced (LIT) image, which is called image-to-image registration. Image-to-image registration is the matching of one image to another so the same geographic area is positioned coincident with respect to the other. This type of geometric correction is used when it is not necessary to have each pixel assigned a unique x, y coordinate in a map projection. Nearest Neighbor interpolation was adopted to accurately retain pixel properties. This yielded an image with proper orientation and each pixel was tagged with its geographic position in UTM projection and WGS84 as datum. Image registration was performed with a RMSE of 0.43 pixels, which is equivalent to 12.9 m. Later the image was subset using vector shapefile of the chosen study area for further processing.

3.4.9 Minimum Noise Fraction Transformation

Minimum Noise Fraction (MNF) transformation is essentially used to find the inherent dimensionality of data, to segregate noise in it, and to increase the computational efficiency of subsequent processes. Objective of MNF is to select components so that Signal to Noise Ratio (SNR) is maximized. This transformation is a modified Principal Component Analysis originally proposed by Green et al., (1988) and implemented in image processing. MNF transform is essentially a noise adjusted two cascaded PC transformations which estimates and equalizes the amount of noise in each image band. The first PC transformation de-correlates and rescales the noise in the data. Here the noise statistics are calculated based on a shift difference method. This first step results in transformed data in which the noise has unit variance and no band-to-band correlations.

The second step is another PC transformation of the noise-whitened data. For the purposes of further spectral processing, the dimensionality reduction of the data is carried out by examination of the final Eigen values and the image bands.

In order to improve the results of data processing, only the coherent bands (i.e., the bands with higher Eigen values) are selected by eliminating redundant band.

As stated earlier, MNF minimizes the noise Fraction (NF) or equivalently maximizes the signal-to-noise ratio (SNR) of linear combinations, $a^T x(r)$, of zeroth-mean original (spatial) variables $x(r)$. Here the total $x(r)$ is written as a sum of a signal part, $x_S(r)$, and a noise part, $x_N(r)$.

$$x(r) = x_S(r) + x_N(r) \quad (3.2)$$

Since these two parts are considered to be uncorrelated, the variance-covariance matrix S of x may be written as a sum of the signal and noise dispersions.

$$S = S_N + S_S \quad (3.3)$$

The noise fraction NF is here defined as the ratio of the variance of the noise and the variance of the total, so for a linear combination $a^T x(r)$ of zeroth-mean $x(r)$ we get,

$$NF = \frac{a^T S_N a}{a^T S a} \quad (3.4)$$

The signal to noise ratio, which is defined as the ratio of the variance of the signal and the variance of the noise, is expressed in the equations 3.5 and 3.6.

$$SNR = \frac{a^T S_S a}{a^T S a} \quad (3.5)$$

i.e., $SNR = \frac{1}{NF} - 1 \quad (3.6)$

In this work, 14 bands up to eigenvalue of 1.523 (88.03%) were selected in VNIR range in MNF transformation followed by inverse MNF transformation to obtain back all 44 VNIR bands ranging from 460nm to 910nm.

3.4.10 Spectral sub set

To match the spectral bandwidth of spectroradiometer and Hyperion data, Hyperion imagery was spectrally subset and spectroradiometer data was resampled to match that of Hyperion image. Hyperion imagery was geometrically corrected to overly GPS data. Extracted endmembers from pure pixel (PPI) were matched with field spectra collected from spectroradiometer. Figure 3.10 shows the spectral signature of a particular Arecanut crop from field visit. And Figure 3.11 shows the corresponding spectra extracted from Hyperion image pixel, from the figure it is observed that coefficient of determination (R^2) 0.95 and it is a good fit. Figure 3.12a&b shows the scatter plot between image spectra corresponds to field spectra.

This infers that there is a close similarity between endmember spectra extracted from image with the field spectra.

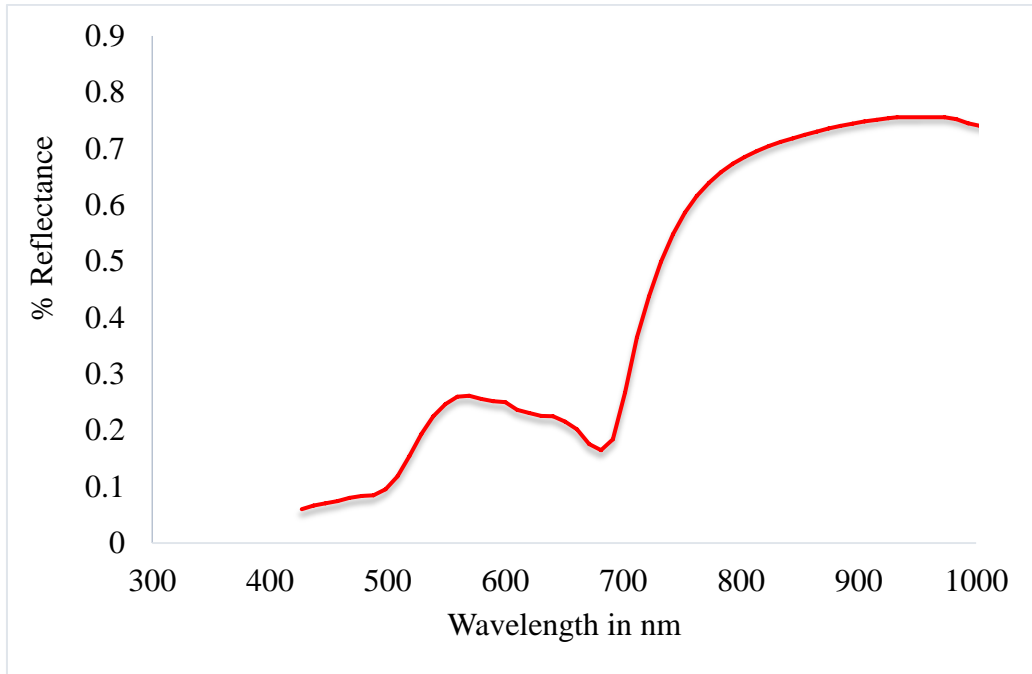


Figure 3.10 Sample field spectra obtained from Spectroradiometer

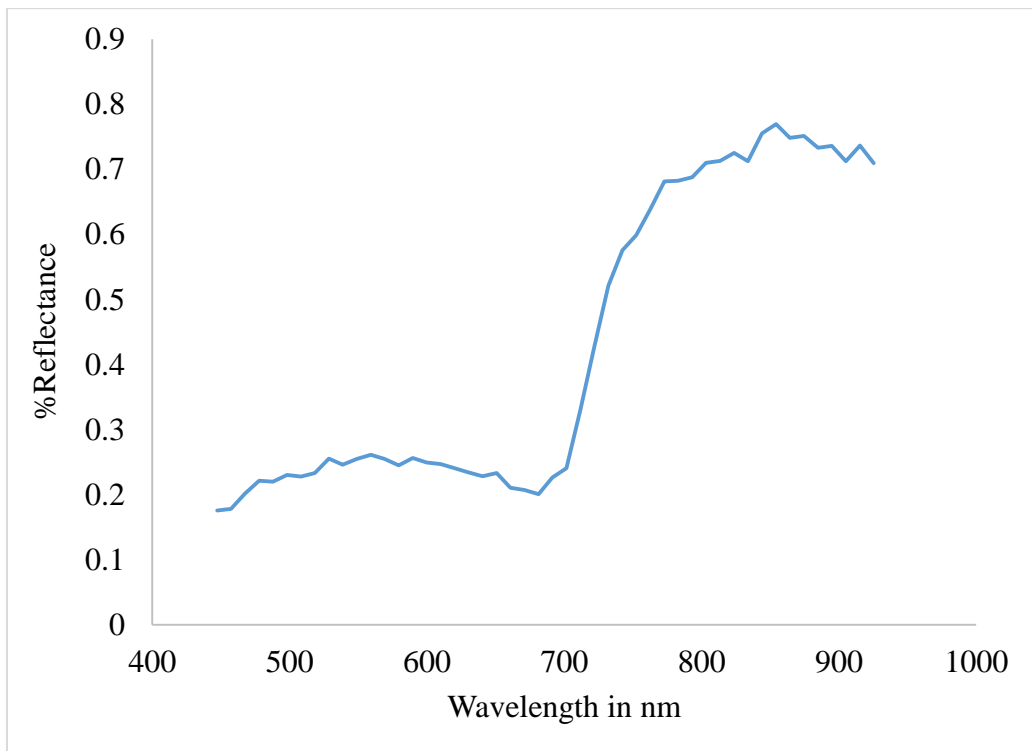


Fig. 3.11 Extracted endmember from Hyperion image

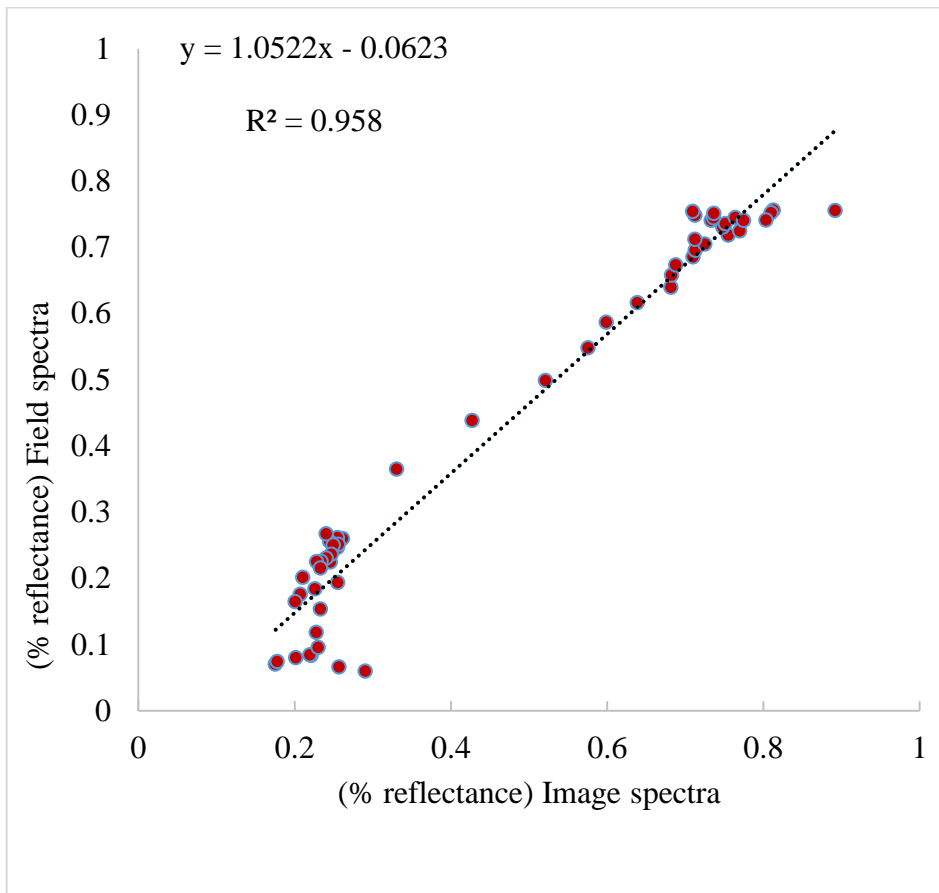


Figure 3.12 (a) Scatter plot between image spectra corresponds to field spectra

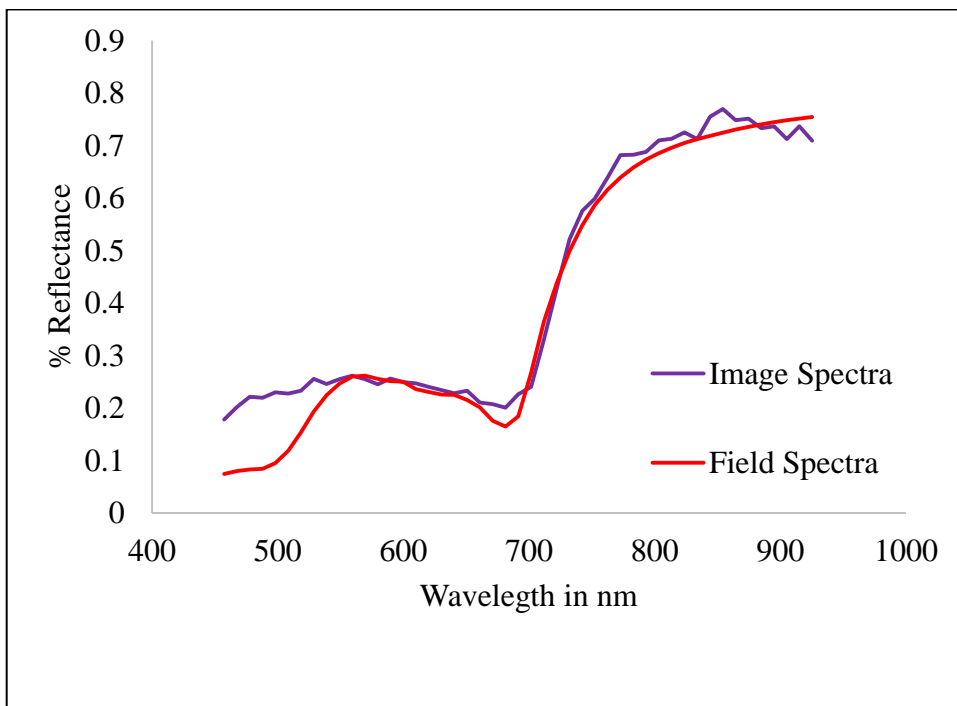


Fig. 3.12 (b) Spectral matching

3.5 Application Software

Environment for Visualizing Images (ENVI 5[®]), Erdas Imagine and ArcGIS software packages were used for image processing procedures and generating thematic maps. MATLAB[®] and Microsoft Excel[®] were used for data analysis and calculations.

ENVI and Erdas Imagine are geospatial raster data processing tools which allow users to process and display satellite images for mapping use in geographic information system (GIS). ENVI[®] is used for hyperspectral image processing, whereas Erdasimagine for modelling multiband images, band math operations and post-processing procedures. ArcGIS[®] was essentially used for generating thematic maps.

3.6 Image Classification

Various classification methods are available for classifying hyperspectral imagery. From the review of literature, most popular supervised classification methods found are Spectral Angle Mapper classifier (SAM), Support Vector Machine classifier (SVM) and Minimum Distance classifier. These supervised classification methods were compared in this study to find the most suitable classifier and to map arecanutcrop within class (age wise) seperability.

3.6.1 Spectral Angle Mapper (SAM) Classification

Classification was aided using spectral angle mapper (SAM) algorithm with reflectance signatures from spectroradiometer. SAM is a spectral classification that uses an n-dimensional angle to match pixels to reference spectra. As depicted in Figure 3.13, the algorithm determines the spectral similarity between two spectra by calculating the angle between the spectra, treating them as vectors in a space with dimensionality equal to number of bands. This technique, when used on calibrated reflectance data, is relatively insensitive to illumination and albedo effects.

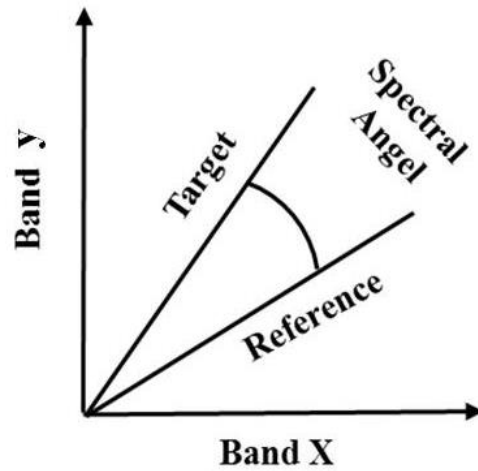


Figure 3.13 Principle of Spectral Angle Mapper Classifier

End member spectra used by SAM either it may be from (American Standard Code for Information Interchange)ASCII files, spectral libraries, or can be extracted directly from the image. SAM compares the angle between end member spectrum vector and each pixel vector in n-dimensional space. Smaller angles represent closer matches to the reference spectrum. Pixels further away than the specified maximum angle threshold in radians are not classified.

$$\text{Spectral Angle, } a = \cos^{-1} \left(\frac{\sum_{i=1}^{nb} t_i * r_i}{\sqrt{\sum_{i=1}^{nb} t_i^2 * \sum_{i=1}^{nb} r_i^2}} \right) \quad (3.7)$$

Where, t = target spectra and r= reference spectra

Classification accuracy assessment is a method to evaluate the performance of classification algorithm in transforming image to thematic map. This can be used to compare the accuracies of two classifiers.

In this work accuracy assessment was carried out using ERDAS® Imagine accuracy assessment tool based on error matrix analysis. Accuracy assessment involves the comparison of classified map and the reference test information. This information can be presented in an error matrix where columns represent the referenced data while rows represent the classified data.

Overall accuracy (OA) is the summed average accuracies of individual classes and is expressed as percentage (%). OA represents the probability that a randomly selected point is classified correctly on the map.

And the kappa coefficient (k) expresses the proportionate reduction in error generated by a classification process compared with error of completely random classification.

$$k = \frac{N \sum X_{ii} - \sum (X_{i+} * X_{+i})}{N^2 - \sum (X_{i+} * X_{+i})} \quad (3.8)$$

Where X_{ii} represent diagonal values of the matrix with classes as rows and columns, X_{i+} is the row pixel sum and X_{+i} is the column pixel sum. N is the Sum of pixels considered for accuracy assessment.

3.6.2 Support Vector Machine Classification

Support Vector Machine (SVM) is a supervised classification method derived from statistical learning theory that often yields good classification results from complex and noisy data. It separates the classes with a decision surface that maximizes the margin between the classes. The surface is often called the optimal hyperplane, and the data points closest to the hyperplane are called support vectors. The support vectors are the critical elements of the training set.

Support vector machine identifies a hyper- plane between two classes that produces optimal separation between the classes. To classify a data of N dimensions, (N – 1) dimensional hyper plane is developed. There are linear and non-linear kernels for support vector machine. When the training data are not linearly separable, non-linear kernels are used.

The mathematical representation of each kernel is listed below:

Linear $K(x_i, x_j) = x_i^T x_j$ (3.09)

Polynomial $K(x_i, x_j) = (g x_i^T x_j + r)^d, g > 0$ (3.10)

RBF $K(x_i, x_j) = \exp(-g \|x_i - x_j\|^2), g > 0$ (3.11)

Sigmoid $K(x_i, x_j) = \tanh(g x_i^T x_j + r)$ (3.12)

Where:

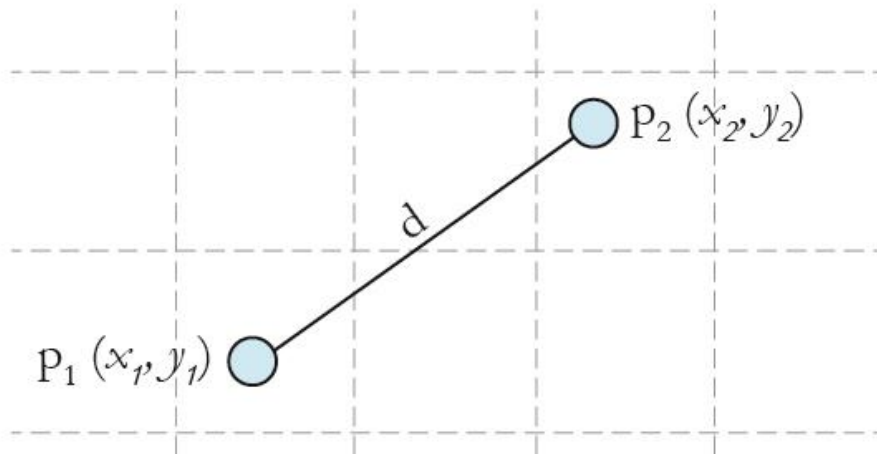
g is the gamma term in the kernel function for all kernel types except linear.

d is the polynomial degree term in the kernel function for the polynomial kernel.

r is the bias term in the kernel function for the polynomial and sigmoid kernels.

3.6.3 Minimum distance classification

Minimum distance classification, Minimum distance classifier uses the mean vectors of each reference spectra and calculates the Euclidean distance from each unknown pixel to the mean vector for each class



$$\text{Euclidean distance (d)} = \sqrt{(x_2 - x_1)^2 + (y_2 - y_1)^2} \dots\dots\dots(3.13)$$

3.7 Vegetation Indices

The Advantages of indices over classification are sets distinguish between soil and vegetation, by reducing atmospheric and topographic effects if possible. Indices can be customized for particular applications. Vegetation monitoring is usually accomplished by simple regression approach, using remote sensing data and by computing vegetation indices (VIs).

Several vegetation indices have been developed by linear combination or ratios of red, green and near-infrared spectral bands. Vegetation indices are more sensitive than individual bands to vegetation parameters (Baret and Guyot, 1991; Qi et al., 1993).

The mathematical transformation of spectral bands accentuates the spectral properties of green plants so that they appear distinct from other image features. This combination of two or more spectral bands results in the formation of vegetation indices. A vegetation index can be calculated by rationing, differencing, rationing differences and sums and by forming linear combinations of the spectral band data (Huete and Jackson, 1991).

3.7.1 Hyperspectral Vegetation Indices

Vegetation interacts with solar radiation in a different way than other natural materials. The vegetation spectrum typically absorbs in red and blue wavelengths, reflects in green wavelength, strongly reflects in near infrared (NIR) wavelength, and displays strong absorption features in wavelengths where atmospheric water is present. Different plant materials, water content, pigment, carbon content, nitrogen content, and other properties cause further variation across the spectrum. Measuring these variations and studying their relationship to one another can provide meaningful information about plant health, water content, environmental stress, and other important characteristics. These relationships are often described as vegetation indices (VIs).

Vegetation index can be calculated by rationing, differencing, and sums and by forming linear combinations of the spectral band data. The mathematical combination or transformation of spectral bands accentuates the spectral properties of green plants so that they appear distinct from other image features. This combination of two or more spectral bands results in the formation of vegetation indices. In this study different indices were attempted for monitoring arecanut crop, Disease index to identify the disease severity of arecanut plantations. To segregate Arecanut crops into different age group Age Index. And Crop water requirement index to estimate the age based arecanut crop water requirement.

3.8 Crop Water Requirement through NDVI based Crop Coefficient

Several methods are available for building indices depending upon the data availability and applications considered. This study utilizes NDVI based crop coefficient (K_c) method to estimate crop water requirement CWR due to lack of climatic data availability.

Image ratio based Normalized Difference Vegetation Index (NDVI) can be expressed mathematically as,

$$NDVI = \frac{NIR-RED}{NIR+RED} \quad (3.10)$$

The Normalized Difference Vegetation Index (NDVI) is a numerical indicator that uses the visible and near-infrared bands of electromagnetic spectrum, and is adopted to analyse remote sensing measurements and to assess whether the target being observed contains live green vegetation or not. Generally, healthy vegetation will absorb most of the visible light that falls on it, and reflects a large portion of the near-infrared light. Unhealthy or sparse vegetation reflects more visible light and less near-infrared light. Bare soils on the other hand reflect moderately in both the red and infrared portion of the electromagnetic spectrum. The NDVI value ranges between -1 and +1. However, no green leaves give a value close to zero and in general, pixels with value above 0.4 indicates vegetation. Higher values of NDVI indicate higher degree of photosynthetic activity or in other words healthy or dense vegetation.

Kamble et al. (2013) developed and validated equation to calculate K_c using NDVI based on regression analysis between NDVI derived from remotely sensed data and AmeriFlux measured crop coefficient under irrigated and rainfed crop condition for various crops. This equation can be used with Hargreaves and Samani equation considering computing crop water requirement. There was a strong linear correlation between the NDVI-estimated K_c and the measured K_c with an r^2 of 0.91 and 0.90, while the root-mean-square error (RMSE) for K_c were 0.16 and 0.19, respectively for two different years in which experiments were carried out. Crop coefficient K_c , was computed based on the equation:

$$K_c = 1.457NDVI - 0.1725 \quad (3.11)$$

Crop water requirement is the amount of water required to compensate the evapotranspiration loss from the cropped field, Allen et al. (1998). In other words, water requirement of a crop is equivalent to water loss due to soil evaporation and transpiration from plant canopy. But soil evaporation component is negligibly small as plant foliage shades the soil beneath, along with efficient drip irrigation system considering no irrigation loss. Hence crop water requirement (CWR in mm/day) can be expressed as,

$$\text{CWR} = \text{ET}_c = K_c * \text{ET}_o \quad (3.12)$$

Daily reference crop evapotranspiration (ET_o in mm/day) is computed based on equations presented by Hargreaves and Samani:

$$\text{ET}_o = 0.0135(KT) (R_a) (TD)^{1/2}/(TC+17.8) \quad (3.13)$$

Where TD is temperature difference between daily maximum and minimum temperature ($^{\circ}\text{C}$), TC is the daily mean temperature ($^{\circ}\text{C}$), R_a is extraterrestrial radiation ($\text{MJ m}^{-2} \text{d}^{-1}$) which is a function of latitude of location, inverse relative distance from earth to sun, solar declination etc calculated with reference to FAO 56, and KT is an empirical coefficient which depends on temperature difference.

$$KT = 0.00185(TD)^2 - 0.0433 TD + 0.4023 \quad (3.14)$$

These values were calculated separately (detailed calculations are presented in chapter 5) for the day on which Hyperion imagery was captured. Obtained value of ET_c in mm/day is converted to l/day/plant by considering standard uniform plant to plant spacing (8 ft or 2.4384 m either way i.e. 151 plants in a pixel of 30m X 30m size) in the study area with drip irrigation practiced throughout.

3.9 Arecanut Crop Water Requirement Index (ACWRI)

A vegetation index (also called a vegetative index) is a single number that quantifies vegetation biomass and/or plant vigor for each pixel in a remote sensing image. The index is computed using several spectral bands that are sensitive to plant biomass and vigor. In the present work, using correlation analysis on Arecanut canopy reflectance and corresponding value of crop water requirement, an index was built. Canopy reflectance data is obtained from Hyperion imagery with respect to corresponding

crop water requirement from the map. Values of the index indicate the magnitude of crop water requirement index in a pixel with Arecanut crops. This will be helpful for spatial comparison of crop water requirement in a rapid manner, even without spectral library of the crop.

Correlation and regression are two methods used to investigate the relationship between variables. The main difference between correlation and regression is that, correlation measures the degree to which the two variables are related, whereas regression is a method for describing the relationship between two variables. In this study the correlation and regression analysis were used to identify the important wavebands for Arecanut crop monitoring.

3.10 Correlation Analysis

Correlation analysis is a technique for investigating the relationship between two quantitative, continuous variables. Pearson's correlation coefficient (r) is a measure of strength of the association between two variables.

$$\rho_{XY} = \text{Corr}(X, Y) = \frac{\text{Cov}(X, Y)}{\sigma_X \sigma_Y} = \frac{E[(X - \mu_X)(Y - \mu_Y)]}{\sigma_X \sigma_Y} \quad (3.15)$$

Where E is the expected value operator, cov means covariance, and corr is a widely used alternative notation for the correlation coefficient.

In the present work correlation analysis is helpful in identifying specific wavelengths in electromagnetic spectrum having association with water requirement of Arecanut plants.

3.11 Stepwise Multi Linear Regression (SMLR)

Stepwise regression is a systematic method for adding and removing terms from a multi linear model based on their statistical significance in a regression. The method begins with an initial model and then compares the explanatory power of incrementally larger and smaller models. If a term is not currently in the model, the null hypothesis is that the term would have a zero coefficient if added to the model. If there is sufficient evidence to reject the null hypothesis, the term is added to the model. Conversely, if a term is currently in the model, the null hypothesis is that the term has a zero coefficient. If there is insufficient evidence to reject the null

hypothesis, the term is removed from the model. Depending on the terms included in the initial model and the order in which terms are moved in and out, the method may build different models from the same set of potential terms. The method terminates when no single step improves the model. There is no guarantee; however, different initial model or a different sequence of steps will not lead to a better fit. (Draper and Smith 1998).

This study has employed Stepwise Multi Linear Regression to prepare a thematic map Of age wise Arecanut crop water requirement of the study area. This was executed in MATLAB®.

3.12 Partial Least Square Regression (PLSR)

PLS is a bilinear calibration method using data compression by reducing the large number of measured collinear spectral variables to a few non-correlated principal components (PCs). The PCs represents the relevant structural information, which is present in the reflectance measurements to predict the dependent variable (Hansen and Schjoerring 2003)

PLS regression uses component projection successively to find latent structures. Visual inspection of score-plots and validation residual variance plots were used to find the optimal number of PCs, so that over-fitting was prevented. In most cases, this procedure can reduce the number of spectral variables to a few independent PCs. The final model predicting \hat{y}_i had the following form (Eq. 3.15):

$$\hat{y}_i = b_0 + b_1 t_{1i} + b_2 t_{2i} + \dots + b_n t_{ni} \dots \dots \dots (3.15)$$

Where t_{1i} to t_{ni} are the scores from principal component (PC) 1 to n for variable i. The scores were calculated on the basis of mean-centered data. By linear regression of t versus y in the calibration iteration process, the regression coefficient b_n was obtained. Due to the initial centering of y, the centered mean b_0 was added in order to obtain y_i . Validation of the models was performed by comparing differences in R^2 and root mean square error (RMSE).

RMSE values were calculated according to Eq. (3.16):

$$RMSE = \sqrt{\frac{\sum_{i=1}^n (\hat{y}_i - y_i)^2}{n}} \dots \dots \dots (3.16)$$

Where \hat{y}_i and y_i were the predicted and measured crop variables, respectively, and n the number of samples ($n = 360$). RMSE provides a direct estimate of the modelling Error expressed in original measurement units (Kvalheim, 1987).

The flexibility of the PLS-approach, its graphical orientation and its inherent ability to handle incomplete and noisy data with many variables (and observations) makes PLS a simple but powerful approach for the analysis of data of complicated problems (Wold et al., 2001).

It can also be extended in various directions as PLSR provides an approach to the quantitative modelling of often complicated relationships between predictors (X) and response (Y) with complex problems seldom more realistic than multiple linear regressions (MLR) including stepwise selection variants.

Hence it is found to be appropriate to determine combination of wavelengths to build a model to assess Arecanut crop water demand.

Partial Least Squares (PLS) regression is a multivariate analysis technique used in cases where there are a large number of independent variables or predictors and these independent variables are highly collinear (Wold et al. 2001). The PLS method reduces the entire reflectance spectra to a small number of relevant factors and regresses them to the dependent variable (Gomez et al. 2008).

A number of variants of PLS exist for estimating the factor and loading matrices for modelling. The most common of these are Non-linear Iterative Partial Least Squares (NIPALS) and Statistically Inspired Modification of PLS (SIMPLS) algorithms. This study employed Partial Least Squares regression for modelling the Arecanut crop water requirement from the Hyperion reflectance spectra. The regression was performed in MATLAB®.

Hence it is found to be appropriate to determine combination of wavelengths to build a model to assess Arecanut crop water demand. In the present study X and Y inputs for the PLSR model are obtained crop water requirement values and corresponding spectral signatures from Arecanut crop water requirement map and pre-processed Hyperion imagery pixels respectively.

3.13 Identification of significant wavelengths

The spectral response of functional groups or molecules is often dispersed over several adjacent wavelengths, leading to strong collinearity in some regions of the spectra, while other regions may be corrupted by noise, or in general, may contain irrelevant information (Gosselin et al. 2010). Hence it is necessary that the wavelengths that are relevant for modelling a particular property be identified. This can be carried out either through projection methods, variable selection or a combination of both.

3.13.1 VIP scores and β coefficients

The optionally modified output from the PLSR algorithm can be employed to purely identify a subset of important variables. The Variable Importance in PLS projections (VIP) is such a measure to accumulate the importance of each variable j being reflected by w from each component. The VIP measure v_j is computed as in equation

$$V_j = \sqrt{P \sum_{a=1}^A [(q_a^2 t_a' t_a (w_{aj} / \|w_a\|)^2] / \sum_{a=1}^A (q_a^2 t_a' t_a)} \dots\dots\dots(3.17)$$

Where $(w_{aj} / \|w_a\|)^2$ represents the importance of the j^{th} variable and the variance explained by each component is given by the expression $q_a^2 t_a' t_a$. The v_j weights are a measure of the contribution of each variable according to the variance explained by each PLS component (Mehmood et al. 2012). Variable j can be eliminated if $v_j < u$, for some user-defined threshold $u \in (0, \infty)$. It is generally accepted that a variable should be selected if $v_j > 1$.

Another Variable selection method is to use the vector of regression coefficients (β) which is a single measure of association between each variable and the response. Even in this case, variables having small absolute value of regression coefficients can be eliminated (Mehmood et al. 2012).

The wavelengths that are significant for modelling the crop water requirement from the Hyperion reflectance spectra using PLS regression were identified by setting thresholds for both Variable Importance for Projection (VIP) and the PLS regression coefficients, β . This was implemented in MATLAB[®].

In the following chapter the classification of stressed Arecanut crops from Hyperion/field reflectance data is presented. Also the cause for a particular disorder called crown choke is discussed.

HYPERSPECTRAL DATA: A TOOL FOR MONITORING STRESSED ARECANUT CROPS

4.1 Introduction

There are about 20 locally known diseases which cause various degrees of damage to the Arecanut palm. Among these; Fruit rot, (Koleroga), bud rot, crown rot, Yellow leaf disease, band disease, foot rot (Anaberoga), Inflorescence die back, bacterial leaf stripe and nut splitting cause significant decrease in yield (Sheshagiri et al, 2010). The assessment of diseases in Arecanut plants is necessary, as it results in yield, quality and economic loss. Identifying the diseased crops at its initial stage helps to take proper monitory decisions. These diseases are generally affected in patches of farms.

The first objective of this study is to investigating the feasibility of hyperspectral data for mapping (Classification), stressed Arecanut crops. And to find out the cause for crown choke disease in Arecanut crops.

From the field visit it was observed that, several acres of Arecanut plots were affected by crown choke disease. Crown choke (also known as band disease) is a disorder rather than a disease, which occurs during some stage of development of the palm. The symptoms of the disorder are exhibited on the leaves as well as on the stem near the crown. The leaves become shorter than normal size and are distinctly dark green in colour. The leaflets are characteristically brittle and crinkled with wavy margin. As it progresses, the other symptoms like reduction in intermodal length, tapering of the stem (Patel and Rao, 1958) and failure of production of inflorescence of normal size are expressed by the palm. Figure.4.1b shows the crown choke affected Arecanut palm and Figure 4.1 a shows the healthy Arecanut palm. Sometimes inflorescences produced are small and malformed. In the acute stage, as a result of failure of natural opening of the leaves, which remain tightly binding the top portion of the stem and the crown exhibit rosette shape. This condition prevents the normal growth of the bud.

Sometimes multiple shoots are developed or the newly formed shoots may emerge through the sides of the tightly folded lower leaves (Joshi and Joshi, 1949). Roots are also poorly developed, brittle and crinkled. But in ideal case studies have shown that, under well drained deep soil conditions, healthy Arecanut roots traverse down to about three meters and the roots confine to only about 1.40 meters under shallow soil condition (Shama Bhat and Leela, 1969; Bhat, 1978).

In this study, the area under investigation is adversely affected by crown choke disorder.

From the field visit it was observed that, large quantity of tank silt is being applied to areca plantations haphazardly by the growers. The practice has temporarily increased the Arecanut yields but on long run it has led to soil compaction, hardening, poor root aeration, rotting and disorders like crown choke.

Figure 4.1 shows the typical crown choke affected and healthy Arecanut plant. The present study makes an attempt to use EO-1 Hyperion imagery to classify the crown choke disease affected area with healthy Arecanut plantations. To identify the cause for crown choke disease, grid wise soil and water samples were collected from the disease affected plots and subjected for physicochemical analysis.



Figure 4.1 (a)Healthy and (b)Crown choke disease affected Arecanut plant

Methodology followed for classification of health status of the crop is shown in Fig. 4.2.

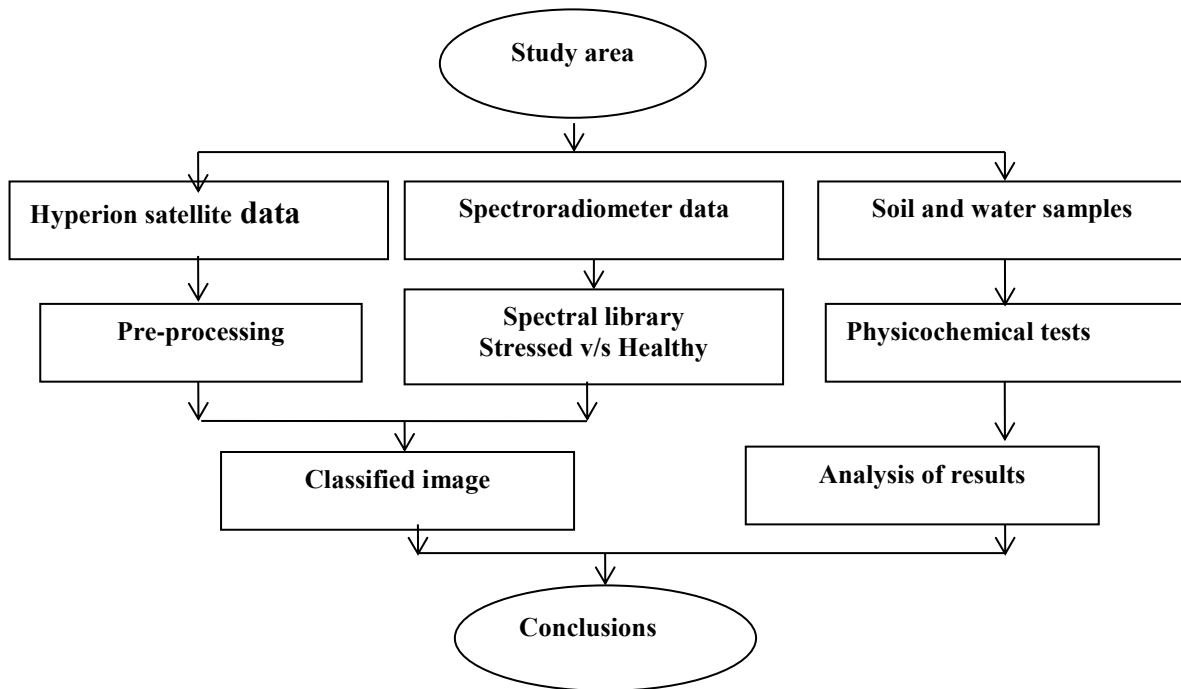


Figure 4.2 Methodology for classifying the diseased vs healthy Arecanut crop

4.2 Spectral library of healthy Vs diseased Arecanut crops

Signatures collected from the field, facilitates construction of spectral library (reference spectra). This includes stressed crop (crown choke disorder crop) and healthy crops of 2, 4 and 20 years Arecanut crops. It serves as the endmember for Spectral Angle Mapper (SAM) classification. Figure 4.3 shows the endmember collection spectra used for SAM classification. Stressed crop shows less reflectance than the different age groups of healthy crops. At near infrared region reflectance is drastically reduced for diseased Arecanut crop but for healthy the reflectance is very high. This particular region is helpful for discrimination of healthy Vs stressed Arecanut crop. In this study the stressed crop represents the crown choke disorder. Figure 4.4 shows the SAM classified map for healthy vs stressed Arecanut crops with spectral angle 0.2 radian.

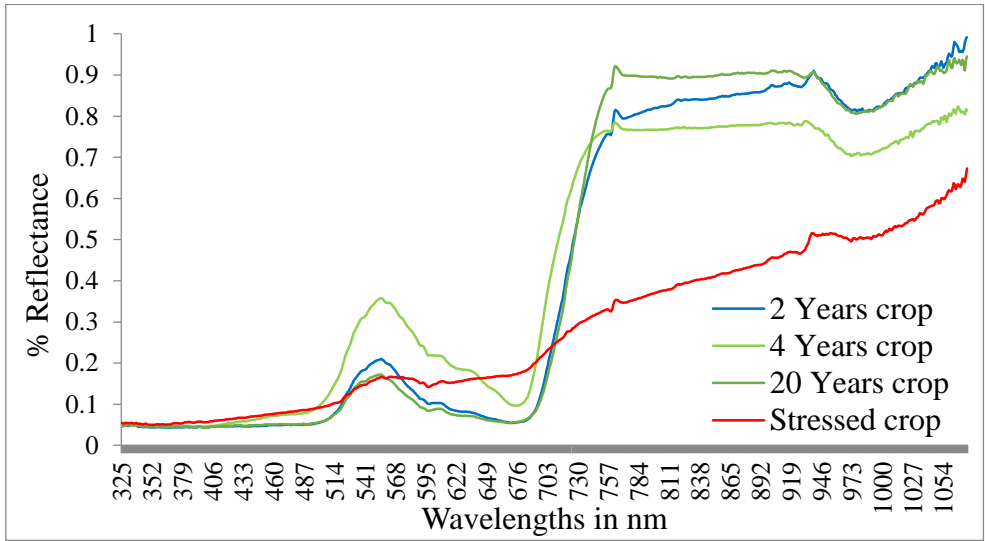


Figure 4.3 Spectral library plots of healthy Vs Stressed Arecanut crops

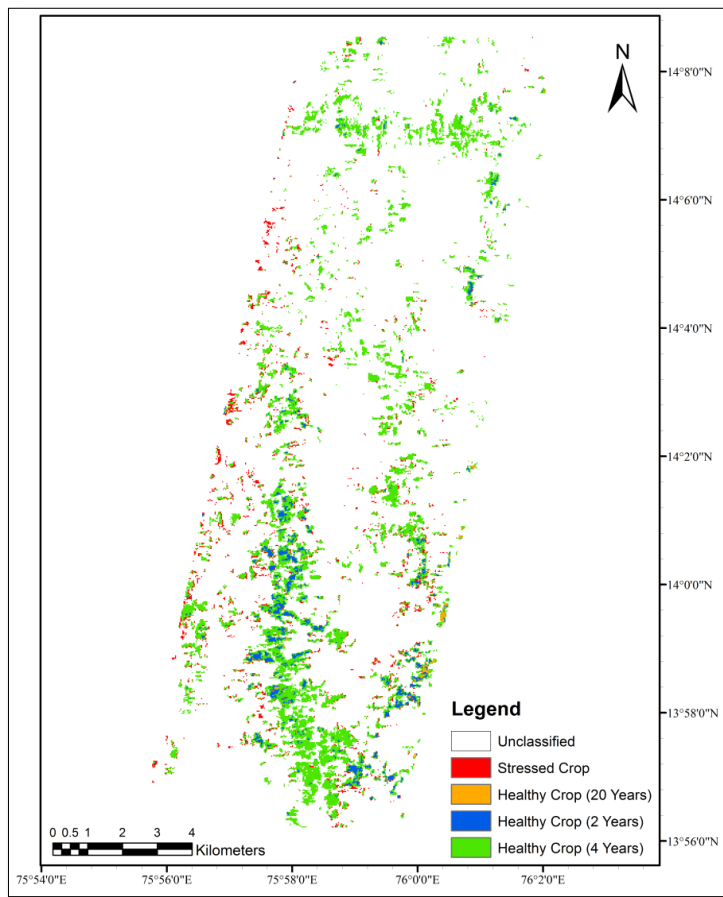


Figure 4.4 SAM classified image with spectral angle 0.2 radiance

Classification accuracy assessment is necessary for comparing the performance of various classification techniques (Congalton and Green, 1998). Classification accuracy assessment is recognized as a critical component of any mapping project. Table 4.1 shows the confusion matrix of SAM classification.

Table 4.1: Confusion matrix of SAM classification

ACCURACY TOTALS						
Class	Reference	Classified	Number	Producers	Users	Class
Name	Totals	Totals	Correct	Accuracy	Accuracy	Kappa
Stressed Crop	7	10	7	100.00%	70.00%	0.63
Healthy Crop (20 Years)	8	10	7	87.50%	70.00%	0.62
Healthy Crop (2 Years)	10	10	8	80.00%	80.00%	0.73
Healthy Crop (4 Years)	11	10	9	81.82%	90.00%	0.86
Totals	40	40	31			
Overall Classification Accuracy = 77.50%						
Overall Kappa Statistics = 0.7						

Overall classification accuracy observed is 77.5% of healthy and stressed Arecanut crops. Usually in remote sensing 80-85% classification accuracy is known as good and in this case, it is within class classification hence it is acceptable. Kappa coefficient is nearer to 1 as Kappa is always less than or equal to 1 and a value of 1 implies perfect agreement and values less than 1 imply less than perfect agreement. From the classified image it can be observed that more than 10 % of the total areas are affected by crown choke disease. To identify the cause for this particular type of disorder soil and water samples were collected from the study area and analysed in laboratory.

4.3 Physicochemical analyses

Characterization of surface soil (0-20 cm) for fertility status was studied by taking twenty representative samples from typical Arecanut gardens. The collected soil samples were air dried under shade. Standard laboratory procedures as per relevant IS codes were adopted for the analysis of nutrients.

Particle size analysis by soil hydro meter method, pH, electrical conductivity by conductometric method, organic carbon by Walkely and Black's wet oxidation method, nitrogen estimation by Kjehl Tech method, phosphorus by Spectro photometry, potassium and sodium by flame photometry, exchangeable calcium and magnesium by Versenate titration and available sulphur by Turbidometry. Available Fe, Mn, Zn and Cu by absorption spectrophometry method. As observed from the analysis, majority of the soil samples were alkaline in nature. The electrical conductivity was found to be critical for half of the soil samples and the average organic carbon content was found be high. Figure 4.5 shows the actual location map of the soil and water sample points.

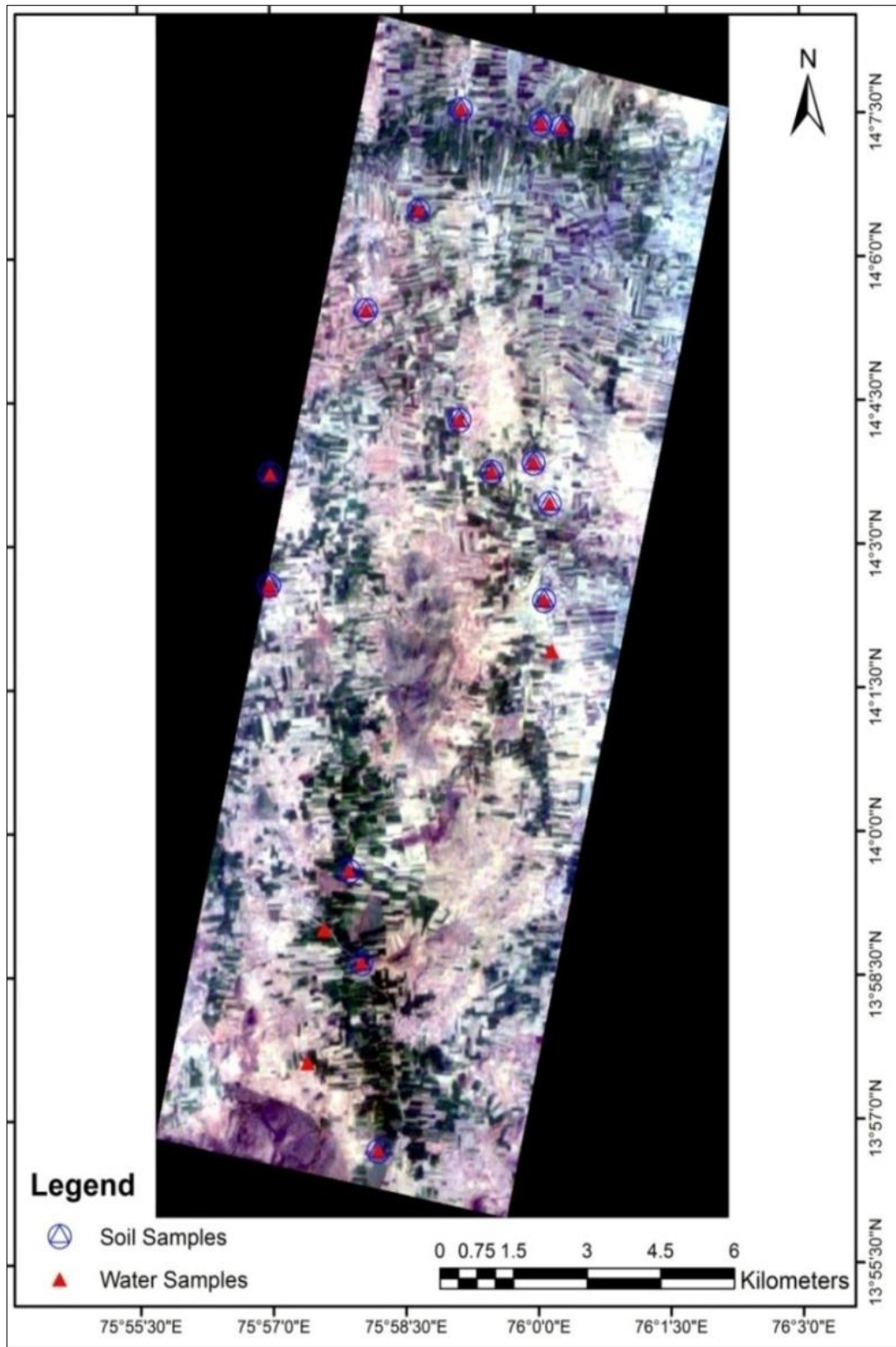


Figure 4.5 Soil and water sampling locations on the Hyperion image



Figure 4.6 Soil sampling



Figure 4.7 Soil and Water Samples

Figure 4.6 shows the collection of soil samples from the field, top soil was collected by digging a 20 cm pit and trimming side wall to ensure that sample must contains all the layers. Each collected soil sample consist the average of five samples collected from a radius of 5 meters. Figure 4.7 shows the packed soil and water samples for the laboratory analysis.

The measured soil pH showed in the Figure 4.8, is ranges in between 7.4 to 8.5. Most of the samples were alkaline in nature and one is acidic, two samples showed neutral.

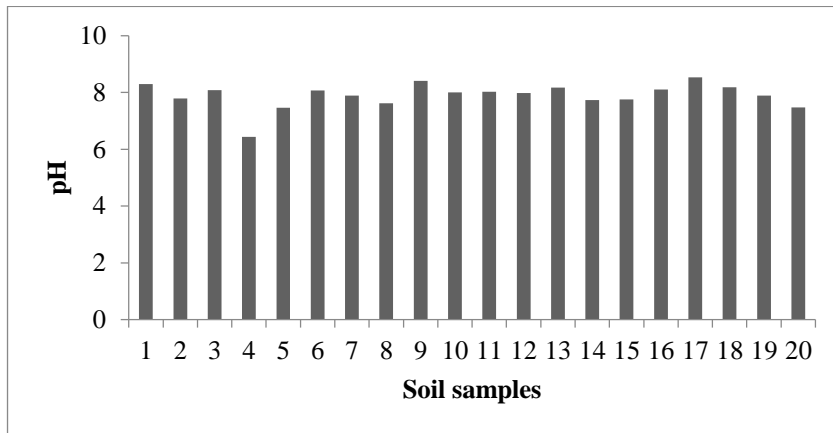


Figure 4.8 Spatial variation of Soil pH

The measured soil electrical conductivity showed in Figure 4.9 is varying in the range of 0.4 to 1.6. Only 9 samples were measured under safer limit, around 10 samples in critical range and one sample under unsafe.

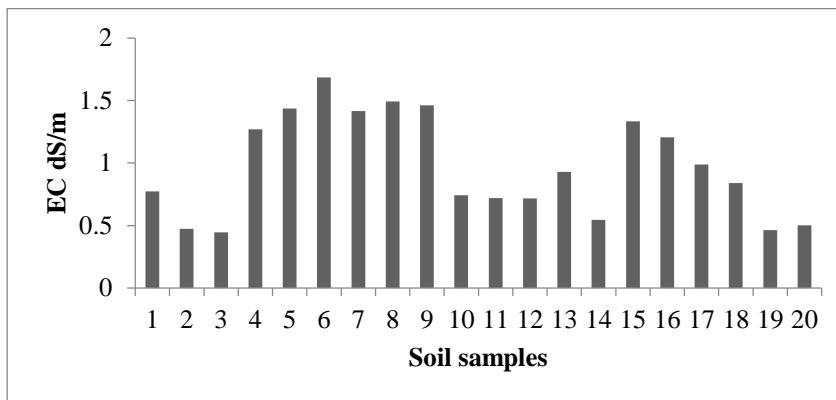


Figure 4.9 Spatial variation of Soil electrical conductivity

The measured soil organic carbon is shown in Figure 4.10 and it ranges from 0.4 to 1. And it was found to be low for 3 samples and within a permissible limit for 5 and rich for 12 samples.

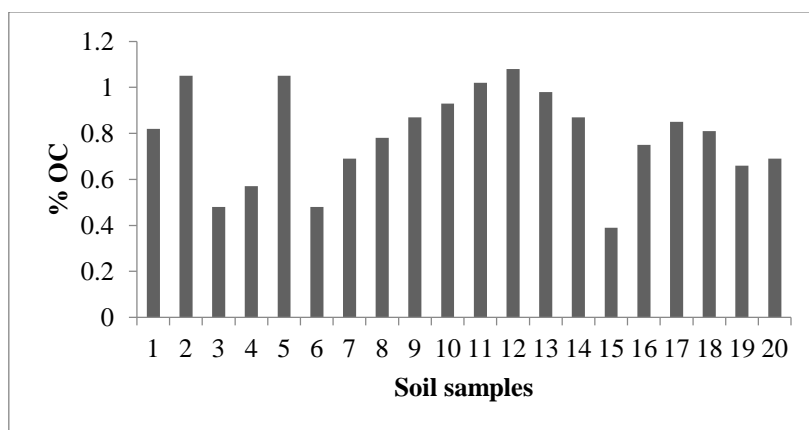


Figure 4.10 Spatial variation of Soil organic content

Table 4.2 shows the statistics of available surface soil nutrients status in the Arecanut farms. The average Nitrogen was found to be low whereas the average phosphorus, potassium and sulphur status was found in the range of medium to high among twenty samples.

Table 4.2 Statistics of available surface soil nutrients status of Arecanut farms

Avg. N (kg/ha)			Avg. P ₂ O ₅ (kg/ha)			Avg. (K ₂ O kg/ha)			S (kg/ha)		
Range	Nature	No. of samples	Range	Nature	No. of samples	Range	Nature	No. of samples	Range	Nature	No. of samples
<280	Low	20	<22.9	Low	02	<141	Low	01	<10	Low	00
280-560	Med	0	22.9-56.6	Med	07	141-336	Med	06	10-20	Med	08
>560	High	0	>56.6	High	11	>336	High	13	>20	High	12

Figure 4.11 represents spatial variation of available surface soil nutrients.

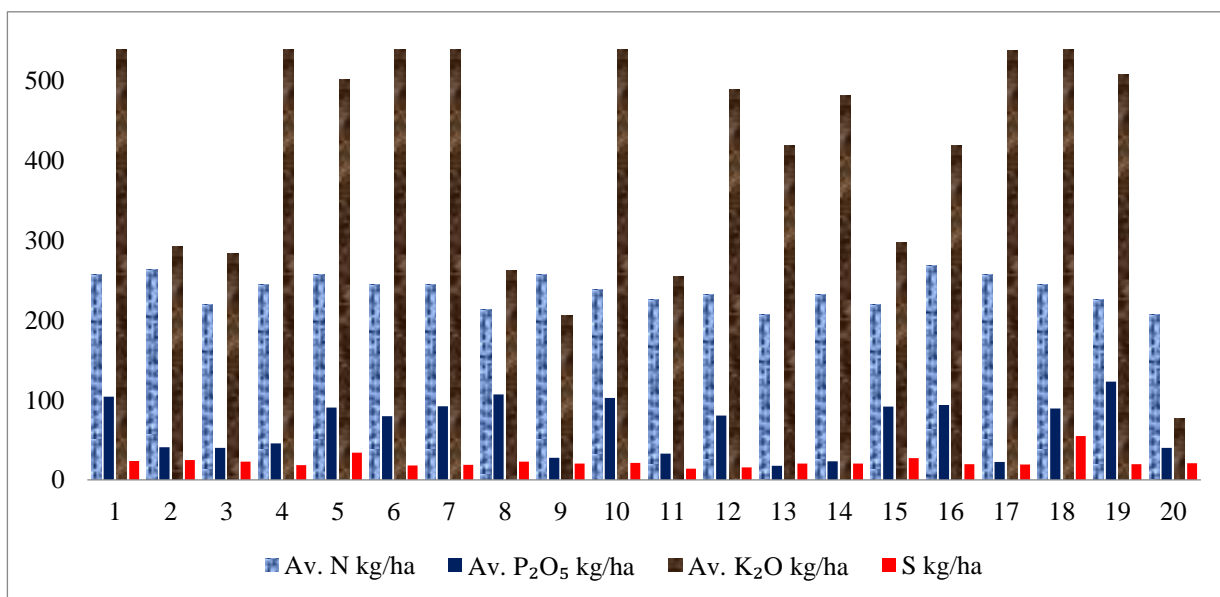


Figure 4.11 spatial variations of available surface soil nutrients.

From the available micro nutrients status in the study area it was found that except zinc, the iron, magnesium, and copper contents were high. Table 4.3 shows the range of micronutrient values and the number of soil samples in each range. Figure 4.12 represents the statistics of soil nutrients.

Table 4.3 shows the statistics for available surface soil micro nutrients status of Arecanut farms.

Table 4.3 Statistics of available surface soil micro nutrients status of Arecanut farms

Fe (ppm)			Mn (ppm)			Zn (ppm)			Cu (ppm)		
<2.0	Low	0	<2.0	Low	0	>0.6	Low	10	<2.0	Low	00
>2.0	High	20	>2.0	High	20	>0.6	High	10	>2.0	High	20

Figure 4.13 bar chart representations of the available soil micro nutrients Fe, Mn, Zn, Cu

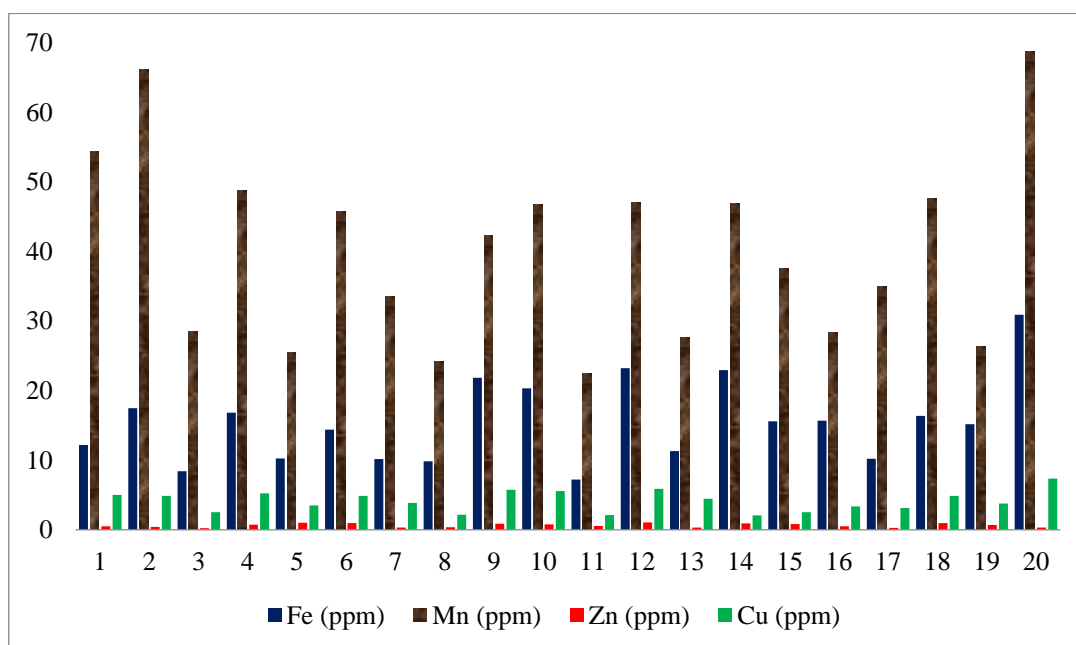


Figure 4.12 Soil micro nutrients Fe, Mn, Zn, and Cu

From the analysis of chemical properties of soil, it may be inferred that, chemical properties may not be the serious cause for disease under study.

4.4 Water quality analysis

To analyse the irrigation water quality source of irrigation water samples collected from field were subjected to laboratory analysis and the following results obtained from the standard tests. Figure 4.13 shows the variation of irrigation water pH level.

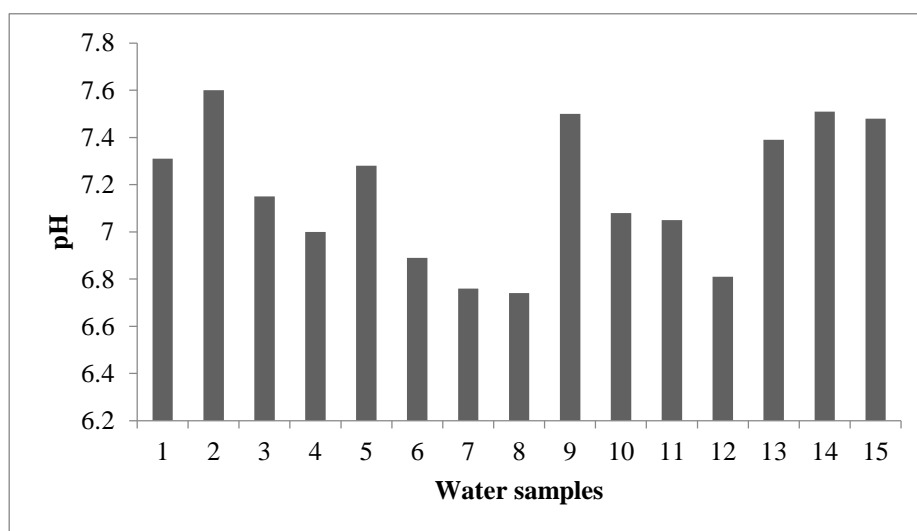


Figure 4.13 Irrigation water pH across the study area

Generally if pH value is less than 6.5, it should be used with amendments. Usually 6.5 to 7.5 are considered as safe and if it is more than 7.5 it should be used after treatment. From the analysis it was found that the pH of irrigation water is safe and it is within the permissible limit.

The permissible limit of EC should be less than 0.25. If it ranges between 0.25 to 0.75 leaching is required and if it is 0.75 to 2.25 and above 2.25 not safe. The analysis shows that the irrigated water having greater EC values than the permissible limit. Hence proper care should be taken before irrigation. Figure 4.14 shows the irrigation water electrical conductivity range.

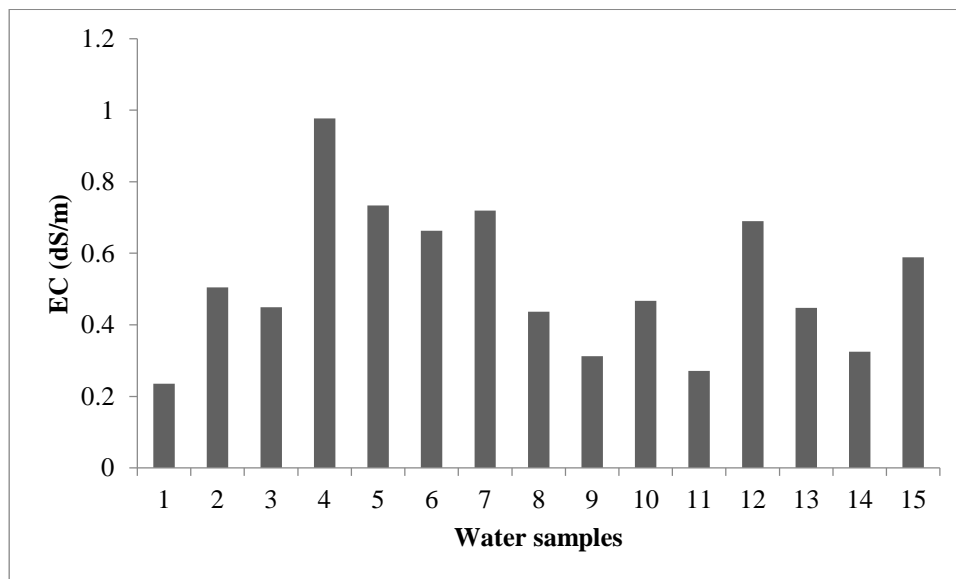


Figure 4.14 Irrigation water electrical conductivity

The Ca, Mg, Ca+Mg and HCO_3 are safe and within permissible limit. Figure 4.15 shows the variations of Ca, Mg, Ca+Mg.

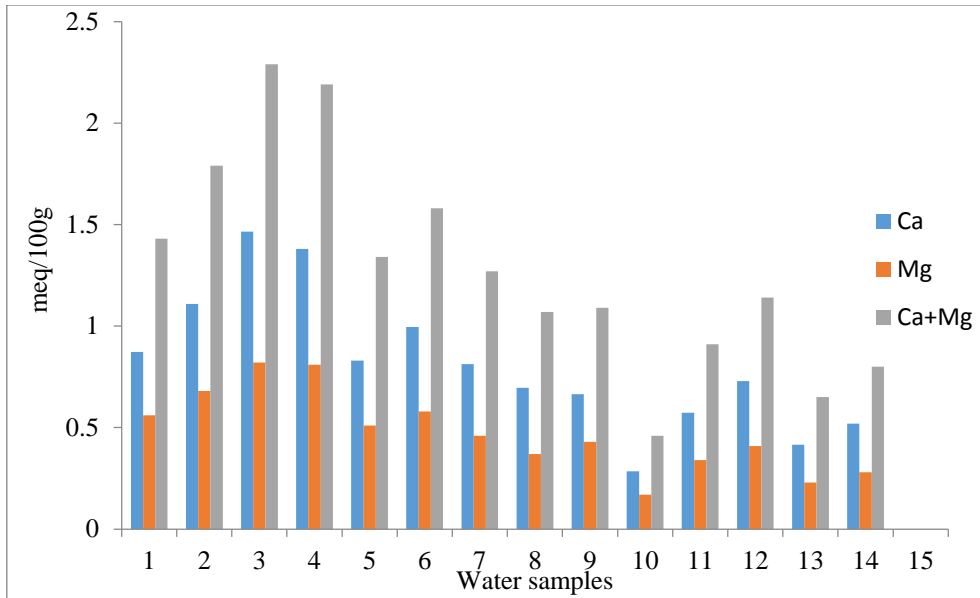


Figure 4.15 Irrigation water Ca, Mg, Ca+Mg

Figure 4.16 represents variations of HCO_3 and it is within permissible limit as per standards.

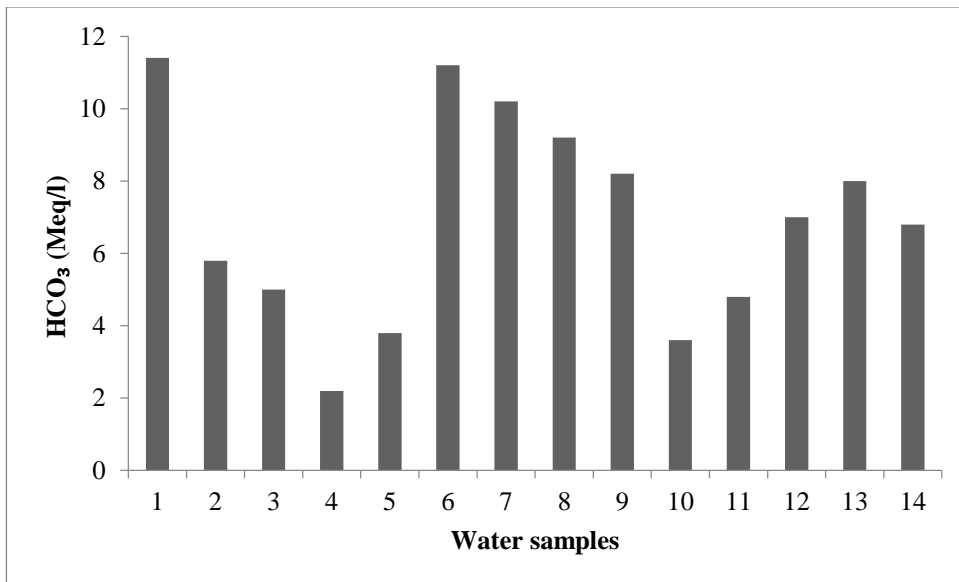


Figure 4.16 Irrigation water HCO₃

Fifteen water samples were collected from the study area; from the water quality analysis it was found that, the irrigated water quality is good and it is within the permissible limit. The average p^H was found to be 7.1 and it is safe as per the standards. The average EC was found to be 0.5 dS/m which is slightly greater than the safer limit. And the carbonate, bicarbonate, magnesium ions were within the permissible limit. From the analysis of chemical properties of water, it may be inferred that, chemical properties of water may not be the cause of the disease under study. Hence the physical properties of the soil were put under investigation.

4.5 Physical properties of the soil

Figure 4.17 shows the traded fresh Arecanut plants substitute for the deteriorated Arecanut plant due to crown choke disorder. When test pit was excavated under the deteriorated plant.



Figure 4.17 Field soil sampling picture under the crown choke affected plant

From the observation it was noticed that top 20 cm soil was varying with the beneath soil. Figure 4.18 shows the variation of soil type under the deteriorated plant, and this may be due to the addition of tank silt from the nearby ponds. Roots were not crossed beneath; instead it was crisscrossed at top few centimetres.



Figure 4.18 Excavated soil sampling duct

From Figure 4.18 it can be clearly seen that added tank silt at the top layer. Five test plots were selected from the adversely "crown choke" disease affected Arecanut farms. At each location 4 core samples were collected to a total depth of 1 meter at 15cm intervals. Soil samples were tested for bulk density, grain size analysis, porosity. Figure 4.19 shows the sample collection for bulk density and grain size analysis at varying depth. Clockwise Figure shows the (a) & (b) preparation of top layer soil strata by removing vegetation, c) placing core cutter and (d) to (e) collection of soil samples at varying depths.



Figure 4.19 Field soil sample collection to analyse physical properties

Figure 4.20 shows the bulk density test and initial soil moisture tests at field.



Figure 4.20 Bulk density and soil moisture measurements at field.

Figure 4.21 shows the hydrometer analysis test in the laboratory to identify the particle size distribution, and hydraulic conductivity.



Figure 4.21 Hydrometer analyses in the laboratory

Table 4.4 shows range of physical properties of the soil from the test plots. Few observations from this table are high value of Bulk density, high % of silt content, very low value hydraulic conductivity and considerably less value of porosity.

Table 4.4 Soil Physical properties

	Bulk Density (g/cm ³)	Moisture (%)	Dry Density (g/cm ³)	Specific Gravity	Silt Content (%)	Hydraulic (cm/sec)	Conductivity
Max	2.12	28.9	1.71	2.57	82		
Avg	1.89	22.2	1.55	2.38	72	3.2×10^{-7}	
Min	1.71	16.3	1.37	2.29	62		

By analysing the test mine shown in Figure.4.22 which was excavated below the death plant of crown choke affected Arecanut plant, it can be observed that the roots were distributed only less than 30 cm depth and below 30 cm there were no roots. From the literature it is found that, a healthy Arecanut plant of 20 years will have roots up to 3-meter depth. But in the test plot it was observed that the roots of 20-year palm have hardly reached less than 50 cm. From the physical properties and also from field observation, one may infer that there is no breathing space for the roots. Primary reason is poorly graded soil stratum which ceases the root development. Impervious nature of the surface causes irrigated water to be simply drained off from the surface not reaching the roots.

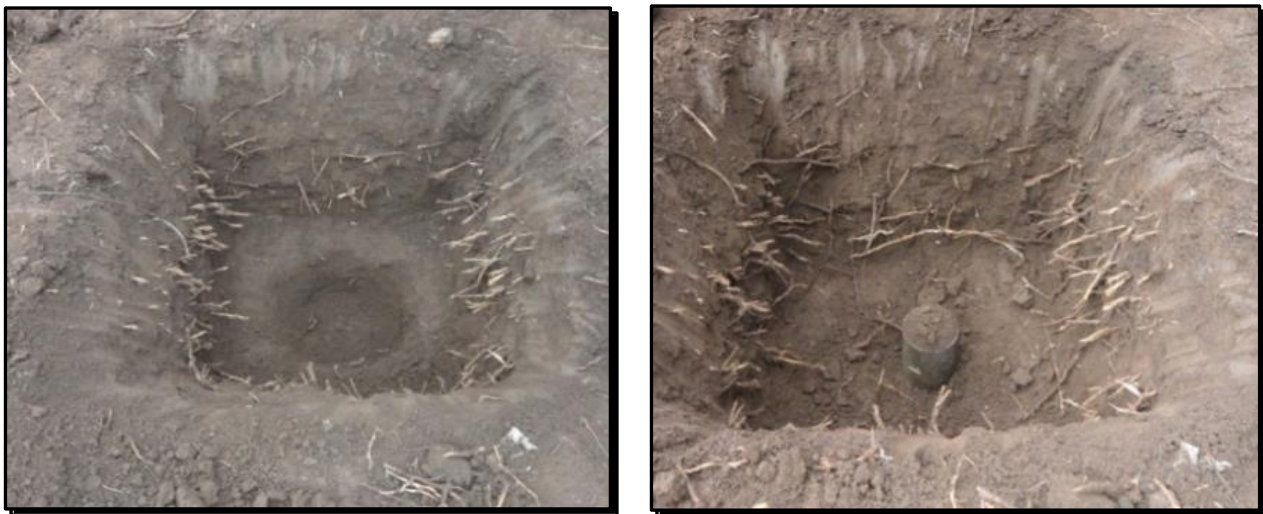


Figure 4.22 Test plots

4.6 Summary

Overall classification accuracy observed was 77.5% for healthy and stressed Arecanut crops. From the classified Hyperion image it was found that more than 10 % of the total areas are affected by crown choke disease.

The Arecanut crop is affected by crown choke disease for long years and has affected the yield and life span of the palm. From the investigation it may be concluded that the poor gradation of soil stratum ceases the root development. Impervious nature of the surface causes irrigated water to be simply drained off from the surface not reaching the roots. Due to this impervious nature, the waterlogging takes place and leads to salinity. The only way to manage the problem is better soil management and improved drainage system. Further investigation is needed on blending of the soil for new plantation and for the existing one. Improved drainage system has to be thought of. Soil aeration can be improved by, removing the hard pan of sub soil and application of organic matter. The practice of addition of tank silt on a large scale should be discontinued.

The next chapter explain the feasibility of hyperspectral data for mapping (Classification) different age group, Arecanut crops.

HYPERSPECTRAL DATA: A TOOL FOR AGE BASED CLASSIFICATION OF ARECANUT CROP

5.1 Introduction

The present chapter objective is to investigate the feasibility of hyperspectral data for mapping (Classification) the distribution of different age group, Arecanut crops. To monitor plantation crop, age based crop mapping is one of the important input for crop water requirement and yield estimation. The aim of the study is to classify Arecanut crops into different age groups. For this, reflectance spectra were collected from different ages (1 to 50) of Arecanut crops. From the spectral patterns it was observed that, four distinct groups can be formed with clear spectral seperability. This category consists of below 3 years, 3 to 7, and 8–15 and above 15 years of age. Figure 5.1 shows spectral reflectance curve of Arecanut crops of different age group forming the spectral library. Clear distinction can be seen between these spectra especially in the visible and NIR region Figure 5.1 a&b shows the enlarged portions of visible and NIR region. This region can be treated as an effective tool for the discrimination of Arecanut crops based on age. To classify Arecanut crop into different age various popular algorithms were considered and compared in this study.

5.2 Classification

Supervised classification methods viz Spectral Angle Mapper classifier (SAM), Support Vector Machine classifier (SVM) and Minimum Distance classifier were compared to find the most suitable classifier, to map within class (age wise) seperability utilizing hyperspectral data.

5.2.1 Spectral Angle Mapper (SAM) Classification

Supervised classification on Hyperion imagery was carried out by SAM classifier; SAM enables to classify the targets based on either spectral library or with respect to training sites. This study attempts classification (i) using the developed spectral library and (ii) training sites.

5.2.1.1 Spectral library of different age group Arecanut crops

Reflectance spectra were collected from different ages of Arecanut crops ranging from 1 to 50 years. From these patterns it was observed that, four distinct groups can be formed having clear spectral seperability. These categories are crops of below 3 years, 3-7, 8-15, and above 15 years 'of age. Figure 5.1 shows spectral reflectance curves of Arecanut crops at different age groups forming the library. There is a clear distinction between these spectra especially in the NIR region. Hence, this region is effective for discrimination of Arecanut crops based on age. Figure 5.2 a&b shows the enlarged visible and NIR portions of the spectral library.

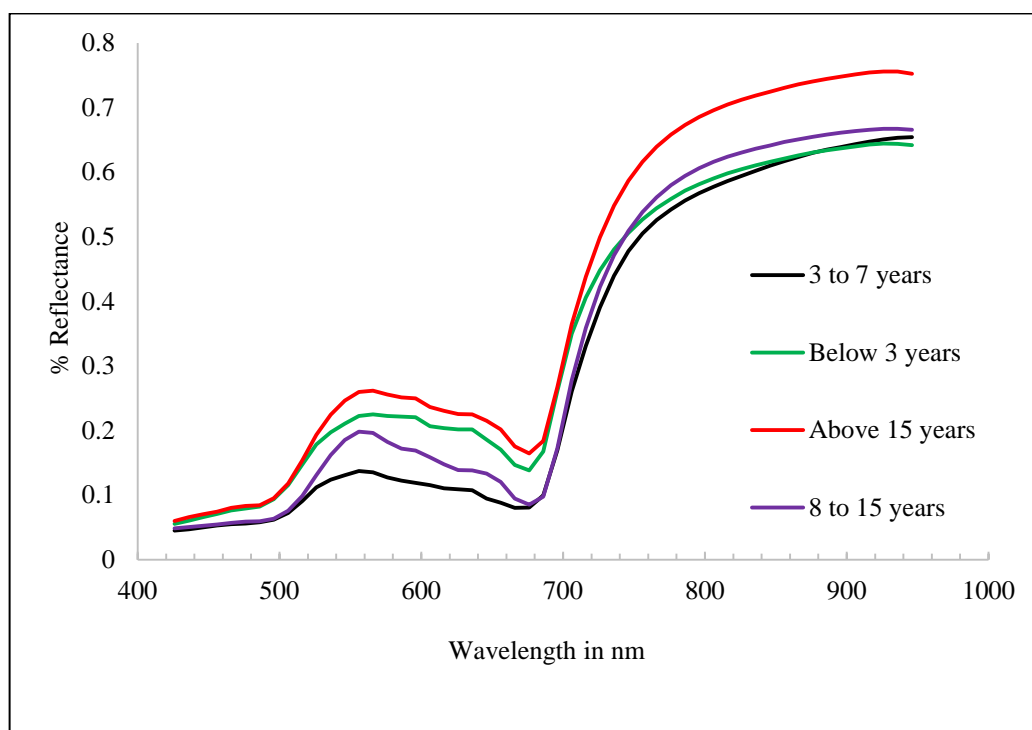
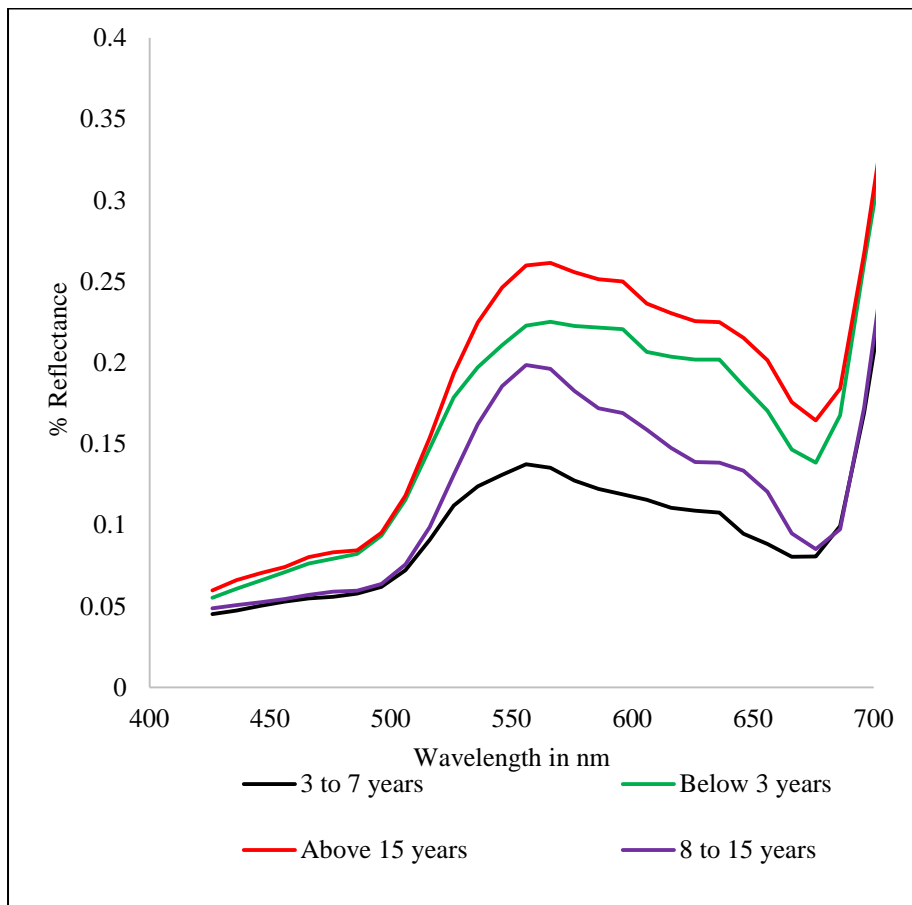
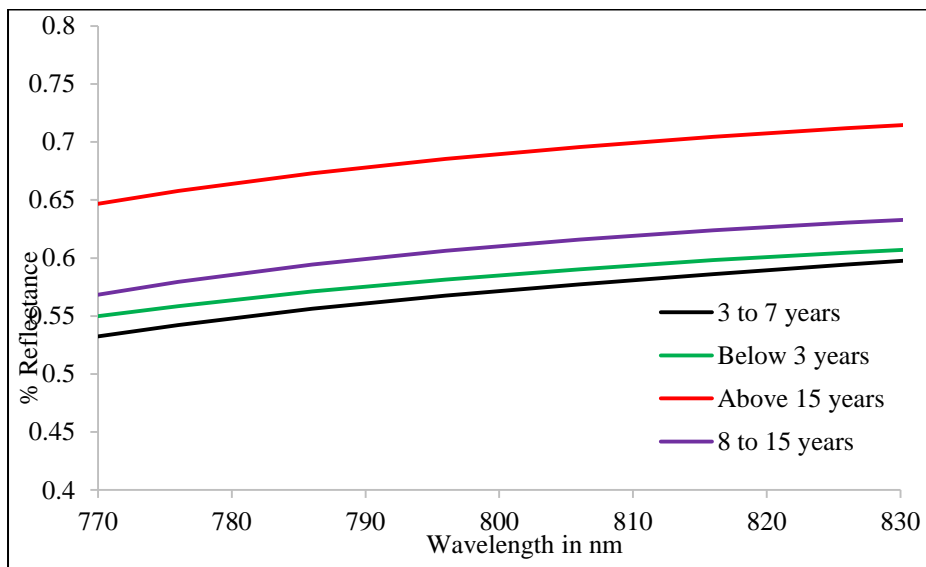


Figure 5.1 Spectral library plots of different age group Arecanut crops.



(a) Visible region.



(b) NIR region.

Figure 5.2 a& b Enlarged visible and NIR region of Spectral library.

5.2.2 Minimum Distance Classification

Minimum distance classifier uses the mean vectors of each reference spectra and calculates the Euclidean distance from each unknown pixel to the mean vector for each class. Figure 5.4 shows the output image of minimum distance classification using training sites for the Hyperion imagery.

5.2.3. Support Vector Machine Classification

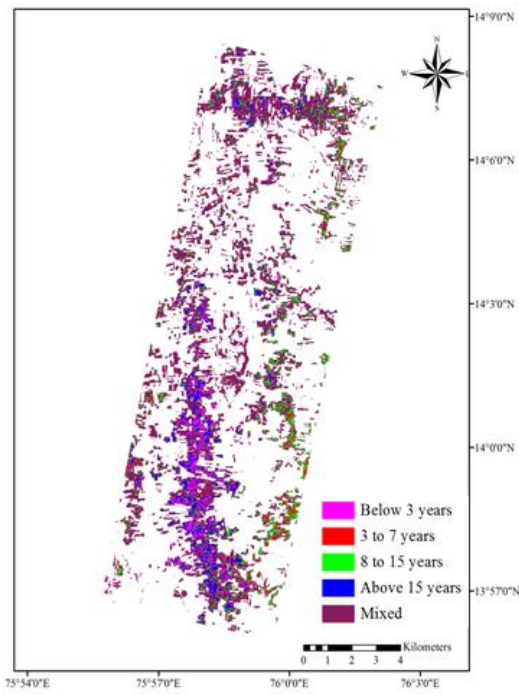
SVM identifies a hyper- plane between two classes that produces optimal separation between the classes. In this study, classification was carried out using linear as well as non-linear kernels from the training sites. The non-linear kernels include polynomial, radial basis function and sigmoid kernels. Figure 5.5 shows the output of support vector machine-based classification using different kernels. Table 5.1 shows the comparison between overall classification accuracies of support vector machine classification using different kernels with other classification methods. It is found that SVM with linear kernel has the highest accuracy compared to other kernels with an overall accuracy of 72.55%. From this one may infer that, even within class variability of crop can be discriminated better with SVM when compared to other classification methods.

5.3 Classification results

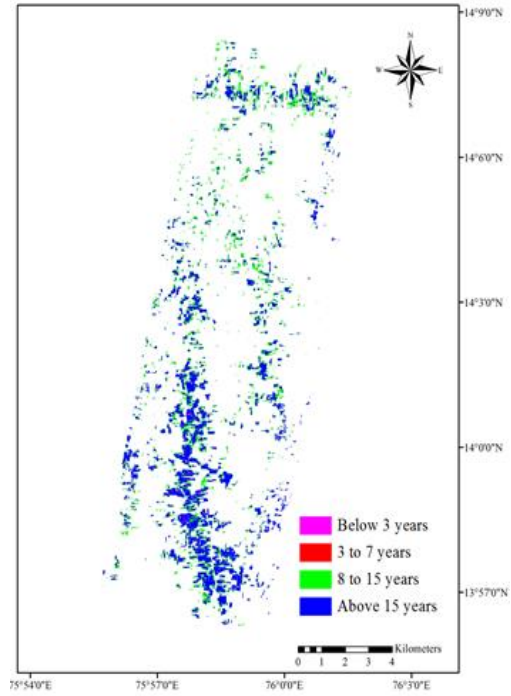
Supervised classification methods namely i) Spectral Angle Mapper classifier (SAM) ii) Support Vector Machine classifier (SVM) iii) Minimum Distance classifier were compared to find the most suitable classifier to map within class (age wise) separability. Table 5.2 & 5.3 shows result of accuracy assessment carried out to compare efficacy of each algorithms.

5.3.1 Classification of Hyperion imagery

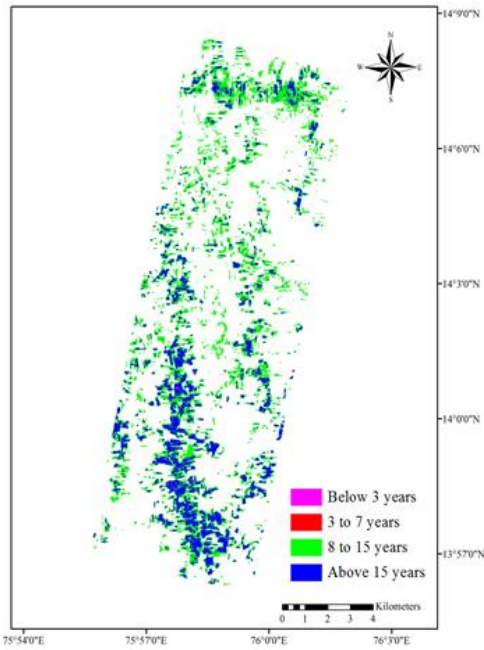
Hyperion imagery was used to carry out supervised classification by SAM classifier using spectral library created for different ages of Arecanut crop and also from training sites. SAM classifies the imagery based on spectral similarity between image spectra and the reference spectra. The spectral similarity is determined by calculating the angle between the reference spectra and the satellite imagery spectra treating them as vectors in an n-dimensional space where n equals to the number of spectral bands of the sensor. Figure 5.3 shows the SAM classified output image using spectral library for varying spectral angles and Figure 5.3 a, shows using training sites.



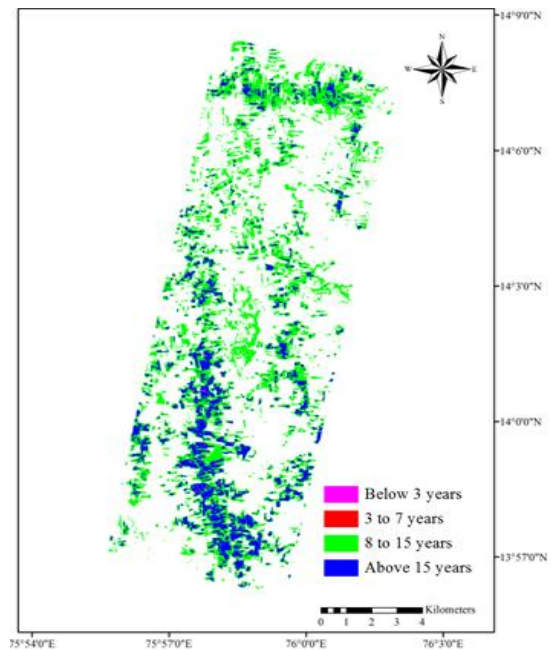
a. SAM classification using training sites



b. SAM classification, spectral angle 0.1



c. spectral angle 0.13



d. spectral angle 0.15

Figure 5.3 SAM classifications using spectral library

5.3.2 Minimum distance classifier results

The minimum distance technique uses the mean vectors of each reference spectra and calculates the Euclidean distance from each unknown pixel to the mean vector for each class. Figure 5.4 shows the output image of minimum distance classification for the hyperspectral imagery.

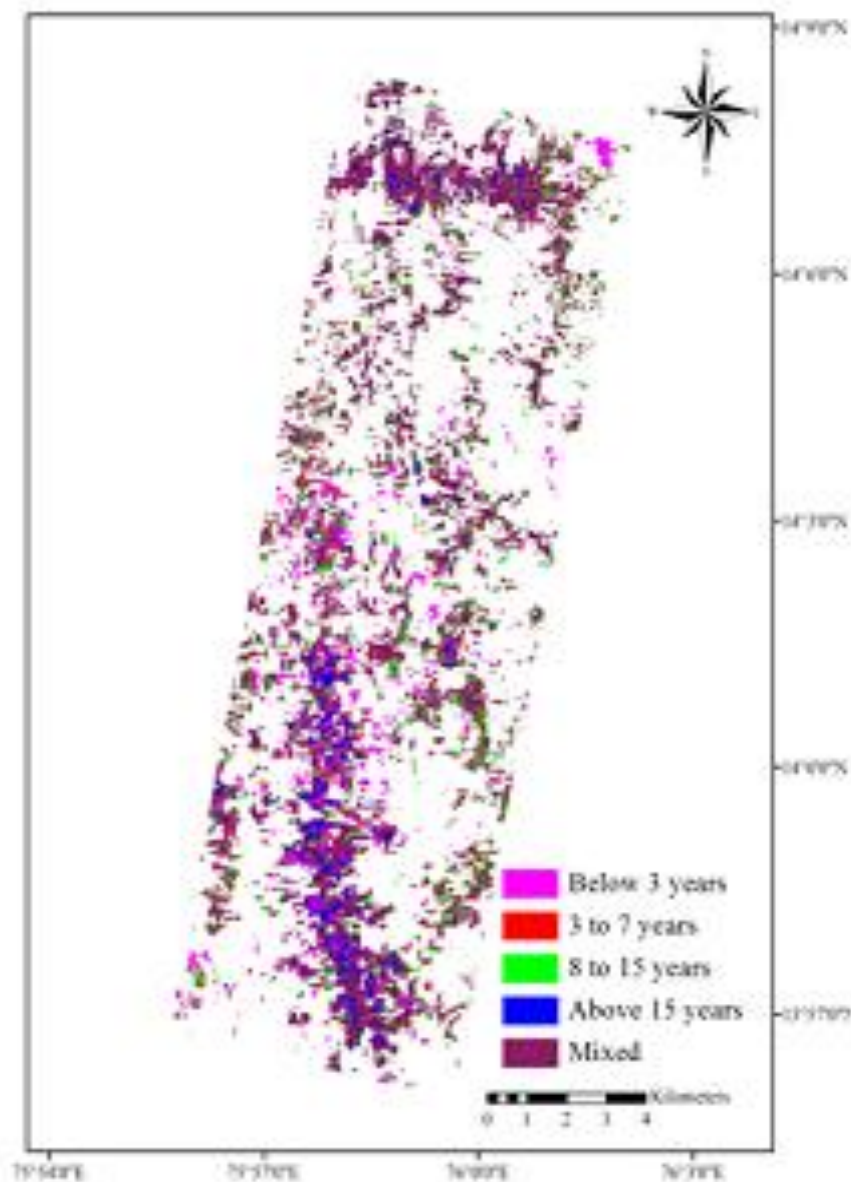


Figure 5.4 Minimum distance classification.

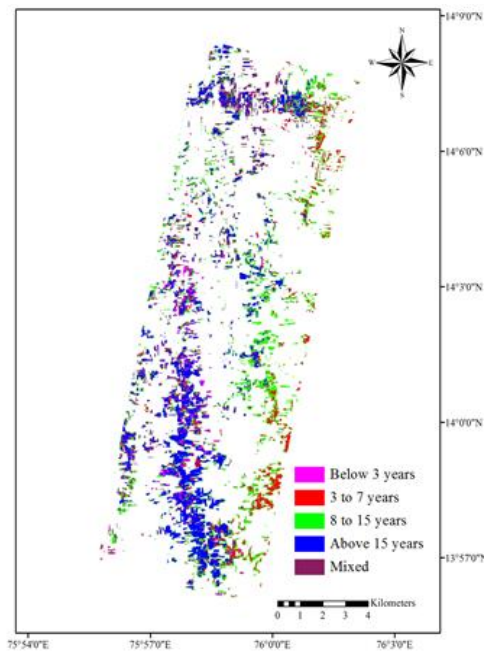
Table 5.1 shows the confusion matrixes of Minimum distance and SAM classification using spectral library and training sites with the varying spectral angle. The results were discussed in detail in the discussion part.

Table: 5.1 Confusion matrixes of SAM and Minimum distance classifier

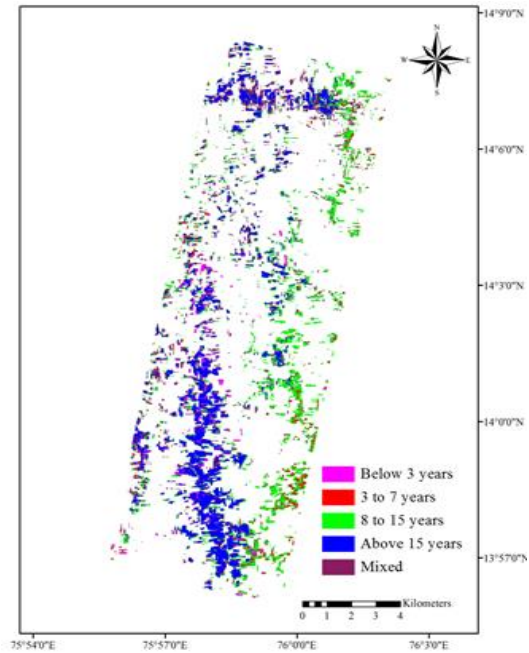
Classes (in age)	Confusion matrix for SAM classification						Confusion matrix for Minimum distance Classification	
	Using Spectral library				Using training sites			
	Angle = 0.1		Angle= 0.13		Angle = 0.1			
	PA (%)	UA (%)	PA (%)	UA (%)	PA (%)	UA (%)	PA (%)	UA (%)
Below 3 years	6.67	100	23.91	84.62	28.57	22.22	82.61	26.21
3 to 7 years	0	0	0	0	20	16.67	20.59	9.72
8 to 15 years	22.5	56.25	30.08	90.59	66.67	61.9	32.81	81.82
Above 15 years	98.21	56.7	97.03	51.89	53.85	66.67	77.45	86.81
Overall accuracy (%)	51.18		57.68		50.83		55.88	
Kappa coefficient	0.21		0.25		0.29		0.39	

5.3.3 Support Vector Machine Classifier

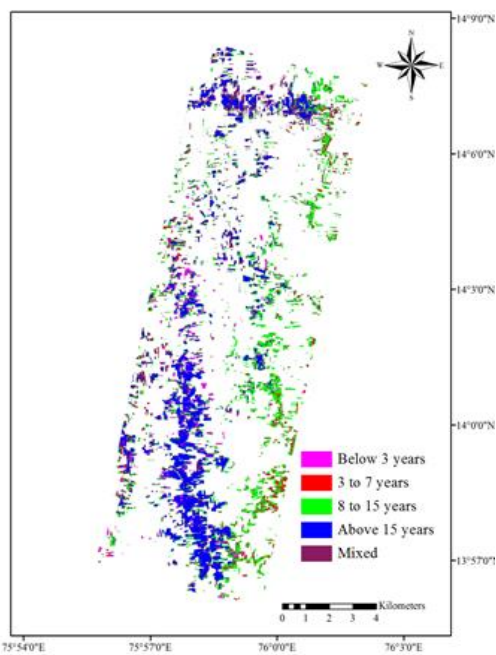
Figure 5.5 shows the output of support vector machine based classification using different kernels.



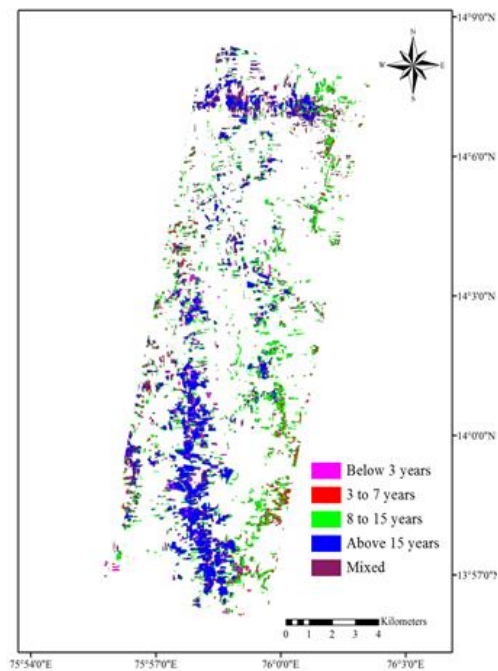
Linear kernel



Polynomial kernel



Radial basis function kernel



Sigmoid kernel

Figure 5.5: SVM classification using training sites with different Kernel Functions

Table 5.2 shows the confusion matrix of SVM classification for different kernel functions with the classification accuracy results for each age group Arecanut crop.

Table 5.2 Confusion matrix of SVM classification

Class	SVM with linear		SVM with polynomial		SVM with Radial basis function		SVM with sigmoid	
	PA (%)	UA (%)	PA (%)	UA (%)	PA (%)	UA (%)	PA (%)	UA (%)
Below 3 years	65.22	45.45	54.35	41.67	47.83	37.29	58.7	38.57
3 to 7 years	12.5	22.22	23.53	29.63	23.53	29.63	11.76	17.39
8 to 15 years	66.93	74.36	55.12	92.72	54.72	92.67	51.95	87.5
Above 15 years	86.25	82.93	97.01	71.43	97.01	71.04	93.66	69.92
Overall accuracy%	72.55		71.93		71.26		68.70	
Kappa coefficient	0.55		0.54		0.53		0.49	

5.4 Optimum Wavelengths Selection and Model Building

It was desired to find the optimum wavelengths combinations for predicting the age of Arecanut crops. The inputs are age of the crop and corresponding reflectance spectra collected from the field. A set of latent variables and scores were observed for the input dataset and finally optimum bands were obtained. The obtained optimum bands were 701, 719, 756 and 1015 nm using which; the following model was developed for predicting age of Arecanut crops (Equation 5.1).

A simple regression equation was developed to predict age of the Arecanut crop using optimum wavelengths to facilitate estimation from satellite data.

$$Y = 157.82 - 5.425 \lambda_{701} + 466.468 \lambda_{719} - 21.931 \lambda_{756} - 434.235 \lambda_{1015} \quad (5.1)$$

Where, Y – predicted age in years

λ_{701} , λ_{719} , λ_{756} , λ_{1015} Reflectance corresponding to **701 nm, 719 nm, 756 nm, and 1015 nm** wavelengths respectively.

70% of data is used for calibrating model, remaining 30% of data is used to validate. The model gave RMSE of 3.22 years with the R^2 of 0.86. Table 5.3 shows the comparison between the predicted and observed ages of Arecanut crops.

Table 5.3 Observed Vs predicted age in years.

Observed age	Predicted age	RMSE (in year)
3	2.38	0.62
4	1.58	2.42
20	20.07	0.07
50	43.9	6.1

The model predicted 3 years aged crop as 2.38 years, it predicted accurately for 20 years crop and lower accuracy for above 50 years crops. Table 5.4 shows comparisons of overall accuracy and Table 5.5 shows the statistics for each age group accuracy.

Table 5.4 Overall classification accuracy comparisons.

	Spectral Angle Mapper Classifier			Minimum Distance Classifier	Support Vector Machine Classifier			
	Using Spectral library		Using training sites		Using training sites with different kernel functions			
	Angle = 0.1 Rad	Angle= 0.13 Rad	Angle = 0.1 Rad		Linear	Polynomial	Radial basis function	Sigmoid
Overall Accuracy (%)	51.18	57.68	50.83	55.88	72.55	71.93	71.26	68.70

Table 5.5 Statistics of various age group classes area under Arecanut crop and SVM individual class classification accuracy.

Group Class	Spectral Angle Mapper Classifier				Minimum distance Classifier	Support Vector Machine Classifier (linear kernel)					
	Using Spectral library			Using Training sites		Area				Individual class User's and Producer's Accuracy (PA)	
	0.1 Rad	0.13 Rad	0.15 Rad	0.13 Rad		Area		in Km ²	13.62	PA (%)	UA (%)
	% area	% area	% area	% area		% area	% area				
Below 3 years	0.068	0.065	0.068	0.92	0.95	3.1	4.557	13.62	65.22	45.45	
3 to 7 years	0.0	0	0	0.88	1.42	1.38	2.0286		12.5	22.22	
8 to 15 years	3	4.6	12.9	9.78	4.39	3.44	5.0568		66.93	74.36	
Above 15 years	4.3	8	4.8	2.21	4.5	1.35	1.9845		86.25	82.93	
Others	92.632	87.335	82.232	86.21	88.74	90.73	133.3731		Overall Accuracy	72.55 %.	
Total	100	100	100	100	100	100	147				

5.5 Summary

Spectral pattern of Arecanut crops of different ages (1 to 50) has revealed that four distinct groups can be formed with clear spectral separability. This category consists of below 3 years, 3–7, and 8–15 and above 15 years of age. SAM classification carried out using spectral library created for different ages of Arecanut crop and also training sites obtained for each age group from the field visit. For classification using spectral library, spectral angle is varied from 0.1 to 0.15 to check the increased accuracy in each age group. Increase in spectral angle did not show much difference for the crop below 3 years of age group, whereas the crop above 15 years age group and 8 to 15 age group showed significant increase i.e. 4.3 to 4.8% and 3 to 12.9%, respectively.

SAM classifier resulted in close spectral similarity between 3 to 7 years age crops with 8 to 15 year's crop, whereas the accuracy achieved by the SVM classifier with linear kernel yielded minimum user's accuracy of 22.22% for 3–7 years of Arecanut crops to maximum of 82.93% for above 15 years of Arecanut crops. Individual age group classification producer's accuracy varied minimum of 12.5% for 3–7 years age group and maximum of 86.25% for above 15 years age group. SVM outperformed better even for individual age group classification. Table 5.5 provides an area statistics in % of various age group classes of Arecanut crop classified with various classification methods in the study area. From SVM, with linear kernel classification method results, it was found that total area under Arecanut crop cultivation is 13.62 km² among the 147 km² study area. This includes below 3 years of 4.55 km², 3–7 years of 2.02 km², 8–15 years of 5.05 km² and above 15 years crops of 1.98 km². The results also illustrate that classification accuracy of spectral library-based classification is comparable with classification using training samples, suggesting that; spectral library built using spectroradiometer can be effectively used for classification. Minimum distance classifier showed better classification accuracy than SAM because of close similarity of classes. Support Vector Machine supervised classification identifies the class associated with each pixel on image and provides good classification results even for complex and noisy data. In this study, SVM with linear kernel showed highest classification accuracy. The obtained results are on par with the study carried out by Jovivek et al. (2009) and Petropoulos et al. (2013). Lower accuracy of SAM could also be due to higher variation in reflectance values of pixels belonging to same class.

The study proved that spectral library can even be built for plantation crops which have long life, like 50 years and it will assist crop classification based on age, avoiding the laborious site visits. Spectral library is developed for different age groups of Arecanut crops showed clear spectral separability. They are being, below 3 years, 3–7 years, 8–15 years and above 15 years. Based on compared classification algorithms accuracy assessment, it can be concluded that, SVM with linear kernel function is the most accurate classification method for within class separability with an overall accuracy of 72%. The total area under Arecanut crop cultivation was found to be 13.62 km² among 147 km² of study area. Also, SVM classifier with linear kernel yielded minimum user's accuracy of 22.22% for 3–7 years of Arecanut crops to maximum of 82.93% for above 15 years Arecanut crops. Individual age group classification producer's accuracy varied minimum of 12.5% for 3–7 years age group and maximum of 86.25% for above 15 years age group. SVM outperformed better even for individual age group classification. In the next chapter development of hyperspectral vegetation indices for Arecanut crop monitoring is presented.

HYPERSPECTRAL VEGETATION INDICES FOR ARECANUT CROP MONITORING

6.1 Introduction

Narrow bands in hyperspectral data facilitate computation of several spectral indices and can facilitate improved classification accuracy. The objective of this chapter is development of hyperspectral vegetation indices for stressed and different age groups Arecanut crop identification and intensity of stress.

On time mapping of spatial spread of disease severity helps in taking decision for necessary remedial measures. Crown choke disorder in Arecanut crop not only injures the yielding stage of plant's life but also cause irreparable damage to farmer's years of effort.

Crown choke disease in Arecanut crop is unique in nature with distinctly dark green in visibility compared to healthy one. To segregate this disease affected crop with healthy arecanut crop there is a need to develop a disease index for finding disease severity in arecanut crops. It is explored to derive an algorithm, to differentiate healthy versus diseased Arecanut crop. From the analysis it is observed that red edge region is the key feature to identify vegetation stress. In this study combination of visible as well red edge region combinations were tried for deriving a disease index. The concept used in building disease index is that, it should use easy-to-use mathematical algorithms, transforming multi-band data into a single band showing the severity of the disease. Additionally, the algorithm must have the ability to illustrate the healthy versus stressed Arecanut crop even with a few band combinations.

Chlorophyll pigment is an excellent indicator of vegetation stress. A set of band combinations were found helpful in distinguishing stressed and healthy vegetation. After the spectral analysis, three key features were identified and used for band combinations. Also from the literature it was found that red edge region is the most important region in detecting vegetation variances. Sample laboratory measurements of healthy and stressed vegetation reflectance spectra are shown in Figure 6.1 and 6.2 respectively.

The proposed Disease Index is expected to be sensitive to Arecanut crown choke disorder. The spectral reflectance curve of healthy green vegetation has a significant minimum reflectance in the visible portion of the electromagnetic spectrum resulting from the pigments in plant leaves. Reflectance increases dramatically in near infrared for healthy plants compare to stressed vegetation, this information is useful to identify stressed vegetation because; stressed vegetation has a significantly lower reflectance in the infrared. The ASD data was processed in view spec pro to find the spectral signatures of the available vegetation data. View spec pro is a software application which is used to analyze the ASD data. The reflectance data was then exported in excel format for further processing. The reflectance of each Arecanut vegetation sample was then obtained corresponding to their wavelength.

Figure 6.3 shows healthy and diseased Arecanut crop spectral signatures. Identifying prominence bands due to distinctiveness at 550, 675 and 750nm the Arecanut Disease Index is intended.

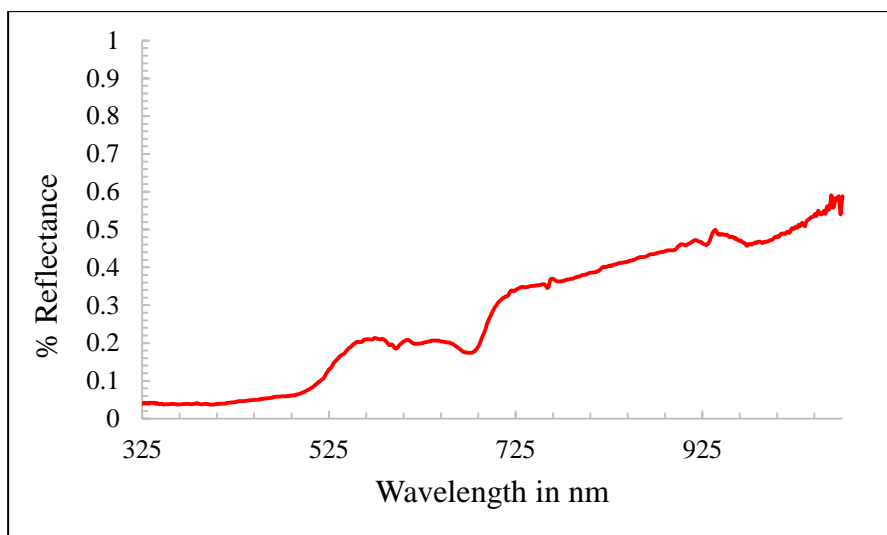


Figure 6.1 Diseased Arecanut crop Spectra

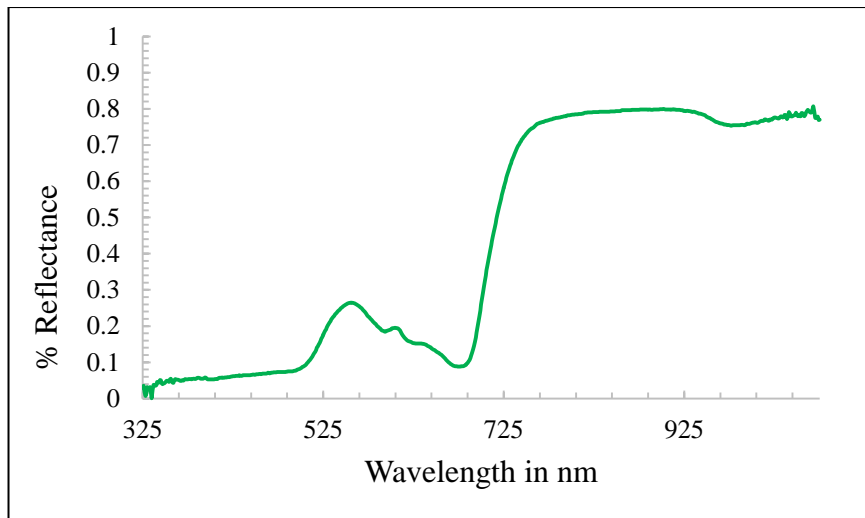


Figure 6.2 Healthy Arecanut crop spectra

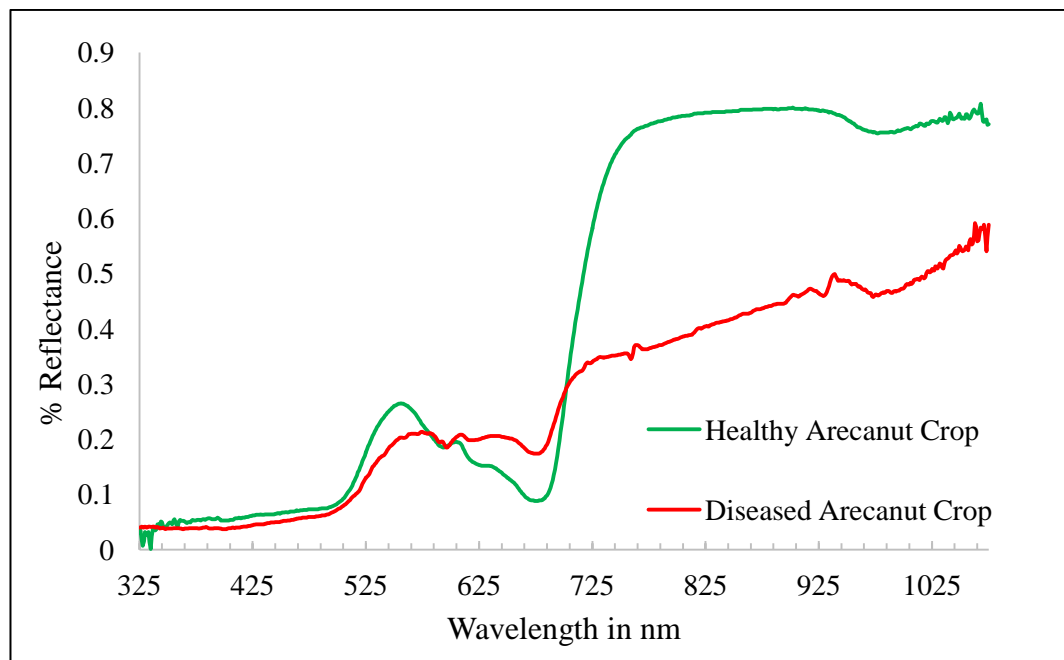


Figure 6.3 Stressed and healthy vegetation reflectance spectra

6.1.1 First Order Derivative Reflectance

The first order derivative shows the rate of change in the reflectance curve. The average first order derivative reflectance spectra of the healthy and the diseased plants as obtained from the processed spectroradiometer data is shown in the Figure 6.4.

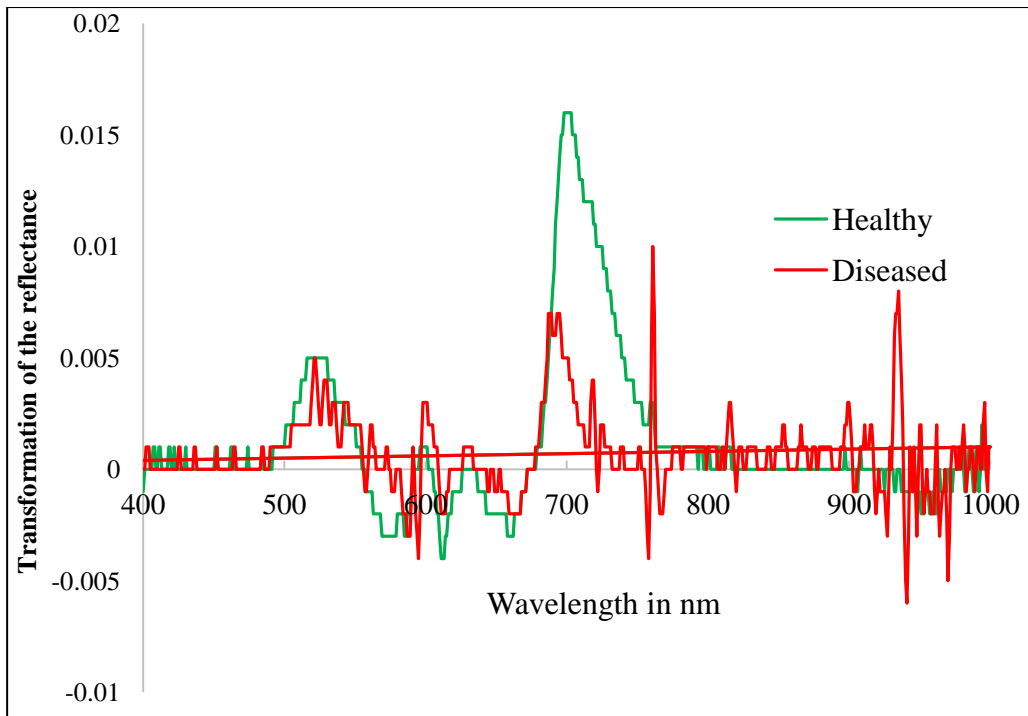


Figure6.4 First order reflectance curves.

It was seen that the maximum value in first order derivative reflectance curve comes in the red edge region, where rate of change was maximum it may be due to the change of reflectance from low red reflectance to high NIR reflectance. In the present study, the maximum first derivative occurred at approximately 700–760 nm. The maximum the first derivative in the green was at 520 nm and minimum at 520-580 nm. The healthy plants have highest value in the first derivative both at red edge and green region compared to diseased plants. As the disease intensity increased these maximum values became lower. This indicates a healthy plant has sharpest change in reflectance value in red edge compared to diseased plants. It was clearly observed that as the disease intensity increases there is a shift in the wavelength towards the red edge portion. The maximum of healthy one is at 720nm while for the disease intense plot the maximum is at 700nm (red edge). The red edge position moves towards right with a shift of about 20nm.

Megaha et.al (2014) have analysed correlation coefficient between the Arecanut crops of diseased intensity percentage and the absorbance at each wavelength which indicates the strength of the relationship between disease severity and leaf absorbance at the various wavelengths. Disease intensity and the spectral reflectance values, shown in the form of a curve in refer Figure6.5. There was a very high correlation (-0.8 to + 0.8) between disease intensity with spectral reflectance.

The correlation coefficient increased from 0.3 at 540 nm to 0.7 at 580 nm. There was a low correlation between 520–560 nm and it again increased to around 0.75 in 610–630 nm region. Beyond 700 nm, the spectral reflectance has very high negative correlation with the disease intensity. This shows that, hyperspectral data are highly useful for disease detection and disease intensity estimation. With these backgrounds Arecanut crop DI is proposed.

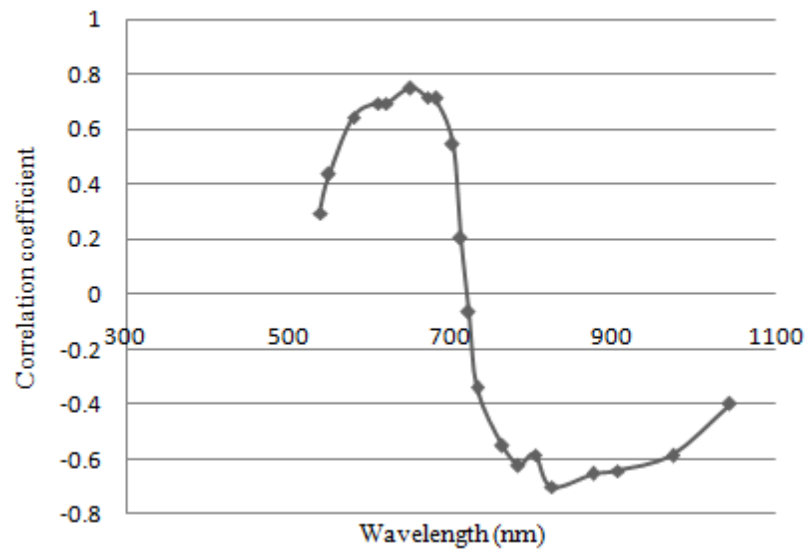


Figure 6.5 Correlation Coefficient vs. Wavelength.

(source: Megha et al., 2014)

6.2 Arecanut Disease Index

The resulting Arecanut Disease Index is inspiration of the study carried out by Kuhn et al., (2004), they focused on Hydrocarbon Index (HI) development and testing for the direct detection of hydrocarbons. Figure 6.6 and 6.7 shows index points for healthy and stressed Arecanut crop.

Present study tries to identify index points for the developing DI. Figure 6.8 shows the index points those form a triangle to derive DI. The index points set for the wavelengths are $\lambda_A = 550\text{nm}$, $\lambda = \lambda_B \approx 675\text{nm}$ and $\lambda_C = 750\text{nm}$. The disease index (DI) uses the vertical line $DI = BB'$, as indicator of severity of disease. The index points A, B and C form a triangle ($DI > 0$). As an approximation, it can be assumed that the larger the DI value, the healthier the crop. If not the disease severity is high. The observed minimum and maximum derived DI value ranges from 0.45 to 1.5 respectively, for the region under investigation.

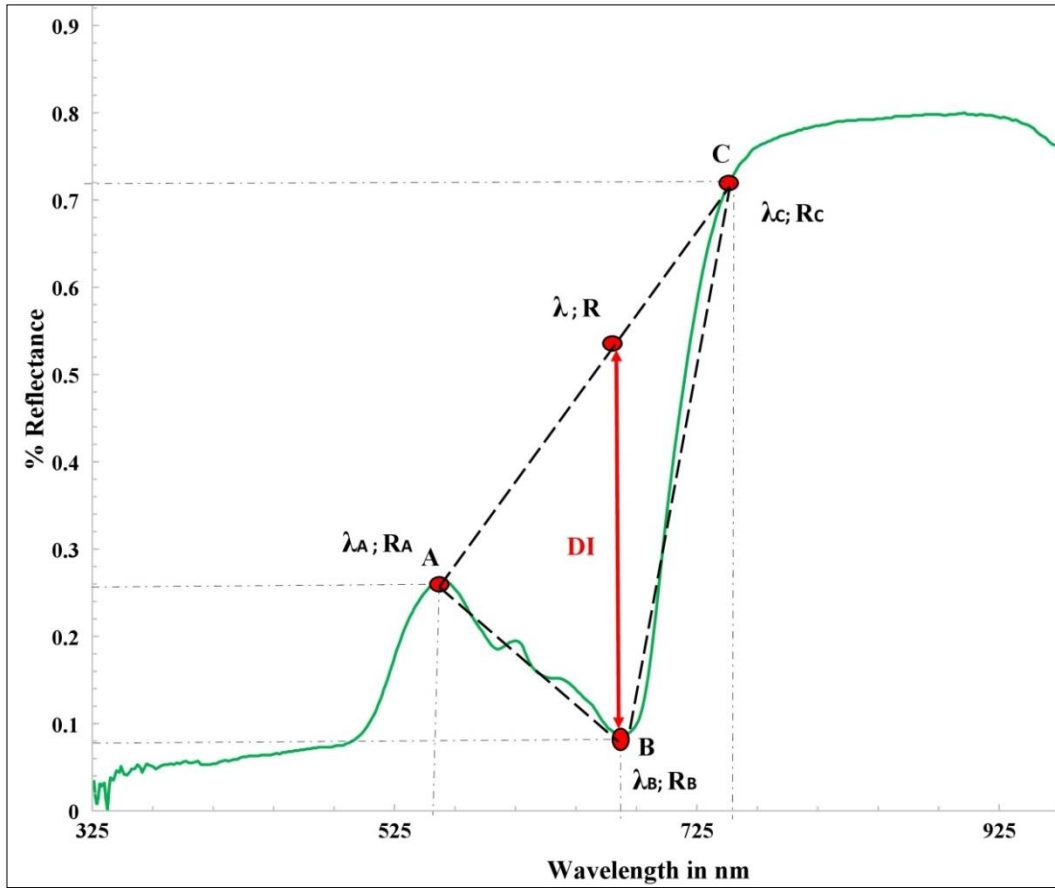


Figure 6.6 Index points for healthy Arecanut crop spectral signature

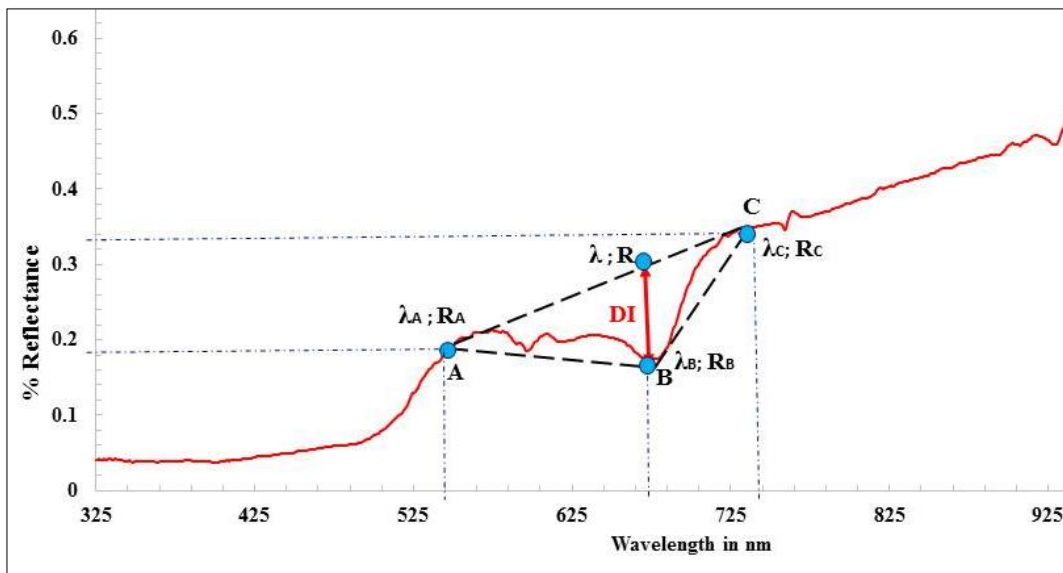


Figure 6.7 Index points for stressed Arecanut crop spectral signature

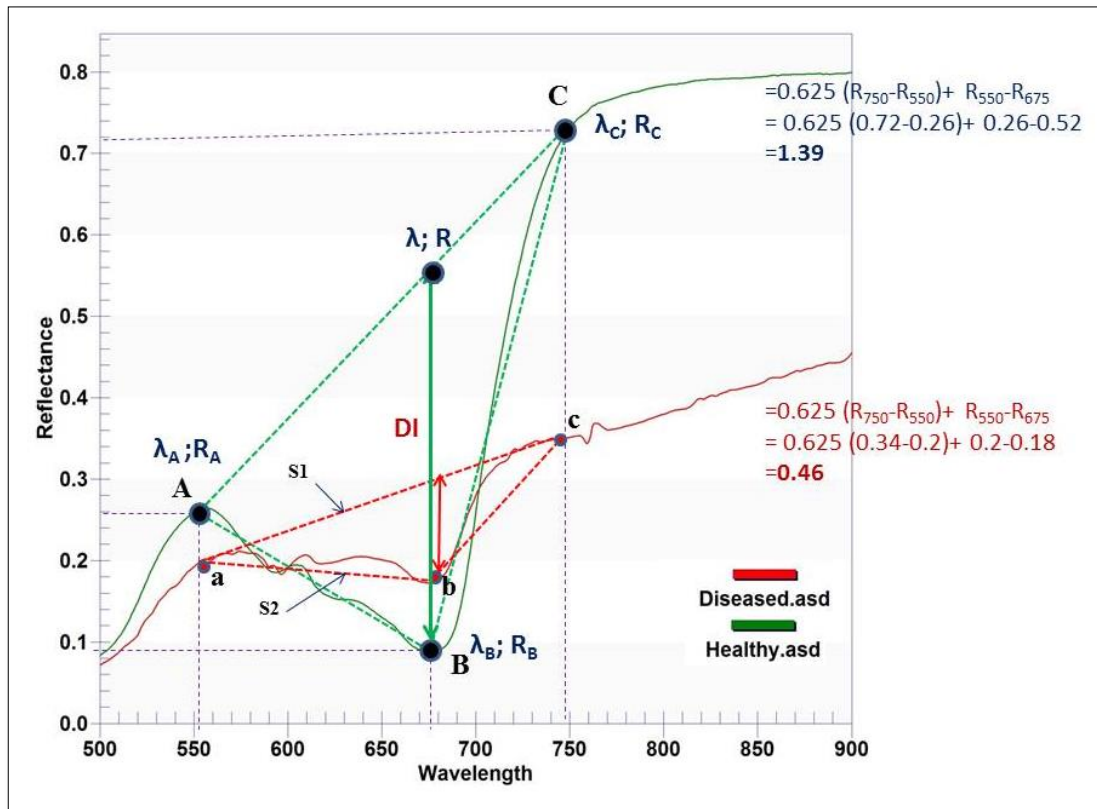


Figure 6.8 A, B, C Index points those form a triangle to derive DI.

If the disease severity is more, the DI value will be less than 0.5 and for healthy the range of DI is 1 to 1.5. As an approximation, it can be assumed that the larger the DI value, the larger the indication of healthy. If not the index points a, b and c lie almost a nearly smaller triangle compare to triangle A, B and C. The Disease Index can be calculated using these three points as follows, (equation of a straight line through two known points).

$$(\lambda_A; R_A), (\lambda; R) \text{ and } (\lambda_C; R_C)$$

Where $\lambda; R$ is a variable

$$\therefore R = R_B'$$

$$\frac{R - R_A}{R_C - R_A} = \frac{\lambda - \lambda_A}{\lambda_C - \lambda_A}$$

$$\therefore \lambda = \lambda_B'$$

$$R_B' = \frac{\lambda_B - \lambda_A}{\lambda_C - \lambda_A} (R_C - R_A) + R_A$$

$$DI = R_B' - R_B$$

$$DI = \frac{\lambda_B - \lambda_A}{\lambda_C - \lambda_A} (R_C - R_A) + R_A - R_B$$

$$DI = \frac{675 - 550}{750 - 550} (R_C - R_A) + R_A - R_B$$

$$DI = \frac{5}{8}(R_{750} - R_{550}) + R_{550} - R_{675} \dots\dots\dots(6.1)$$

Substituting the reflectance values to corresponding wavelengths' in equation 6.1 forest healthy Arecanut crop DI value is

$$= \frac{5}{8}(R_{750} - R_{550}) + R_{550} - R_{675}$$

$$= \frac{5}{8}(0.72 - 0.26) + 0.26 - 0.52$$

$$DI = 1.39 \approx 1.4$$

Substituting for critical diseased Arecanut crop DI value is

$$DI = \frac{5}{8}(R_{750} - R_{550}) + R_{550} - R_{675}$$

$$= \frac{5}{8}(0.34 - 0.2) + 0.2 - 0.18$$

$$DI = 0.46 \approx 0.5$$

The derived index value ranges from minimum of $0.46 \approx 0.5$ to maximum value of $1.39 \approx 1.4$ hence it is difficult to understand these range of values, it should be normalized for better understanding

6.2.1 Normalization of an Index

The process of transforming the derived index from its value into a range of 0 and 1 is called normalization. Suppose the dissimilarity index is in the range of (d^{\min}, d^{\max}) and is not in the range of $(0, 1)$. If it is required to transform it into range of $(0, 1)$.

Put notation ' d ' to the original dissimilarity and ' δ ' to the normalized dissimilarity. There are several ways to normalize an index. In principle, to aggregate a sequence of numbers into range of $(0, 1)$ there is a need to make them positive and divide with something that is bigger than the nominator. Using this principle, it can make use any inequality to normalize the index.

If it is know the maximum and minimum value of index, then transformation is in the form of equation number 6.2

$$\delta = \frac{d - d^{\min}}{d^{\max} - d^{\min}} \dots\dots\dots(6.2)$$

It will change transform it into range of $[0, 1]$. If $d = d^{\min}$, then $\delta = 0$. If $d = d^{\max}$, then $\delta = 1$. A special care must be taken to avoid division by zero when d^{\max} is zero. If the value of index is always zero or positive, and the maximum value of index, then it can be set $d^{\min} = 0$ and the equation (6.2) can be simplified into

$$\delta = \frac{d}{d^{\max}} \dots\dots\dots(6.3)$$

Figure 6.9 shows the normalized disease index map, the value corresponds to less than 0.5 represents the crops under crown choke disorder, 0.5 to 0.75 are moderately healthy and above 0.75 values represents the in good health.

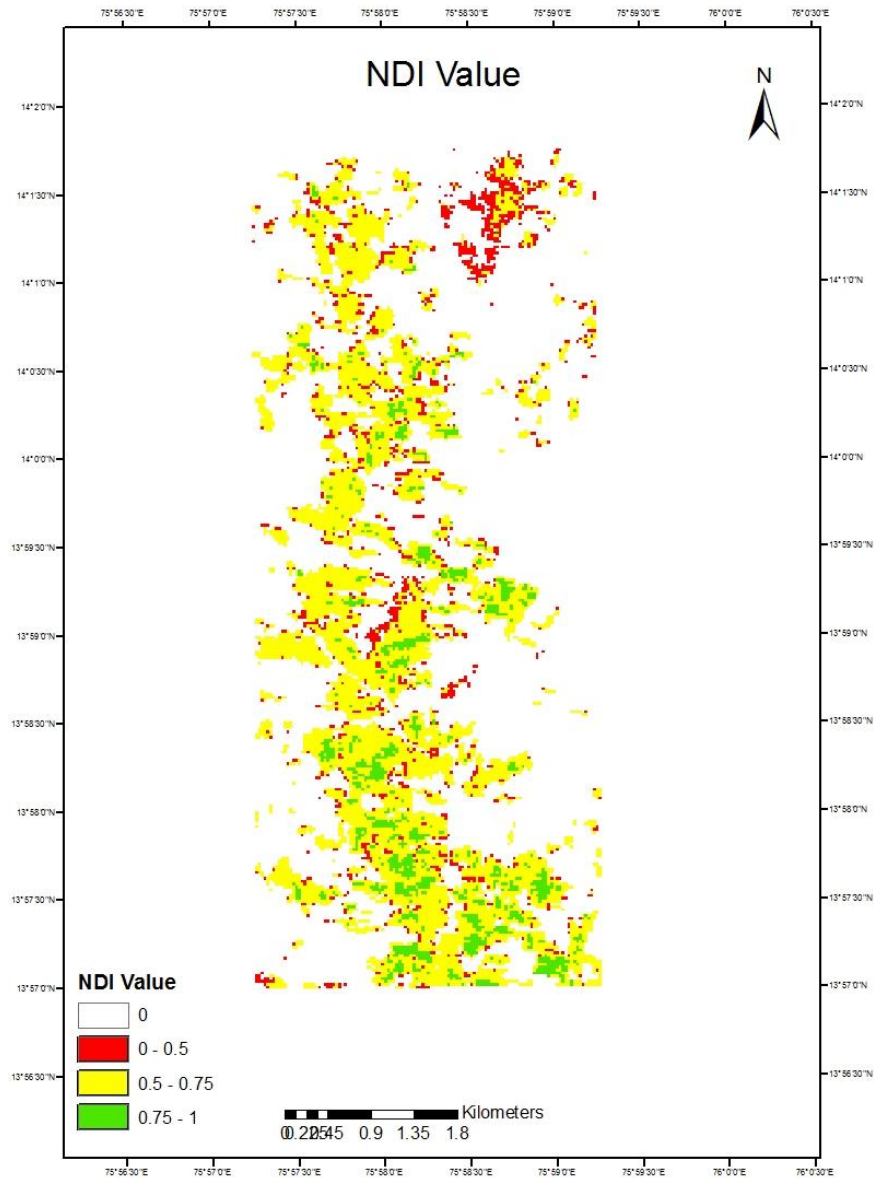


Figure 6.9 Normalized Disease Index map

6.3 Age Index

Chapter 5 gives the detailed description about the Arecanut crop classification based on different age group. The analysis concludes that it is possible to discriminate Arecanut crops into different age group. The spectral library plot showed in Figure 6.10 shows clear distinction between Arecanut each age group, more clearly at visible and NIR region. Taking advantages of this discrete separability using the age index has been proposed.

Index is designed by the wavelength combinations of 540, 680 and 780nm, to segregate Arecanut crops into different age groups. The main objective is to simplify the classification for a better accuracy. Three index points were identified as sensitive towards age of the crop and named it as points A, B and C. Figure 6.11 shows the index points A, B and C those form a triangle to derive AI.

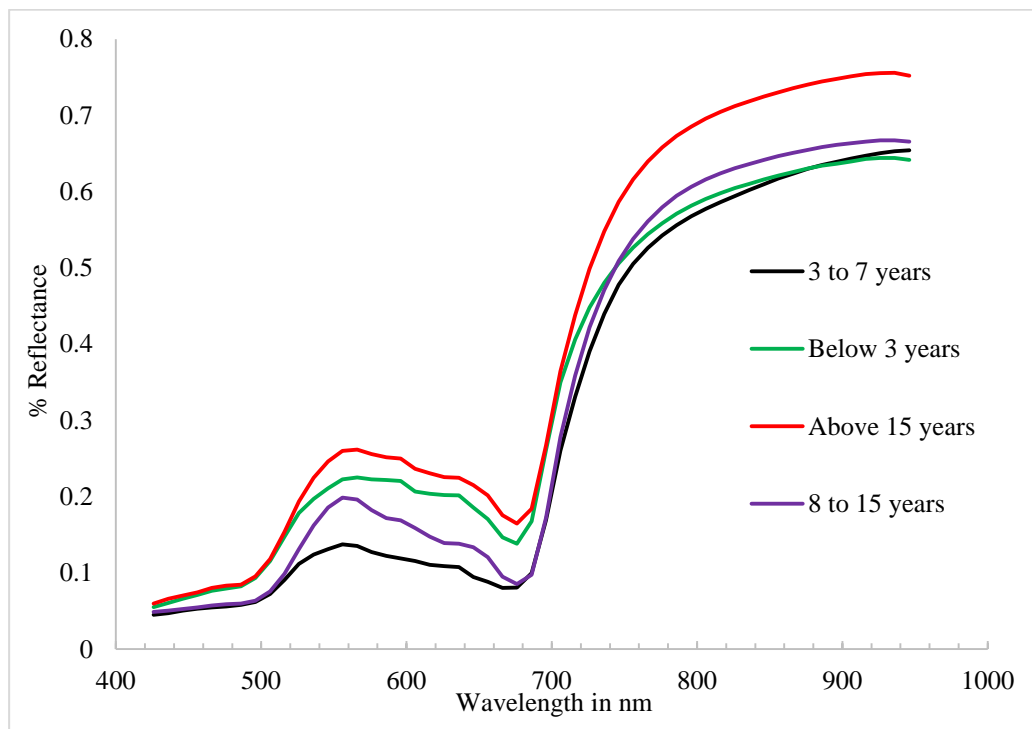


Figure 6.10 Spectral library of different age group Arecanut crops

The idea behind selecting NIR region is to segregate the stressed vegetation, (if considered crop is diseased then $CB' = AB''$ and the ratio become null). There is a clear distinction between the age groups at visible and NIR portions. Hence, these regions can be optimally used for deriving an age index by calculating the difference. Higher the difference more will be age and lower values corresponds for younger age. The derived age index is a ratio of differences of three index points. Equation 6.4

represents the age index. The range of AI values varied from minimum of 3 to maximum of 4.5 and the value corresponds to 4.5 is for above 15 years' age crop, value corresponds to 3 belongs to below 3 years crops.

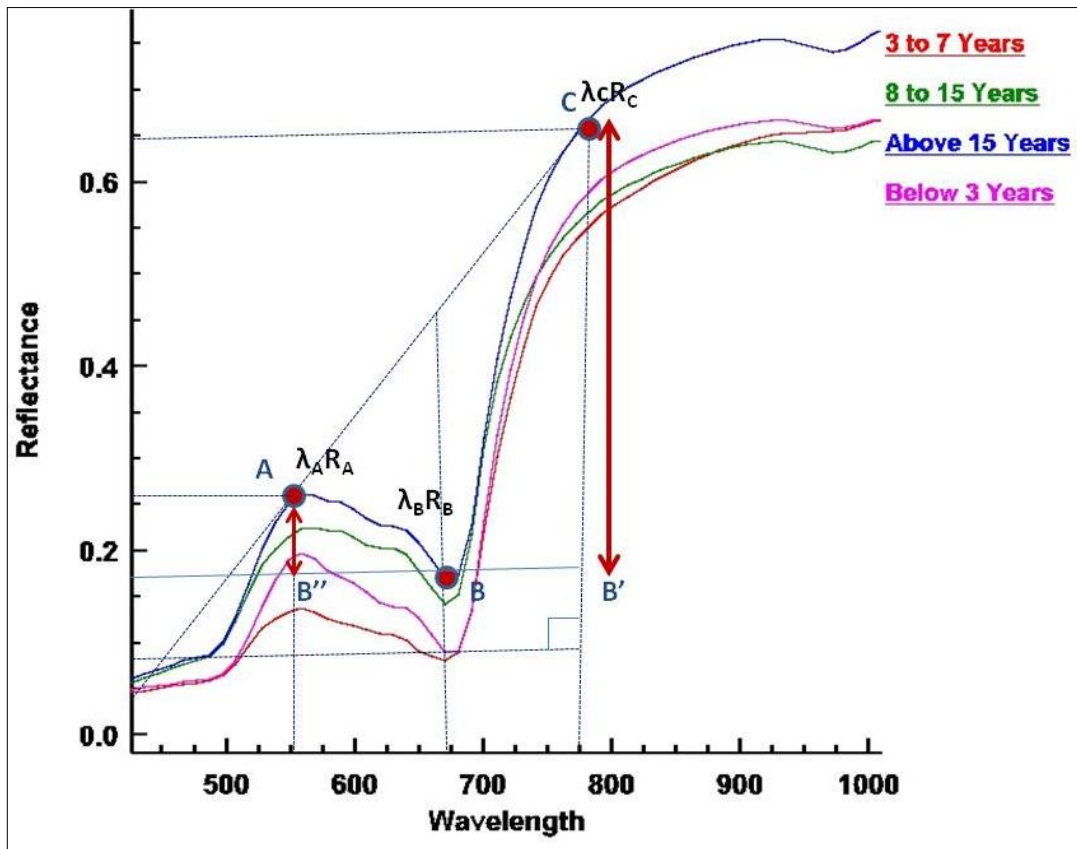


Figure 6.11 Index points A, B and C those form a triangle to derive AI

$$AI = \frac{\lambda_C R_C - \lambda_B R_B}{\lambda_A R_A - \lambda_B R_B} \dots \dots \dots (6.4)$$

Where $B = B' = B''$

Substituting the reflectance values corresponding to wavelengths of 540, 680 and 780nm, for above fifteen years crop.

$$AI = \frac{0.64 - 0.12}{0.24 - 0.12}$$

$$AI = 4.33$$

Here Age Index value for fifteen years crop is 4.33.

Table 6.1 shows the age wise Arecanut crop water requirement; the crop less than 5 years consumes minimum of 19 liter and maximum of 23 liters per day for 9-15-year crop.

Table 6.1 Age wise Arecanut Crop Water Requirement

Crop Class	Area (hectares)	Avg. K_c Values	Avg. CWR (liters/plant)
< 5 Year	217.71	0.76	19.00
5-8 Year	16.83	0.85	21.02
9-15 Year	0.81	0.93	23.01
16- 25 Year	195.48	0.90	22.37
> 25 Year	221.04	0.79	19.69
Stressed	132.93	0.90	22.48

Total Crop Area = 784.80 hectares; Gross CWR = 28056.09 m³.

The derived age index is validated with the calculated crop water requirement and it yielded an R^2 of 0.56 is shown in Figure 6.12. As the crop water requirement is depending on age of the crop there is comparatively good correlation between these two.

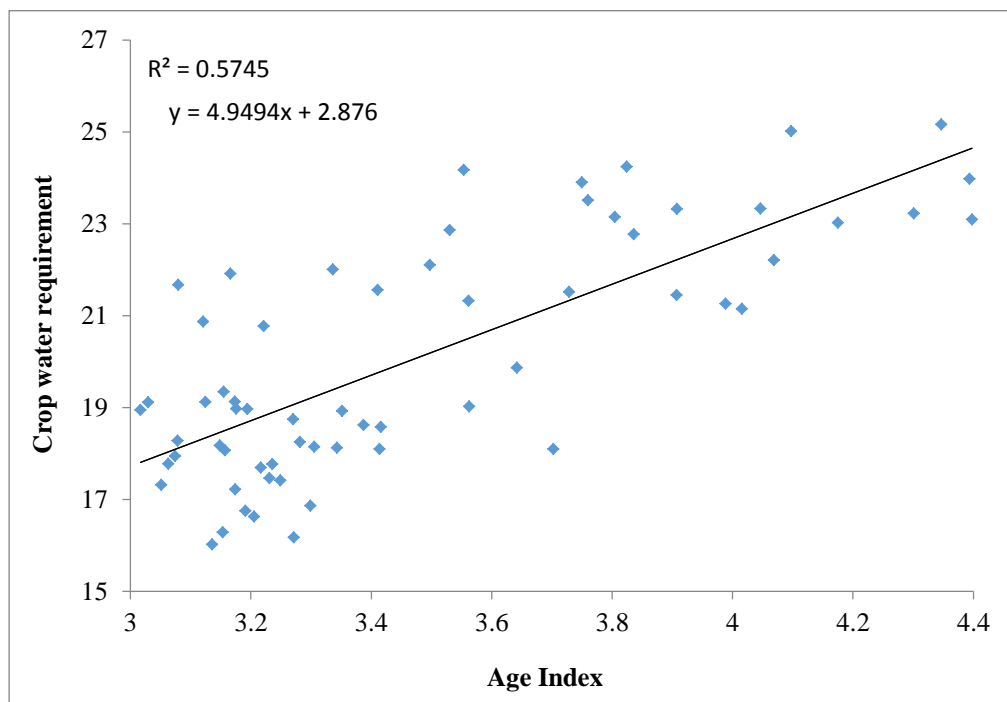


Figure 6.12 Age Index validations

6.4 Summary

With regard to disease Index (DI) spectra obtained from healthy and stressed crops helps in choosing the best possible range, of visible, near infrared and the transition region also known as the red edge position of the spectral curve. The newly derived DI is useful for discriminating stressed Arecanut crops with healthy. And also it indicates that the proposed band combination has better correlation with the chlorophyll content than the other vegetation indices and thus proves to be best. This index uses only three narrow channels centered i.e. R_{750} , R_{550} and R_{675nm} . The derived DI values ranges from 0.45 to 1.5 respectively.

The derived age index is a ratio of differences of three index points corresponds to 540, 680 and 780nm, has the ability to segregate Arecanut crop into different age groups. The range of AI values varied from 3 to 4.5, the value corresponds to 4.5 is above 15 years' age crop. And the value corresponds to 3 belongs to below 3 years crops. The derived age index is validated with the calculated crop water requirement and it yielded an R^2 of 0.56.

In the next chapter hyperspectral vegetation index for age based Arecanut crop water requirement is presented.

HYPERSPECTRAL VEGETATION INDEX FOR AGE BASED ARECANUT CROP WATER REQUIREMENT

7.1 Introduction

The objective of this chapter is to map the age based Arecanut crop water requirement. Irrigation water requirement of crops is defined as, "The quantity of water required by a crop in a given period of time for normal growth under field conditions." It includes evaporation and other unavoidable wastes. Usually water requirement for crop is expressed in water depth per unit area.

$$\text{Irrigation water requirement} = \text{Crop water need} - \text{available rain fall}$$

For design of water harvesting systems, it is necessary to assess the water requirement of the crop intended to be grown. A certain crop grown in a sunny and hot climate needs more water per day than the same crop grown in a cloudy and cooler climate. Apart from sunshine and temperature, other climatic factors which influence the crop water requirement are humidity and wind speed. When it is dry, crop water needs are higher than when it is humid. In windy climates, the crops use more water than in calm climates. The highest crop water needs are thus found in areas which are hot, dry, windy and sunny. The lowest values are found when it is cool, humid and cloudy with little or no wind. In other words, crop water requirement is the amount of water needed to meet water loss through evapotranspiration. Evapotranspiration (ET) is a term describing the transport of water into the atmosphere from surfaces, including soil (soil evaporation), and from vegetation (transpiration). The latter two are often the most important contributors to evapotranspiration.

Other contributions to evapotranspiration may include evaporation from wet canopy surface (wet-canopy evaporation), and evaporation from vegetation-covered water surface in wetlands. The evaporation component of ET is comprised of the return of water back to the atmosphere through direct evaporative loss from the soil surface, standing water (depression storage), and water on surfaces (intercepted water) such as leaves and/or

roofs. Transpired water is that which is used by vegetation and subsequently lost to the atmosphere as vapour. The water generally enters the plant through the root zone, is used for various bio physiological functions including photosynthesis, and then passes back to the atmosphere through the leaf stomata. Transpiration will stop if the vegetation becomes stressed to the wilting point, which is the point in which there is insufficient water left in the soil for a plant to transpire. Crop water requirement depends on two factors first the weather parameters (Reference crop evapotranspiration) and crop parameter (Crop coefficient). The reference crop evapotranspiration ET_0 (sometimes called potential evapotranspiration, PET) is defined as the rate of evapotranspiration from a large area covered by green grass which grows actively, completely shades the ground and which is not short of water. The rate of evapotranspiration depends on the climate. The highest value of ET_0 is found in areas which are hot, dry, windy and sunny whereas the lowest values are observed in areas where it is cool, humid and cloudy with little or no wind. The crop factor (or "crop coefficient") depends on crop type and varies according to the growth stage of the crop. There are four growth stages to distinguish:

- the initial stage: when the crop uses little water;
- the crop development stage, when the water consumption increases;
- the mid-season stage, when water consumption reaches a peak;
- the late-season stage, when the maturing crop once again requires less water.

To overcome these complications faced by the Arecanut farmer's plantation crop monitoring with advanced techniques is important.

In addition to classifying whole image to a set of classes, abundance of certain feature can be mapped to find its geographic presence and distribution using Hyperspectral optical data.

Knowing the exact amount of irrigation water requirement is essential not only for sustainable water resources planning but also for increased yield, particularly in summer. This information is useful for Indian agricultural scenario where monsoon lasts for few months and rest of the year irrigation is necessary. Periodic and precise mapping of total area of Arecanut crop, area under different age groups and crop under stress are some of the inputs not only for estimating crop water requirement but also for policy and decision makers.

Periodic and precise mapping of total area of Arecanut crop, area under different age groups and crop under stress are some of the inputs for estimating crop water requirement. Crop water requirement (CWR) is the total amount of water required to balance the loss of water from crop foliage due to evapotranspiration, which is a function of local climate and crop condition. Estimating crop water requirement by computing crop evapotranspiration is a widely used method. Crop evapotranspiration (ET_c) is governed by weather and crop condition, Ray and Dadhwal (2000).

For increased yield and sustainable water resources planning and management predicting exact amount of irrigation water requirement is essential, particularly in summer. Various methods are available to estimate the crop water requirement, but due to non-availability of data such as wind velocity and other parameters NDVI based crop water requirement method is adopted in this study.

7.2 Crop Water Requirement through NDVI based Crop Coefficient

Image ratio based Normalized Difference Vegetation Index (NDVI) can be expressed mathematically as,

$$NDVI = \frac{NIR-RED}{NIR+RED} \quad (7.1)$$

The Normalized Difference Vegetation Index (NDVI) is a numerical indicator that uses the visible and near-infrared bands of the electromagnetic spectrum, and is adopted to analyse remote sensing measurements and to assess whether the target being observed contains live green vegetation or not. Generally, healthy vegetation will absorb most of the visible light that falls on it, and reflects a large portion of the near-infrared light. Unhealthy or sparse vegetation reflects more visible light and less near-infrared light. Bare soils on the other hand reflect moderately in both the red and infrared portion of the electromagnetic spectrum.

Values of NDVI ranges between -1 and +1. However, no green leaves give a value close to zero and in general, pixels with value above 0.4 indicates vegetation. Higher values of NDVI indicate higher degree of photosynthetic activity or in other words healthy or dense vegetation.

Kamble et al. (2013) developed and validated equation to calculate K_c using NDVI based on regression analysis between NDVI derived from remotely sensed data. Spectral bands 672 nm and 855 nm were implemented to calculate NDVI values and AmeriFlux measured crop coefficient under irrigated and rain fed crop condition for various crops. This equation can be used with Hargreaves and Samani equation to compute crop water requirement. There was a strong linear correlation between the NDVI-estimated K_c and the measured K_c with an r^2 of 0.91 and 0.90, while the root-mean-square error (RMSE) for K_c were 0.16 and 0.19, respectively for two different years in which experiments were carried out. Crop coefficient K_c , was computed based on the equation:

$$K_c = 1.457NDVI - 0.1725 \quad (7.2)$$

Crop water requirement is the amount of water required to compensate the evapotranspiration loss from the cropped field, Allen et al. (1998). In other words, water requirement of a crop is equivalent to water loss due to soil evaporation and transpiration from plant canopy. But soil evaporation component is negligibly small as plant foliage shades the soil beneath, along with efficient drip irrigation system considering no irrigation loss. Hence crop water requirement (CWR in mm/day) can be expressed as,

$$CWR = ET_c = K_c * ET_o \quad (7.3)$$

Daily reference crop evapotranspiration (ET_o in mm/day) is computed based on equations presented by Hargreaves and Samani:

$$ET_o = 0.0135(KT) (R_a) (TD)^{1/2}(TC+17.8) \quad (7.4)$$

Where TD is temperature difference between daily maximum and minimum temperature ($^{\circ}C$), TC is the daily mean temperature ($^{\circ}C$), R_a is extraterrestrial radiation ($MJ\ m^{-2}\ d^{-1}$) which is a function of latitude of location, inverse relative distance from earth to sun, solar declination etc. calculated with reference to FAO 56, and KT is an empirical coefficient which depends on temperature difference.

$$KT = 0.00185(TD)^2 - 0.0433 TD + 0.4023 \quad (7.5)$$

These values were calculated separately (detailed calculations are presented in Appendix page 159) for the day on which Hyperion imagery was captured.

Obtained value of ET_c in mm/day is converted to l/day/plant by considering standard uniform plant to plant spacing (8 ft or 2.4384 m either way i.e. 151 plants in a pixel of 30m X 30m size) in the study area with drip irrigation practiced throughout.

7.3 Arecanut Crop Water Requirement Index (ACWRI)

A vegetation index (also called a vegetative index) is a single number that quantifies vegetation biomass and/or plant vigor for each pixel in a remote sensing image. The index is computed using several spectral bands that are sensitive to plant biomass and vigor.

In the present work, using correlation analysis on Arecanut canopy reflectance and corresponding value of crop water requirement, an index is built. Canopy reflectance data is obtained from Hyperion imagery with respect to corresponding crop water requirement from the map. Values of the index indicate the magnitude of crop water requirement index in a pixel with Arecanut crops. This will be helpful for spatial comparison of crop water requirement in a rapid manner, even without spectral library of the crop.

7.4 Correlation Analysis

Correlation analysis is a technique for investigating the relationship between two quantitative, continuous variables. Pearson's correlation coefficient (r) is a measure of the strength of the association between the two variables.

$$\rho_{XY} = \text{Corr}(X, Y) = \frac{\text{Cov}(X, Y)}{\sigma_X \sigma_Y} = \frac{E[(X - \mu_X)(Y - \mu_Y)]}{\sigma_X \sigma_Y} \quad (7.6)$$

Where E is the expected value operator, cov means covariance, and corr is a widely used alternative notation for the correlation coefficient.

In the present work correlation analysis was helpful in identifying specific wavelengths in electromagnetic spectrum having association with water requirement of Arecanut plants.

7.5 image classification using Spectroradiometer based reflectance spectra

Reflectance spectra of various age groups and stress levels of Arecanut crops signatures for all age group were derived by averaging numerous samples falling in the group and used for image classification through SAM classifier.

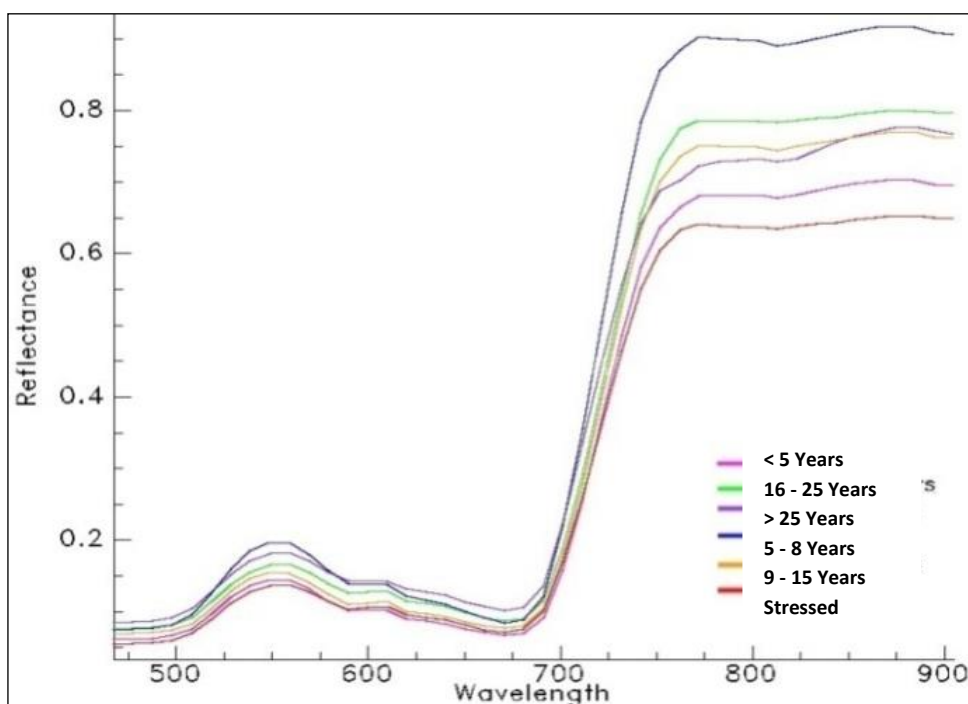


Figure 7.1 Spectral reflectance discrimination of crop

Various age groups and their reflectance behaviour in wavelength range from 460 nm to 910 nm considered for classification are presented in Figure 7.1. Arecanut crops are divided into five different classes based on age and one class of stressed crops affected by crown choke disease. The classes were, < 5 years' age: The juvenile crops, 5-8 years old crops: Slightly older crops in the verge of senescence, 9-15 years old crops: crops which start flowering and yielding. 16-25 years old crops: Adult plants which are in the peak of yielding, >25 years old crops: Older crops with lower yield. Stressed Arecanut crops are generally of age 10 years or older and fail to reflect back radiation in both NIR and visible region compared healthy crops.

The reflectance spectra of Arecanut crop have clear distinction with respect to age of crop. Reflectance in green region (525-575 nm) has clear variation showing increase in greenness of the crop on aging. In the red region (620-750 nm) a decreasing trend in reflectance show higher the chlorophyll content, higher the absorption of light in this range. Major variation is observed in NIR region (750-900 nm) where young (5-9 years old) and mature (16-25 years old) crops have distinctly high reflectance showing higher level of photosynthesis compared to juvenile (<5 years old) and (>25 years old).

Crown choke affected crops showed least reflectance in NIR region which was due to its inability to reflect light in this range due to lesser chlorophyll content.

The Spectral Angle Mapper (SAM) technique is used to classify hyperspectral data Figure 7.2 shows the crop map generated by SAM classifier.

SAM classification was performed with an overall accuracy of 73.68% and overall kappa statistics is 0.67. Obtained accuracy of classification is rational for a within class classification of vegetation.

The study area has 784.80 hectares of land is under Arecanut crop cultivation with 132.93 hectares of stressed plantation. Most of the crop belonged to either old (>25 year) or juvenile (<5 years) class. Precisely 221.04 hectares (28.16 %) of crop were old whereas 217.17 hectares (27.74%) were juvenile. 16.83 hectares of crop were of age 5-8 years old, 195.48 hectares of crop were of age 16- 25 years and merely 0.81 % were found to be healthy crops of age 9-15 years. The major reason for lower crops of middle age is the plant stress due to crown coke disease which was found to have affected 132.93 hectare (16.93%) of cropped area. Figure 7.2 shows the SAM classified map. Figure 7.3 shows the NDVI value variations for Arecanut crop and Figure 7.4 the Arecanut crop coefficient value map.

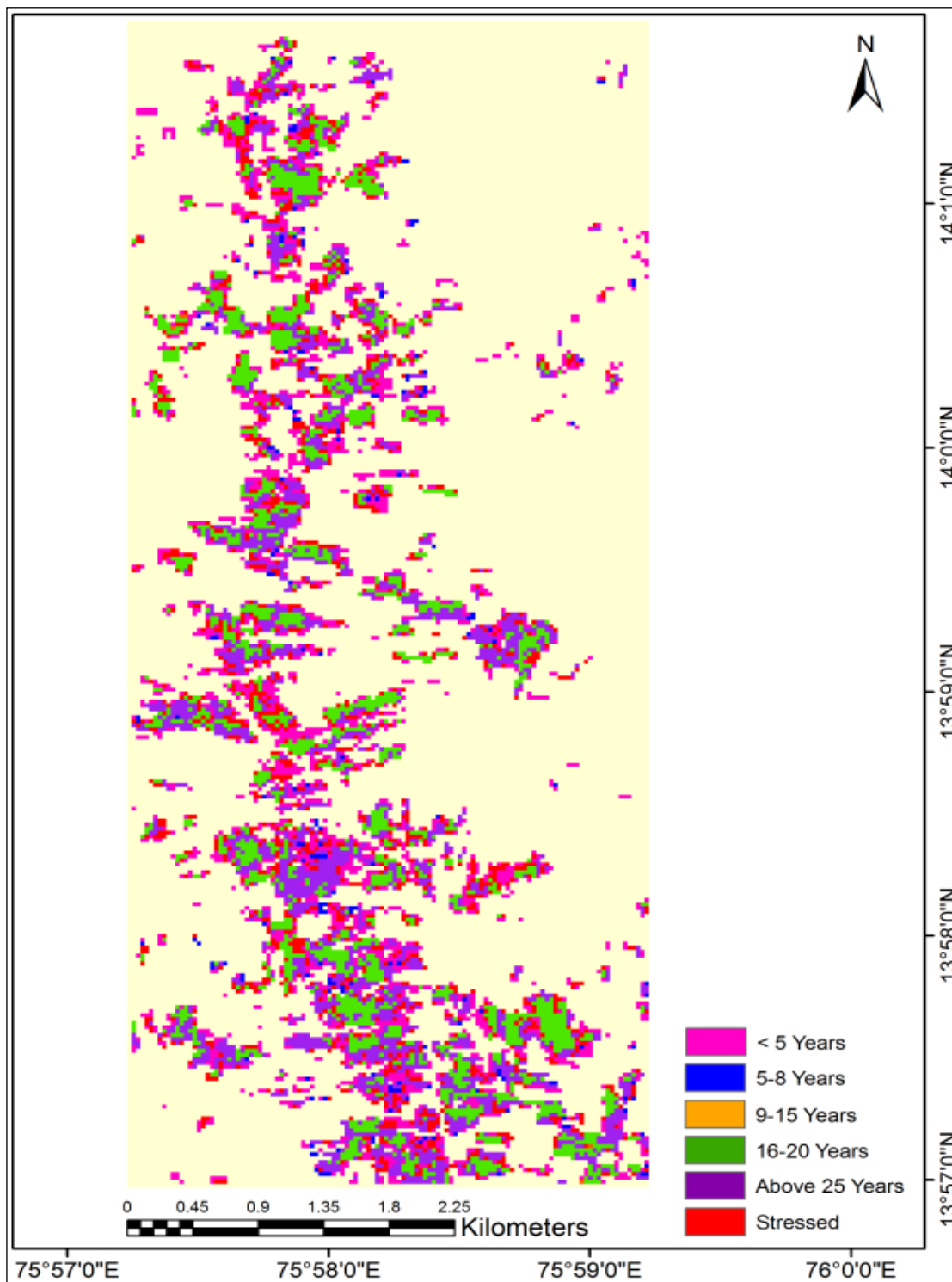


Figure7.2 SAM classified Arecanut crop map

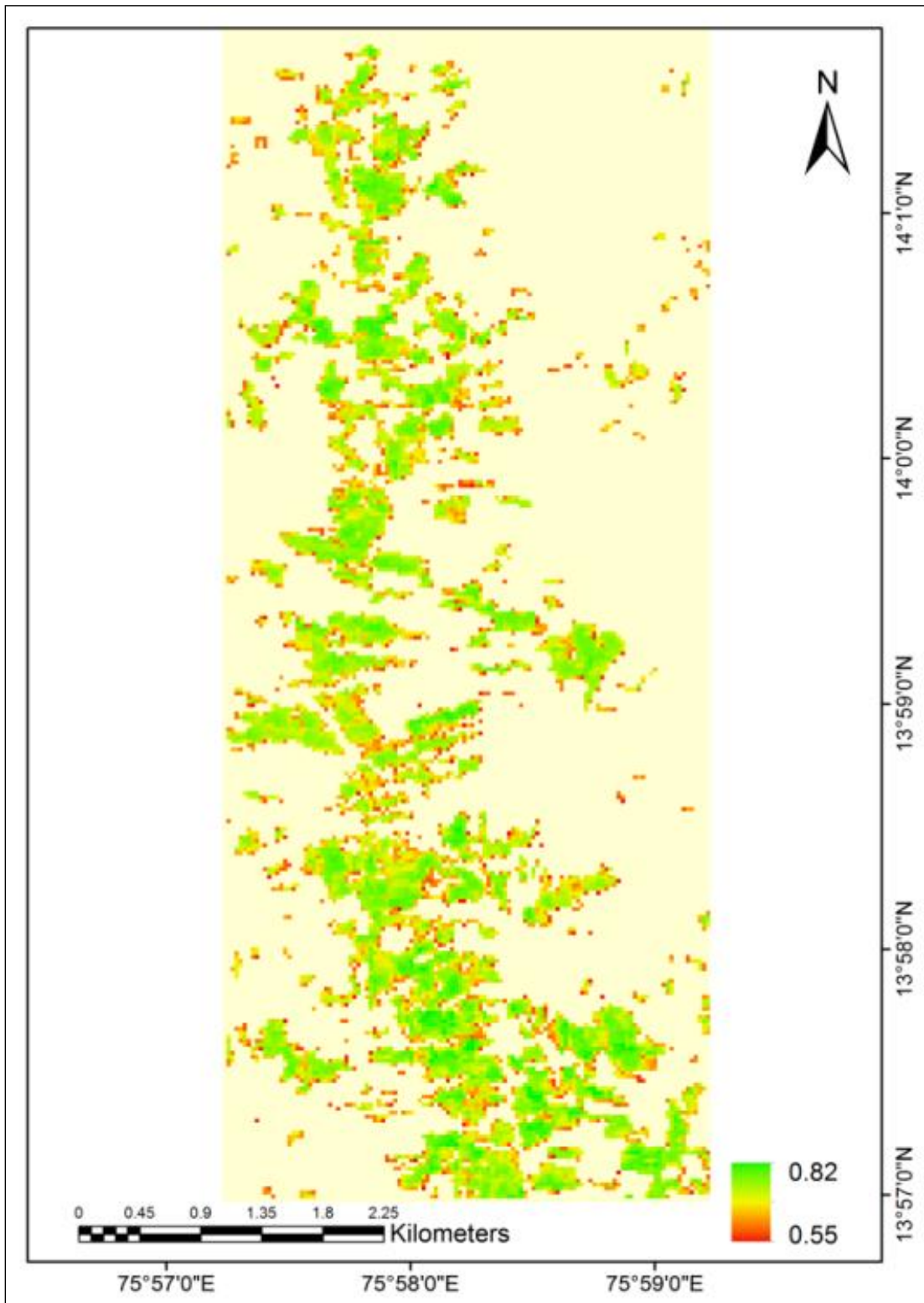


Figure 7.3 Arecanut crop NDVI map

NDVI values of Arecanut crop varied from a minimum value of 0.55 to a maximum value of 0.82. This ascertains the variation in crops in terms of plant vigor either due to variation in age or due to plant stress.

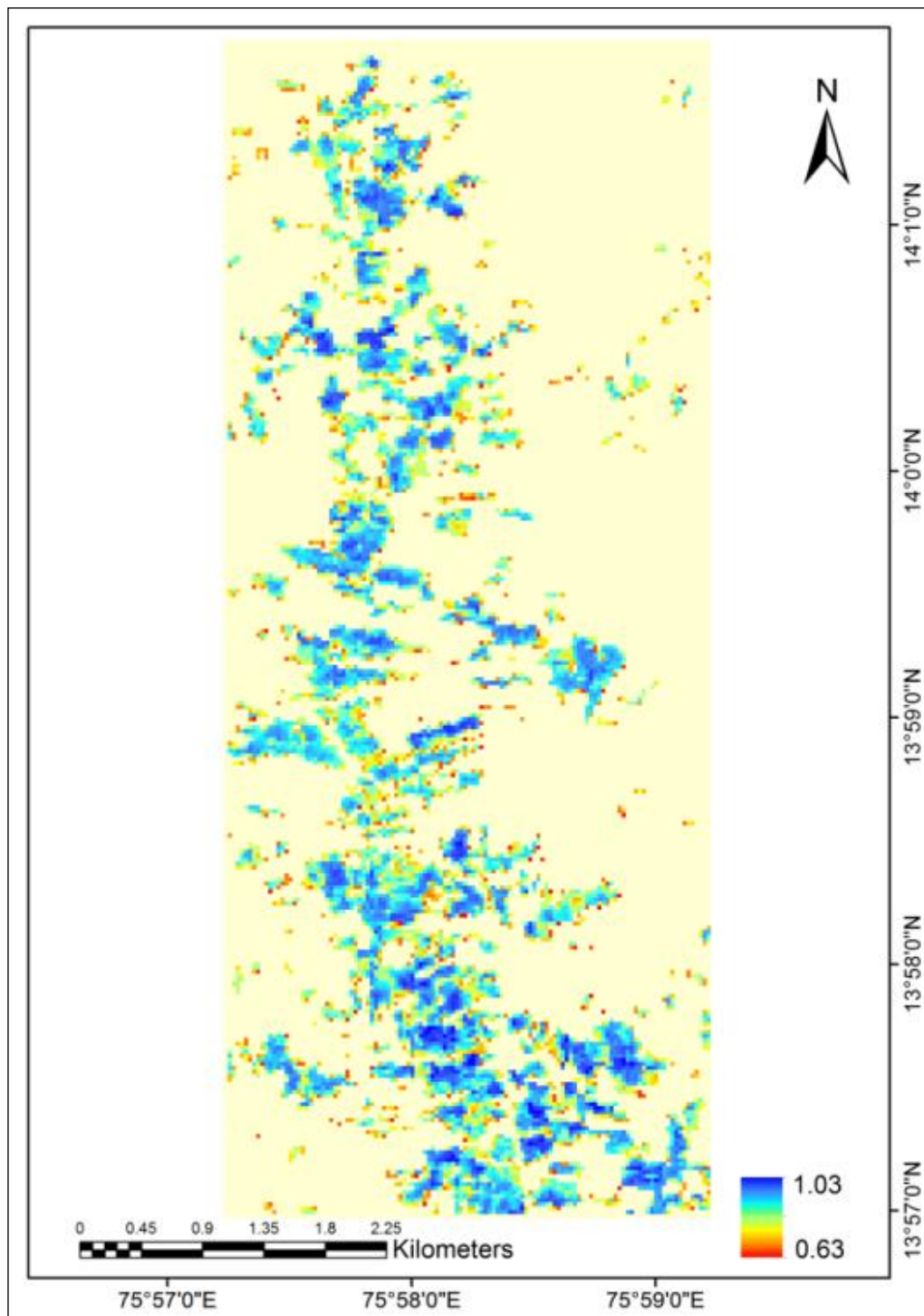


Figure7.4 Arecanut crop K_c map

Crop coefficient map developed based on NDVI (using eqn. 4.2) reveals K_c varied between 0.63 to 1.03 suggesting average crop evapotranspiration lesser than potential evapotranspiration.

From Table 7.1, it can be observed that daily crop water requirement is a function of crop age and varied from 19 liters to 23 liters. The total cropped area of 784.80 hectares had water demand of 28056.09 m³. Image classification showed 132.93 hectares (16.93%) of crops were affected by crown choke disease. Cumulative average water requirement is equal to 21.26 liters. The results are in agreement with the findings of Balasimha et al. (1996). Table 7.1 shows age wise Arecanut crop water requirement.

Table 7.1 Age wise Crop Water Requirement

Crop Class	Area (hectares)	Avg. K_c Values	Avg. CWR (liters/plant)
< 5 Year	217.71	0.76	19.00 ≈ 19.00
5-8 Year	16.83	0.85	21.02 ≈ 21.00
9-15 Year	0.81	0.93	23.01 ≈ 23.00
16- 25 Year	195.48	0.90	22.37 ≈ 22.50
> 25 Year	221.04	0.79	19.69 ≈ 20.00
Stressed	132.93	0.90	22.48 ≈ 22.00
Total Crop Area = 784.80 hectares; Gross CWR = 28056.09 m ³ .			

Figure 7.5 shows the Arecanut crop water requirement map. From the figure it is observed that ACWR differs 15 to 25 l/day/plant for below 5 years crops to 25 years crop respectively.

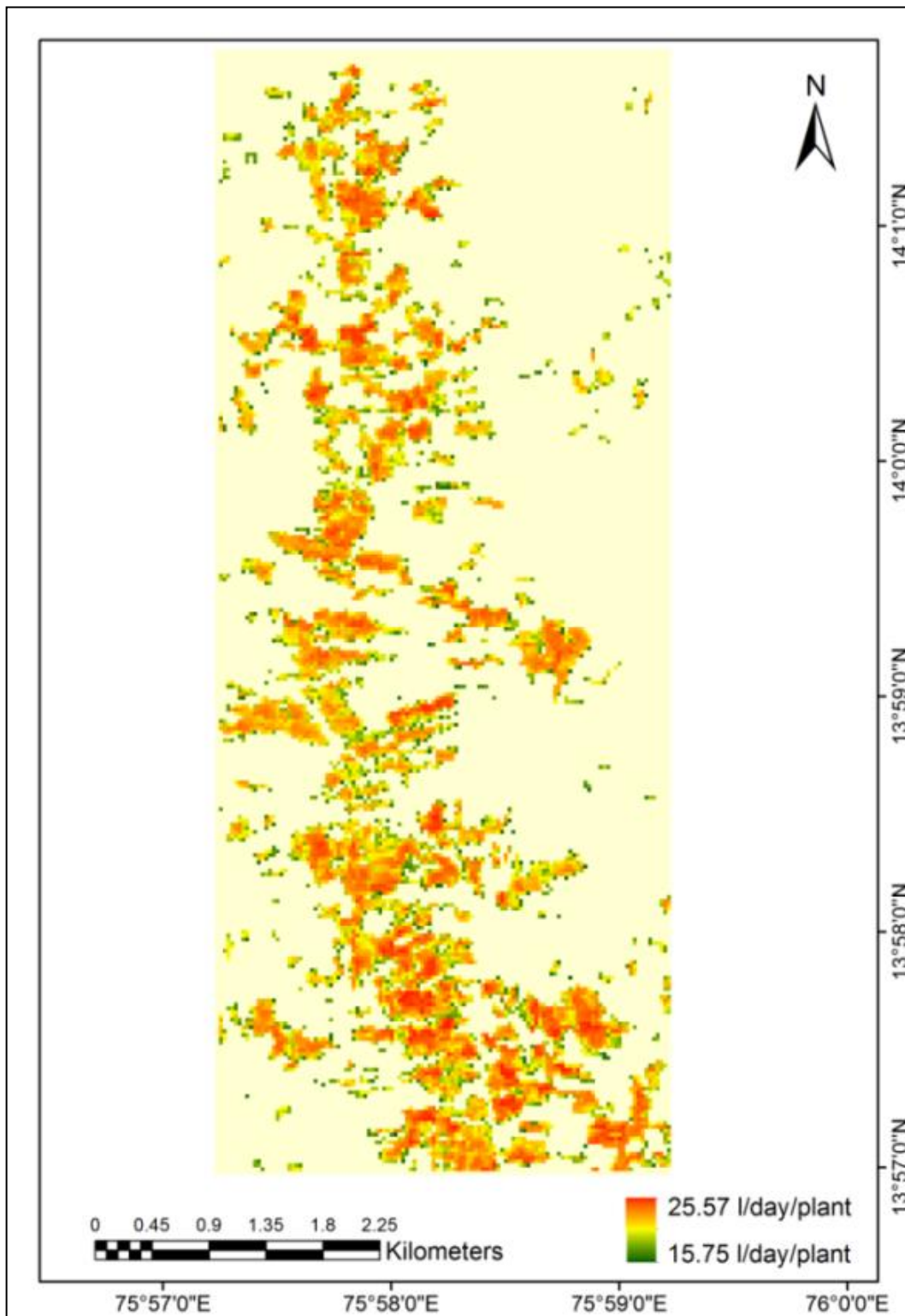


Figure7.5 Arecanut age wise crop water requirement map

7.6 Arecanut Crop Water Requirement Index

The most common vegetation index is the normalized difference vegetation index (NDVI) helps identify areas of varying levels of plant biomass/vigor. Higher values indicate high biomass/high vigor.

The best combination of narrow wavebands for a normalized difference type of vegetation index to assess Arecanut crop water requirement was investigated. Figure 7.6 shows the reflectance plots of data used for correlation analysis and the reflectance data with corresponding CWR values is shown as matrix in Appendix II. The basis of crop variable specific waveband selection was the two-band normalized difference vegetation index.

$$\text{Index} = \frac{\lambda_2 - \lambda_1}{\lambda_2 + \lambda_1} \dots\dots\dots(7.7)$$

75 bands between 467 nm to 1295 nm were selected for the analysis. All possible two-pair combinations ($\lambda_2 > \lambda_1$) of 75 wavelengths (2,775 combinations) were used in Equation 7.7 and a correlation analysis was performed in order to determine the correlation coefficient (r). All the r values were plotted in a matrix plot and the plot revealed a characteristic pattern with a number of “hot spots” with relatively high correlation coefficients. Figure 7.6 shows reflectance plots of data used for correlation analysis.

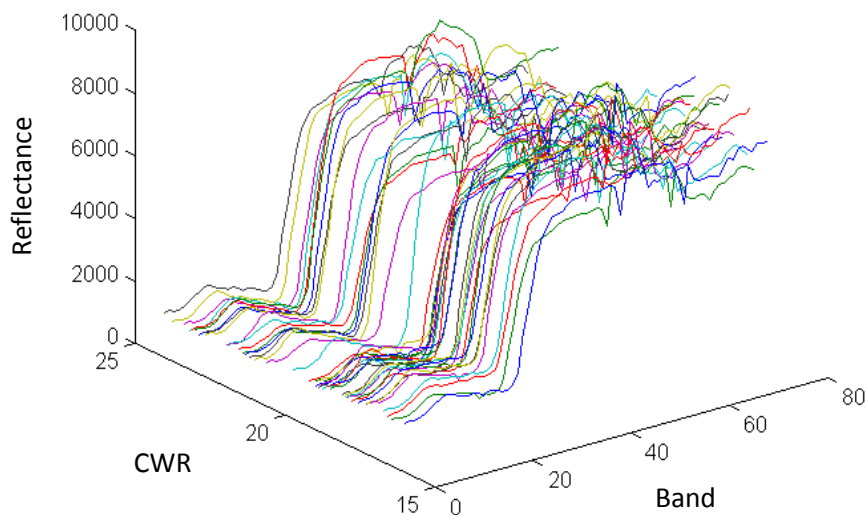


Figure7.6 Reflectance plots of data used for correlation analysis

The analysis results as shown in Figure 7.7 revealed bands $\lambda_2= 844\text{nm}$ and $\lambda_1 =691\text{nm}$ showed the highest correlation ($r= 0.892$), and were selected as key bands to build the index as,

$$\text{Arecanut Crop Water Requirement Index} = \frac{\lambda_{844}-\lambda_{691}}{\lambda_{844}+\lambda_{691}} \quad (7.8)$$

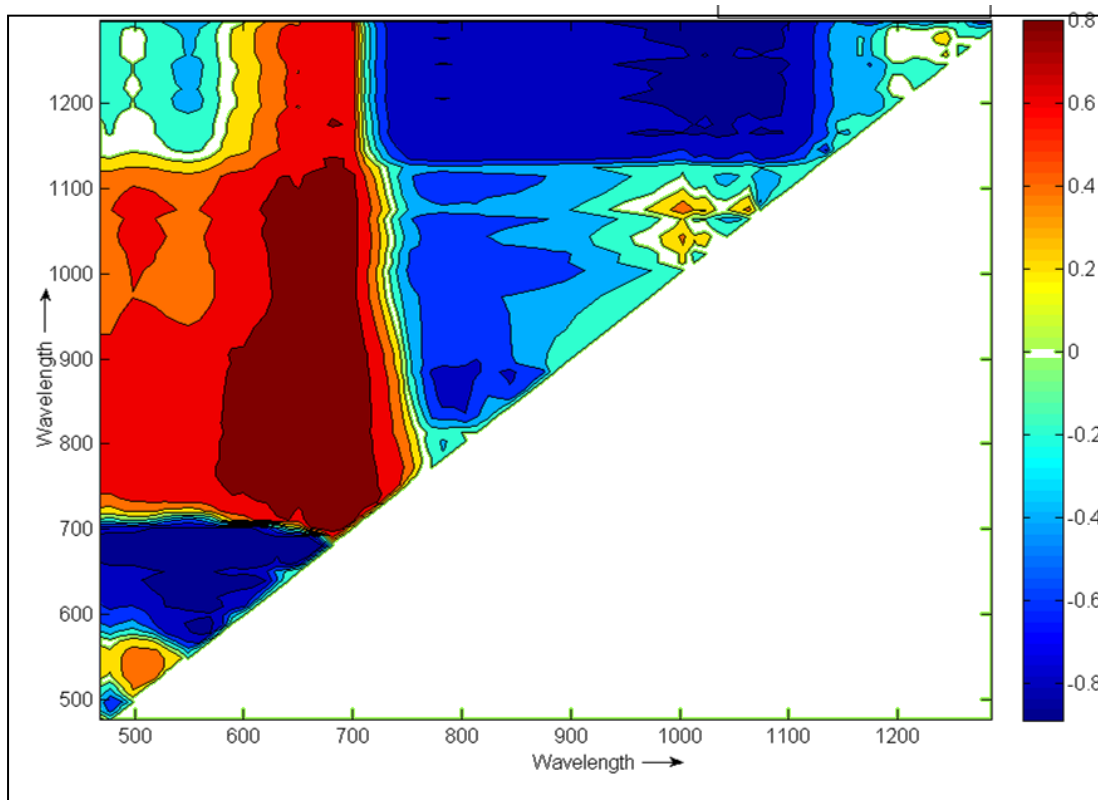


Figure7.7 Coefficient of correlation plot for all band combinations of equation 7.8

Obtained ACWRI was applied onto study area to derive a map as shown in Figure 7.8. All the correlation coefficient (r) values are plotted in a matrix plot and the plot revealed a characteristic pattern with a number of “hot spots” with relatively high correlation coefficients. Half of the plot shows a value of zero because of the rule $\lambda_2 > \lambda_1$ because of which band combination is reduced to half the possible combinations. The other half would just be a mirror image if considered for computation. A hot spot with highest correlation is shown in dark red shade, and interestingly it can be observed that it extends beyond photosynthetically active region/radiation (PAR).

Figure 7.8 shows the variation of the Arecanut crop water requirement with an index value ranging from 0.3 to 0.8.

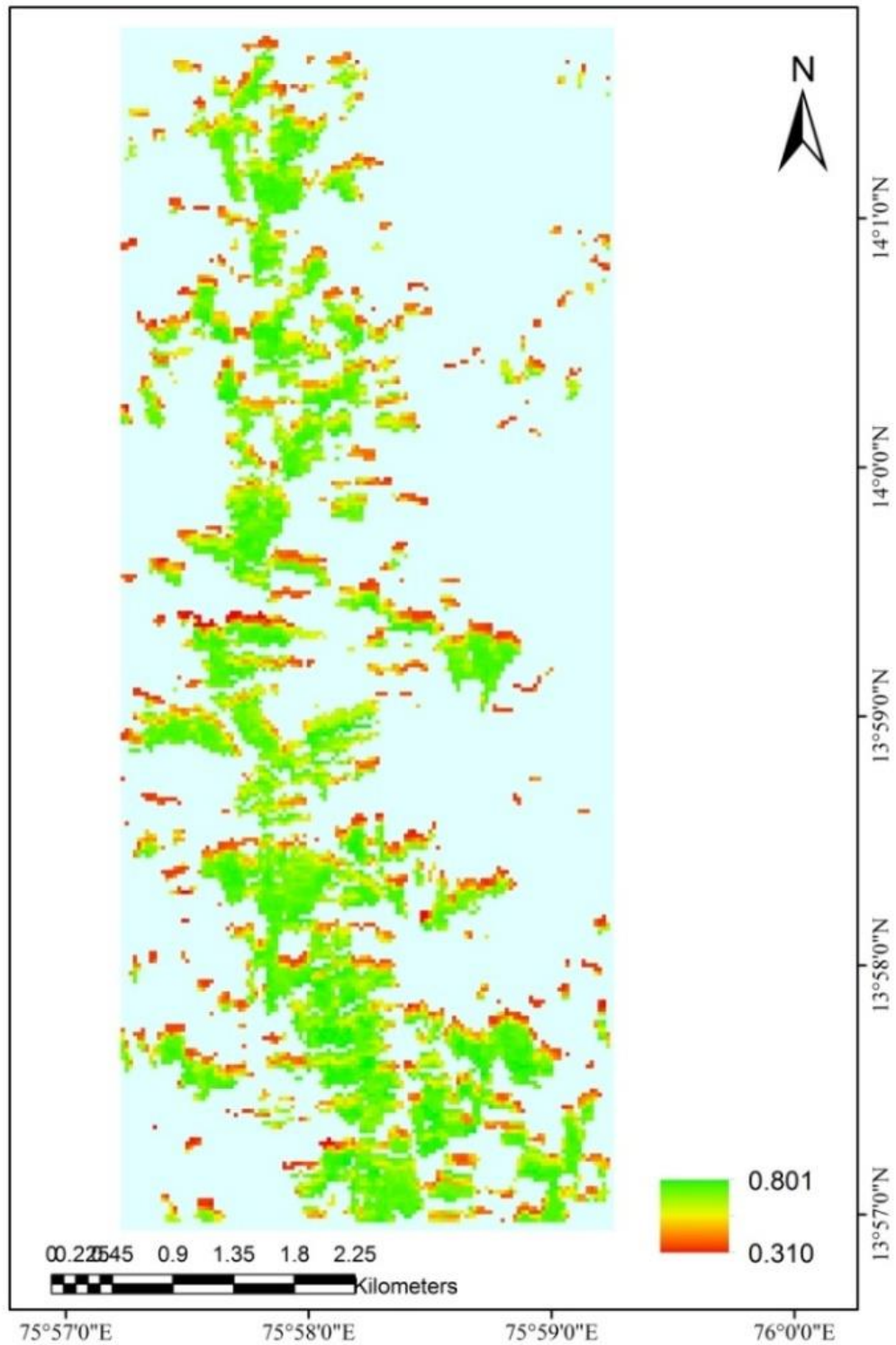


Figure 7.8 ACWRI map of the study area

7.7 Assessment of Arecanut crop water requirement using PLSR model

In the present study using ACWR map, pixel wise Arecanut crop water requirement values and their corresponding spectral signatures from pre-processed Hyperion imagery were extracted and tabulated. In order to establish relation between thus obtained extracted spectral signatures and crop water requirement values, Partial least Regression (PLSR) technique is adopted since the method is proved to be a robust and commonly used statistical technique.

The flexibility of PLS-approach, its graphical orientation and its inherent ability to handle incomplete and noisy data with many variables (and observations) makes PLS a simple but powerful approach for the analysis of data of complicated problems (Wold et al., 2001). It can also be extended in various directions as PLSR provides an approach to quantitative modelling of often complicated relationships between predictors (X) and response (Y) that with complex problems often is more realistic than multiple linear regressions (MLR) including stepwise selection variants. Hence it is found to be appropriate to determine combination of wavelengths to build a model to assess Arecanut crop water demand. In the present study X and Y inputs for the PLSR model are obtained crop water requirement values and corresponding spectral signatures from Arecanut crop water requirement map and pre-processed Hyperion imagery pixels respectively.

In order to establish the relation between thus obtained extracted spectral signatures and crop water requirement values, Partial least Regression (PLSR) technique is adopted. From this ACWR map, pixel wise Arecanut crop water requirement values and their corresponding spectral signatures from pre-processed Hyperion imagery were extracted and tabulated. In order to establish the relation between thus obtained extracted spectral signatures and crop water requirement values, the obtained results from the Partial Least Regression (PLSR) technique is as follows. The selected procedure for identifying the calibration and validation sets is the random selection method to ensure the PLSR model is unbiased. Regression coefficients were obtained from calibration set and then regression was carried out on validation set. The result from PLS modelling shows its capability of estimation of Arecanut crop water requirement (ACWR). Selection of PLSR factors was carried out by computing estimated mean square error prediction. Number of PLSR factors used for ACWR prediction is 7.9. Figure 7.10 shows the ACWR prediction results and comparatively good prediction is observed.

Calibration dataset yielded an R^2 of 0.98 with RMSE of 0.34. Validation dataset yielded an R^2 of 0.97 with RMSE of 0.83. Higher RMSE may be due to high variability, spatial resolution of Hyperion and small sized scattered fields. Figure 7.9 a&b shows the graphical representation of calibration results.

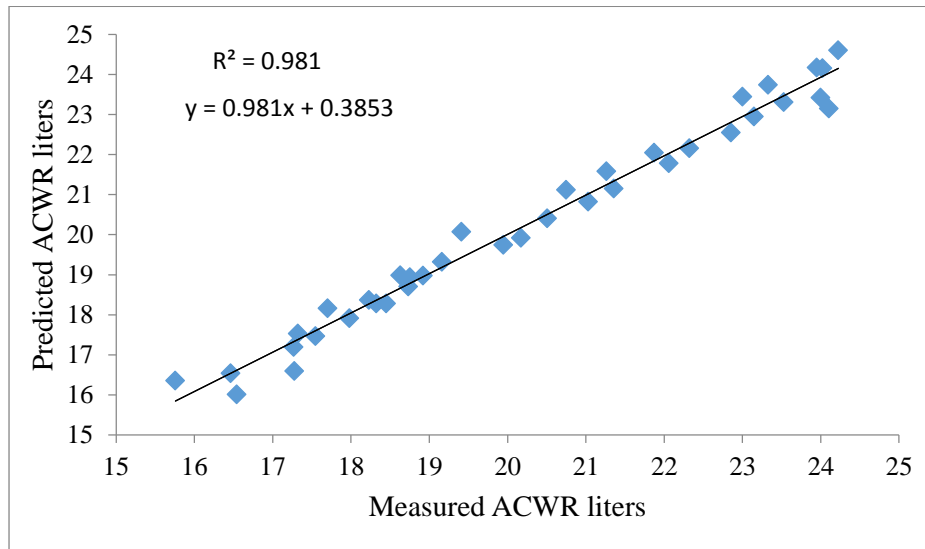


Figure 7.9 (a) PLSR for calibration

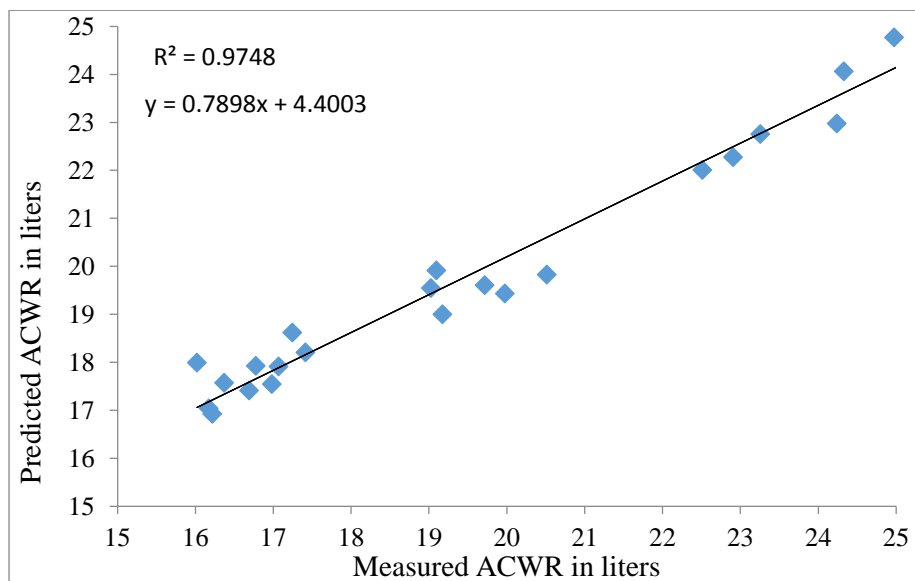


Figure 7.9 PLSR for validation of ACWR

7.8 Arecanut Crop Water Requirement Model (ACWR)

Based on PLSR b-coefficients with 3 factor the important wavelengths found are 548, 681 and 721 the combination of these wavelengths equation is as follows (Eq.7.9)

$$Y = (20.26 - 1.89 * \lambda_{548} - 2.32 * \lambda_{681} + 2.36 * \lambda_{721}) / 100 \dots\dots\dots(7.9)$$

Where Y is the predicated Arecanut water requirement value in terms of l/day/plant and λ_{548} , λ_{681} , λ_{721} are the reflectance values of corresponding wavelengths.

In validation ACWR model with combination of only three wavelengths yielded an R^2 of 0.65. Figure 7.10 shows the model validation graphical representation.

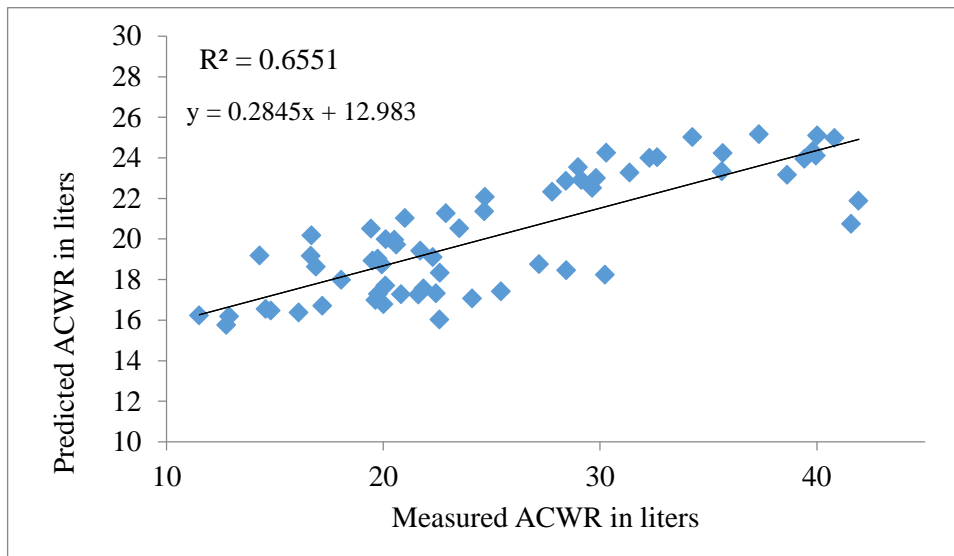


Figure 7.10 Results of Model validation

7.9 Selection of Important Variables

The output from the PLSR algorithm was employed to identify a subset of wavelengths that are significant in predicting the ACWR from spectral reflectance data. For this, both Variable Importance for Projection (VIP) scores and the PLS regression coefficient (β) value were taken as the selection parameters, as observed in similar studies (Mehmood et al. 2012, Rossel et al. 2008). This was executed in MATLAB and the codes used are given in the appendix at the end of this report. Wavelengths corresponding to significantly higher VIP scores and β coefficient values were taken as important from the study undertaken. The graphs representing VIP scores and β coefficient values are illustrated in Figures 7.11 and 7.12.

Selection of important variables is very important when there is collinearity in the dataset. This can be achieved by computing Variable Importance for Projection (VIP) and also by considering b-coefficients. VIP is a weighted sum of squares of the PLS weights, with weights calculated from the amount of Y-Variance of each PLS component (Wold et al.

2001). Greater than 1 rule is used as a criterion for variable selection (Chong and Jun, 2005). Details of VIP are discussed in section 3.13.1 of chapter number 3.

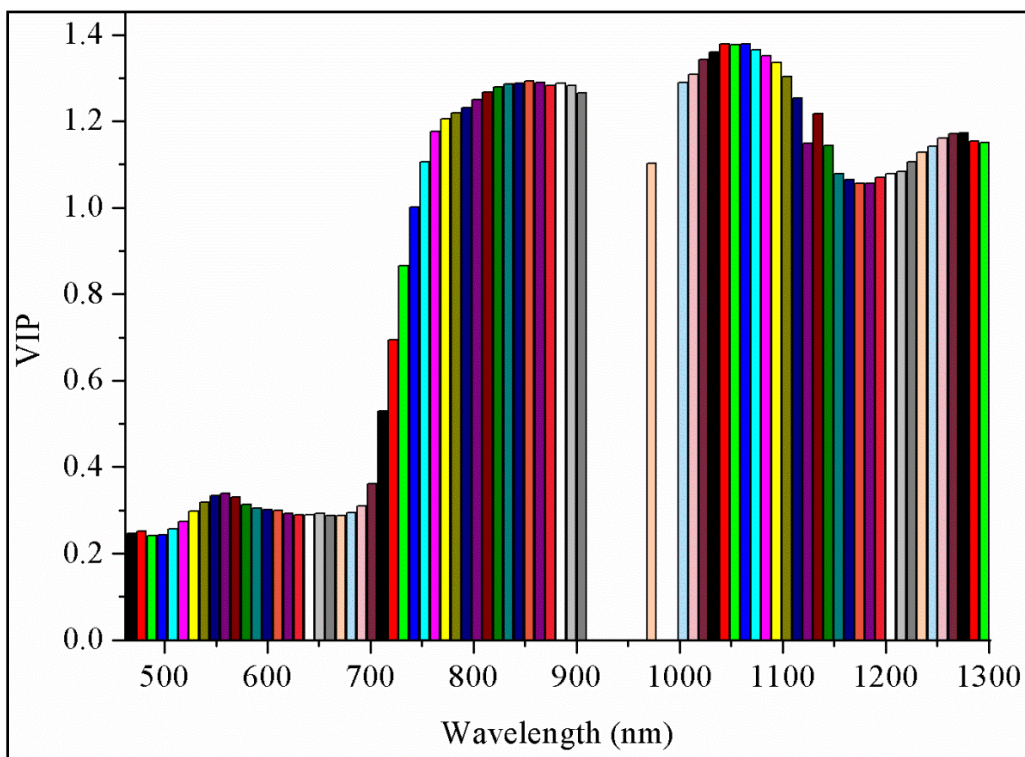


Figure 7.11 VIP scores corresponding to wavelengths

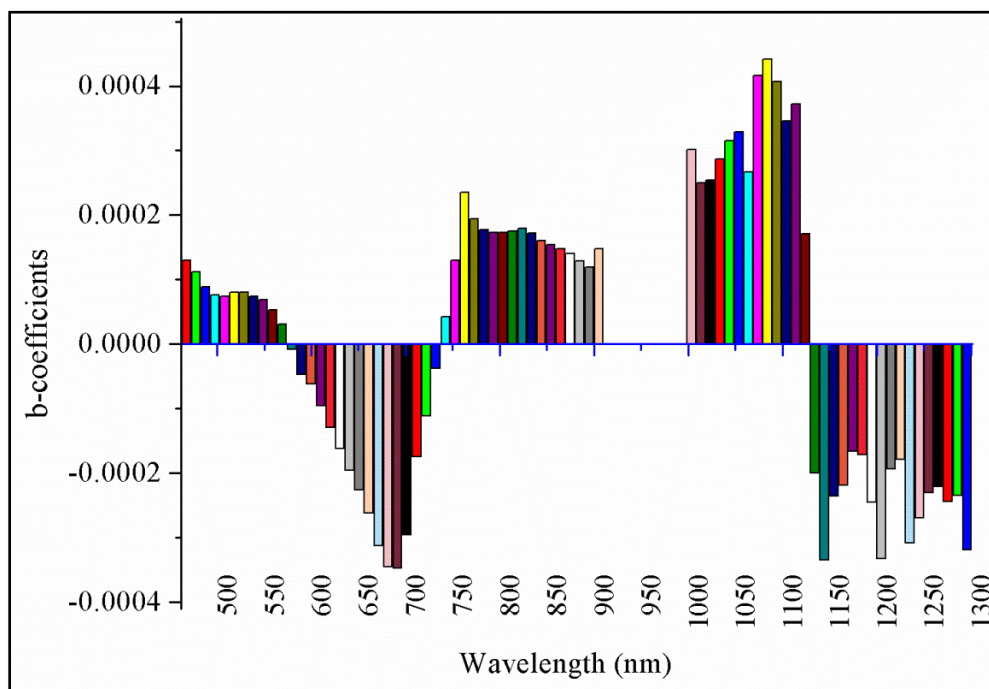


Figure 7.12 β coefficients corresponding to wavelengths for ACWR

After comparing the VIP scores and β coefficient values, a total of eight wavelengths, spanning across VNIR and SWIR regions were identified as significant in modelling the ACWR these were 1043, 1053, 1033, 1083, 1023, 1013, 1104, and 854nm.

7.10 Stepwise Multi Linear Regression (SMLR)

The study employs Stepwise Multi Linear Regression, to evaluate the accuracy compare to PLSR, executed in MATLAB[®] and to prepare a thematic map of age wise Arecanut crop water requirement of the study area using ENVI[®].

Stepwise regression is a systematic method for adding and removing terms from a multi linear model based on their statistical significance in a regression. The method begins with an initial model and then compares the explanatory power of incrementally larger and smaller models. If a term is not currently in the model, the null hypothesis is that the term would have a zero coefficient if added to the model. If there is sufficient evidence to reject the null hypothesis, the term is added to the model. Conversely, if a term is currently in the model, the null hypothesis is that the term has a zero coefficient. If there is insufficient evidence to reject the null hypothesis, the term is removed from the model. Depending on the terms included in the initial model and the order in which terms are moved in and out, the method may build different models from the same set of potential terms. The method terminates when no single step improves the model. There is no guarantee; however, different initial model or a different sequence of steps will not lead to a better fit. (Draper and Smith 1998).

7.10.1 SMLR Results

The obtained Arecanut crop water requirement map pixel values corresponding to pre-processed Hyperion imagery spectral signatures are used for (SMLR) regression. The performance results for ACWR in MATLAB[®] graphical user interface is shown in Figure 7.13 and 7.14. It can be observed that the high R square value and low RMSE values indicates model performance is good. From the results it can be interpreted that band combinations of 681 and 721nm are prominent to predict the age based Arecanut crop water requirement.

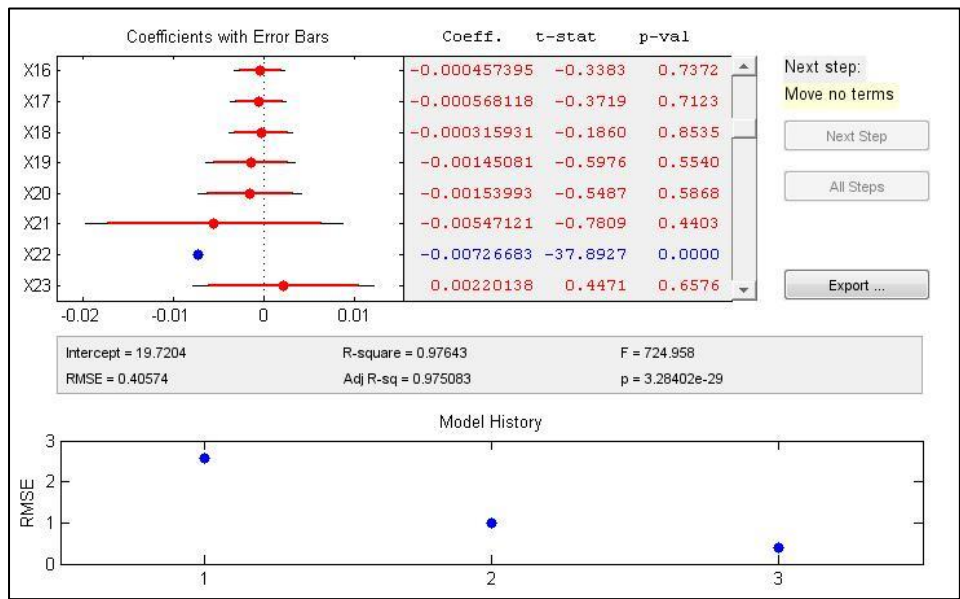


Figure 7.13 SMLR performances for ACWR in MATLAB®

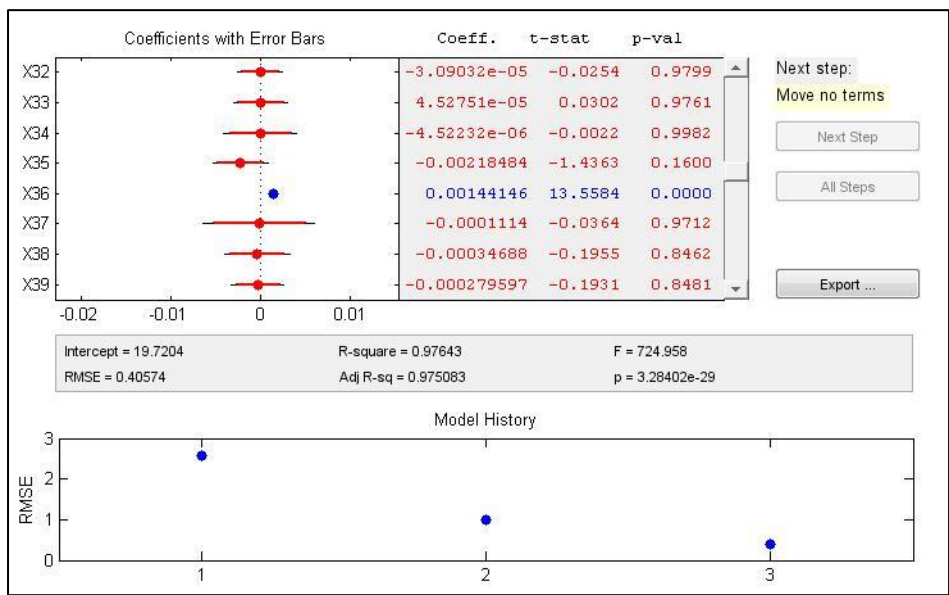


Figure 7.14 SMLR performances for ACWR in MATLAB®

Using obtained results from SMLR an optimum model is developed to predict the age based Arecanut crop water requirement. The prediction equation developed using SMLR and Hyperion reflectance values is presented in the equation 7.10.

$$Y = 19.72 - 0.0072 * \lambda_{681} + 0.0014 * \lambda_{721} \quad \dots\dots\dots(7.10)$$

Where Y is the predicted age based Arecanut crop water requirement in liters/day/plant and λ_{681} and λ_{721} are the reflectance values corresponds to 681 and 721nm wavelength.

The regression of the calibration data gave RMSE of 0.4 and R^2 value of 0.97. The validation resulted in an RMSE of 0.4 and R^2 value of 0.98. The graphical representations of validation results are presented in Figure 7.15. Results show good prediction accuracy of 0.98 for two band combination model.

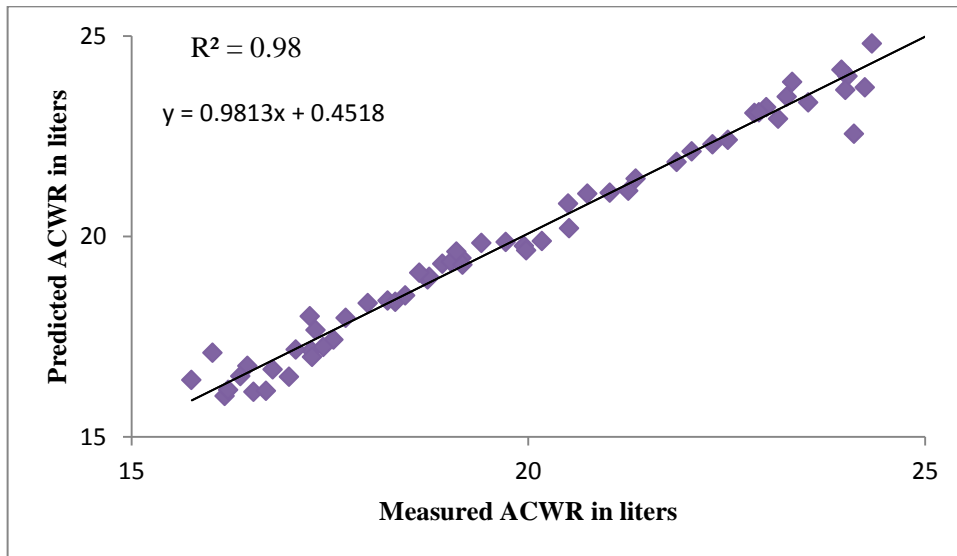


Figure 7.15 Model validation results of SMLR

The study reveals that SMLR model performance is better compare to PLSR model. The developed model is mapped using ENVI band math operation and presented in Figure 7.16. The figure represents the spatial distribution of the age wise Arecanut crop water requirement map. Red color represents area under more than 15 liters crop water requirement. Green is 10 to 15 liters and blue is of below 10 liters.

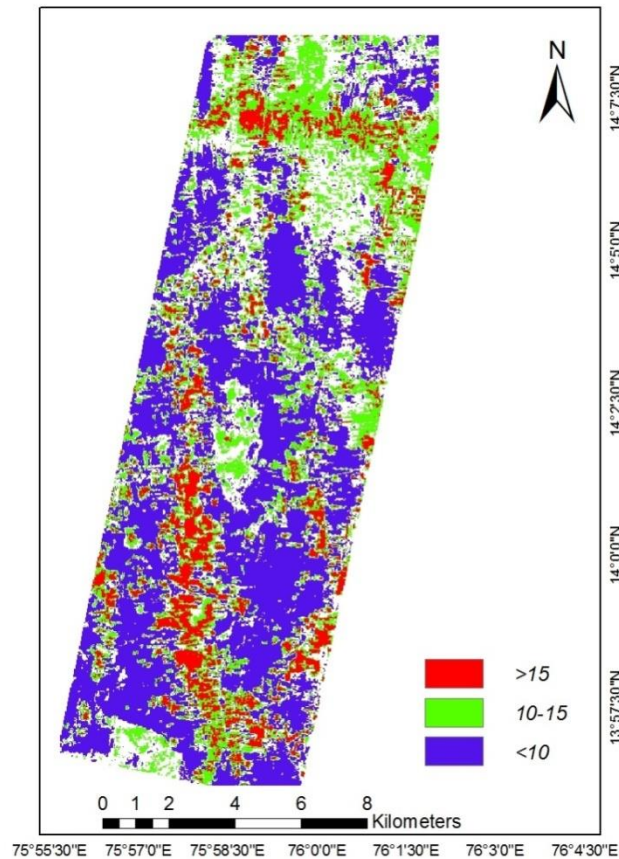


Figure 7.16. Age wise ACWR map by SMLR

7.11. SUMMARY

The approach of remote sensing using Hyperion image showed it has the potential benefit to map Arecanut water requirement map. The study also proposes that the Hyperion coupled with PLSR technique provide a rapid, accurate determination of ACWR. The newly derived Arecanut crop water requirement model (ACWR) will be helpful in assessing spatial variation of Arecanut crop water needs. Bands at 548nm, 681nm and 721nm were found to have good correlation with crop water requirement and suitable to form the model. The ACWR model with combination of only three wavelengths yielded an R^2 of 0.65. This model helps to understand crop water need at field level. This study establishes a newer approach to remotely ascertain water consumption by farmers to tally with available water resources. This helps both farmers and policy makers in determining a trade-off between agricultural productivity and irrigation water consumption for better sustainability and also helps in better water management.

By comparing the VIP scores and β coefficient values, a total of eight wavelengths, spanning across VNIR and SWIR regions were identified as significant in modelling the ACWR these were 1043, 1053, 1033, 1083, 1023, 1013, 1104, and 854nm.

The Arecanut crop water requirement model (ACWR) using SMLR will be helpful in assessing spatial variation of Arecanut crop water needs. Bands 681nm and 721nm were found to have good correlation with crop water requirement and suitable to form the model. The ACWR model with combination of only two wavelengths yielded an R^2 of 0.94.

These studies also help policy makers to evolve a policy with respect support price, subsidy, and other socio economic attributes in order to ensure a sustainable agricultural income for farmers.

The next chapter presents the research conclusions, contributions, limitation and future scope of the study.

CHAPTER 8

CONCLUSIONS

8.1 Introduction

This study evaluates the feasibility of hyperspectral data integrated with field studies to address societal problems say Arecanut crop monitoring. Study proves that hyperspectral data can be effectively used for:

- Discrimination of Arecanut crop into diseased vs. healthy.
- Field studies combined with laboratory experiments helps in identification of cause for disease.
- Arecanut crop can be categorized into different age groups.
- Mapping age based crop water requirement with limited data.
- Hyperspectral enables to develop Narrowband combinations indices to map the parameters such as Disease Index, Age Index, and Age Based Arecanut Crop Water Requirement Index.
- To identify the prominence wavelengths to build simple predictive models such as predication of crop age and its water requirement.

8.2 Summary

8.2.1 Hyperspectral Data: A Tool for Monitoring Stressed Arecanut Crops

Arecanut crop affected by crown choke disease for long years and has affected the yield and life span of the palm. SAM classifier is used to segregate these diseased vs healthy Arecanut plants using built spectral library. Overall classification accuracy was observed as 77.5%. From the classified Hyperion image it was found that more than 10 % of the total areas are affected by crown choke disease.

From physico-chemical analysis it was observed that improper soil management is the main cause for crown choke disorder. On the basis of soil characterization and water quality it is inferred that soil is poorly graded (82% of silt content) with very low hydraulic conductivity of 3.2×10^{-7} cm/sec, and high bulk density of 2.12 g/cm^3 . This impervious nature causes water logging and leads to salinity.

8.2.2. Hyperspectral Data: A Tool for Age Based Classification of Arecanut Crop

The study proved that spectral library can even be built for plantation crops which have long life, like 50 years and it will assist for crop classification based on age, avoiding the laborious site visits. Spectral library developed for different age groups of Arecanut crops showed clear spectral separability.

They are, below 3 years, 3–7 years, 8–15 years and above 15 years. Based on accuracy assessment, it can be concluded that, SVM with linear kernel function is the most accurate classification method. For within class separability with an overall accuracy of 72%. The total area under Arecanut crop cultivation was found to be 13.62 km² among 147 km² of study area. Also, SVM classifier with linear kernel yielded minimum user's accuracy of 22.22% for 3–7 years of Arecanut crops to maximum of 82.93% for above 15 years Arecanut crops. Individual age group classification producer's accuracy varied minimum of 12.5% for 3–7 years age group and maximum of 86.25% for above 15 years age group. SVM outperformed even for individual age group classification.

The developed PLSR model for crop age prediction provides better forecast for 20 years age Arecanut crop and 3 years age Arecanut crop, compared to 4 and 50 years age Arecanut crops. The built model provided predictions with R² of 0.86 and RMSE of 3.22 years. The optimum bands to discriminate Arecanut crops based on age were found to be 701, 719, 756 and 1015 nm. This proves the significance of narrow band combinations, which is having a great ability to characterize crops.

On comparing the developed model and age-wise image classification, it can be concluded that the model based age prediction is more versatile method and can be used on individual plant and don't have the limitations of image pixel resolution as in case of image classification. Image classification also suffers from spectral inseparability when higher number of classes is required, leading to inaccuracy. But image classification is still a good technique when large area of plantation needs to be classified and mapped. The two techniques are complementary to each other but not substitutes.

8.2.3 Hyperspectral Vegetation Indices for Arecanut Crop Monitoring

With regard to disease Index (DI) spectra obtained from healthy and stressed crops helps in choosing the best possible range, of visible, near infrared and the transition region also known as the red edge position of the spectral curve. The newly derived DI is useful for discriminating stressed Arecanut crops with healthy. Also it indicates that the proposed band combination has better correlation with the chlorophyll content than the other vegetation indices and thus proves to be best. This index uses only three narrow channels centered i.e. R_{750} , R_{550} and R_{675nm} . The derived DI values ranges from 0.45 to 1.5 respectively. To stream line the DI, normalization is carried out and the normalized DI ranges in-between 0 to 1.

The derived age index is a ratio of differences of three index points corresponds to 540, 680 and 780nm, has the ability to segregate Arecanut crop into different age groups. The range of AI values varied from 3 to 4.5, the value corresponds to 4.5 is above 15 years' age crop. And the value corresponds to 3 belongs to below 3 years crops. The derived age index is validated with the calculated ager based crop water requirement and it yielded an R^2 of 0.56.

8.2.4 Hyperspectral Vegetation Index for Age Based Arecanut Crop Water Requirement

The understanding of variation in water demand from crop to crop is essential not only for optimizing irrigation but also to increase yield of the crops. This is an essential aspect of precision farming to get most out of available water resource. Like every other crop, daily water needs of Arecanut crops depend on crop age, health and local weather and varies with aging. Daily crop water needs per Arecanut plant were estimated to vary from 19 litres to 23 litres. Study area was estimated to have an irrigation demand of 28,056.09 m^3 for Arecanut crops.

8.2.5 Important Wavelengths and Model Building

The approach of remote sensing using Hyperion image showed it has potential benefit to map Arecanut water requirement map. The newly derived ACWR model will be helpful in assessing spatial variation of Arecanut crop water needs. Bands at 548nm, 681nm and 721nm were found to have good correlation with crop water requirement

and suitable to form the model. ACWR model with combination of only three wavelengths yielded an R^2 of 0.65. This model helps to understand crop water need at field level. This study establishes a newer approach to remotely ascertain water consumption by farmers to tally with available water resources. This helps both farmers and policy makers in determining a trade-off between agricultural productivity and irrigation water consumption for better sustainability and also helps in better water management. The study also proposes that the Hyperion coupled with PLSR technique provide a rapid, accurate determination of ACWR.

By comparing VIP scores and β coefficient values, a total of eight wavelengths, spanning across VNIR and SWIR regions were identified as significant in modelling the ACWR these were 1043, 1053, 1033, 1083, 1023, 1013, 1104, and 854nm.

The Arecanut crop water requirement model (ACWR) using SMLR will be helpful in assessing spatial variation of Arecanut crop water needs. Bands 681nm and 721nm were found to have good correlation with crop water requirement and suitable to form the model. The ACWR model with combination of only two wavelengths yielded an R^2 of 0.94.

8.3 Specific Conclusions

Based on the results obtained from the study following explicit conclusions are drawn,

- The stressed crops showed explicit distinction with lesser reflectance in NIR region owing to the fact that crown choke disease has hindered photosynthesis.
- From the classified Hyperion image it is found that more than 10 % of the total areas (1.3 Km²) of Arecanut crop cultivation are affected by crown choke disease. And from physico-chemical analysis it was observed that improper soil management is the main cause for crown choke disorder.
- Reflectance behaviour of Arecanut crop is observed to be a function of crop age. Distinction is clear throughout the spectral range, especially in the NIR region where mature crops (16-25 years old) had distinctly high reflectance compared to other classes.
- SVM with linear kernel function is the most accurate classification method for within class separability with an overall accuracy of 72%. The total area under Arecanut crop cultivation was found to be 13.62 km² among 147 km² of study area.

- The developed PLSR model for crop age predication provides better forecast for 20 years age Arecanut crop and 3 years age Arecanut crop, compared to 4 and 50 years age Arecanut crops. The built model provided predictions with R^2 of 0.86 and RMSE of 3.22 years. The optimum bands to discriminate Arecanut crops based on age were found to be 701, 719, 756 and 1015 nm.
- This Disease Index uses only three narrow channels centered i.e. R_{750} , R_{550} and R_{675nm} . And derived DI values ranges from 0.45 to 1.5 respectively. Normalized DI ranges in-between 0 to 1.
- The derived age index is a ratio of differences of three index points corresponds to 540, 680 and 780nm, has the ability to segregate Arecanut crop into different age groups.
- The range of AI values varied from 3 to 4.5, the value corresponds to 4.5 is above 15 years' age crop. And the value corresponds to 3 belongs to below 3 years crops. The derived age index is validated with the calculated ager based crop water requirement and it yielded an R^2 of 0.56.
- Image classification employing SAM yielded accurate map with 73.68% classification accuracy. Higher spectral separability of various classes explains such good accuracy. This corroborates the applicability of hyperspectral remote sensing in within class discrimination of Arecanut crops based on age and stress.
- Crop coefficient of Arecanut crops were estimated using NDVI based approach. NDVI valued of Arecanut crops varied from 0.55 to 0.82 where as calculated values of crop coefficient varied from 0.63 to 1.03 using which crop water requirement were estimated.
- Daily crop water needs per Arecanut plant were estimated to vary from 19 litres to 23 litres. Study area was estimated to have an irrigation demand of 28,056.09 m³ for Arecanut crops.
- From the study it is evident that water demand is associated with growth stage. Juvenile crops have comparatively lesser water requirement than the crops of age 9-15 (23.01 litres/plant) which are in yielding stage. Later the water requirement further decreases with increase in crop age. Crops older than 25 years tend to show significant signs of aging and have lesser water requirement (19.69 litres/plant).

- Arecanut crops develop signs of stress (crown choke disease affected) only in adulthood and interestingly consume water quantity comparable with adult healthy crops (22.48 litres/plant). Calculations showing slightly higher amount of water consumption than actual in juvenile crops is because of mixed crops plantation as observed in the study area, to protect smaller crops from sun, whose water consumption is also included.
- In addition to calculated crop water needs, the newly derived Arecanut crop water requirement index (ACWRI) will be helpful in assessing spatial variation of Arecanut crop water needs. Bands at 844nm and 691nm were found to have good correlation with crop water requirement and suitable to form an index. The index proves to be a quick solution to understand crop water requirement.
- From the hyperspectral data significant wavelengths were identified: (i) to map the stressed Arecanut crops (750, 550 and 675nm), (ii) Arecanut crop age predication (540, 680 and 780nm). (iii) And to predict the age wise crop water requirement using statistical models: SMLR reveals that 681 and 721nm are significant. PLSR also in agreement with SMLR i.e 681,721 and 548nm are important. Whereas a VIP technique reveals wavelengths 1043, 1053, 1033, 1083, 1023, 1013, 1104, and 854nm is prominence.

Knowledge of accurate water need by crops helps to optimize consumption of water and avoid over exploitation of groundwater. This study establishes a newer approach to remotely ascertain water consumption by farmers to tally with available water resources. This helps both farmers and policy makers in determining a trade-off between agricultural productivity and irrigation water consumption for better sustainability.

8.7 Contributions from This Research

The study addresses the societal problem and finds feasible solutions for monitoring and mapping the commercial crop say Arecanut. The study proves the potential of hyperspectral data combined with field data can be helpful for discrimination of the Arecanut crops into different age groups. This helps for estimation of exact yield to plan for export. Also segregation of crops in to stress versus healthy information helps to take the proper remedial measures in advance. Age based crop water requirement based on crop age to determine variation in crop water need. Helps irrigation planning and scheduling this avoids excessive irrigation which prevents the ground water exploitation and power loss. Simple predictive models help to develop application software's to forecast water demand.

8.8 Recommendations

From the field visit it was observed that, in plain region and where large quantity of tank silt is being applied to areca gardens haphazardly by the growers. The practice has temporarily increased the Arecanut yields but on a long run it has led to soil compaction, hardening, poor root aeration, rotting and disorders like crown choke are formed.

From the investigation it may be concluded that the poor gradation of soil stratum ceases the root development. Impervious nature of the surface causes irrigated water to be simply drained off from the surface not reaching the roots. Due to this impervious nature the water logging takes place and leads to salinity. The only way to manage the problem is better soil management and improvement of drainage. Further investigation is needed on blending of the soil for new plantation and for the existing one, improved drainage system has to be thought of. Soil aeration can be improved by, removing the hard pan of sub soil and application of organic matter. The practice of addition of tank silt on a large scale should be discontinued.

Optimized irrigation facilitate better yield by avoiding ground water depletion.

8.8 Limitations

- The study uses limited data sets, due to mismatch in path row of available satellite data with the field data and cloud coverage.
- The study uses limited data for calculations of crop water requirement.
- Direct canopy reflectance data collection using spectroradiometer is not carried out due to safety aspects.
- The study not used evapotranspiration measurements at the field level.

8.9 Future scope

- ✓ Establishment of more accurate values for Arecanut crop coefficient and measuring meteorological parameters, with higher spatial interval can aid determining more accurate values of crop water requirement helping farmers.
- ✓ Subpixel level classification techniques and human expertize classification methods can improve the results.
- ✓ Different types of atmospheric correction methods can be tried for best suitable method for plantation crop monitoring.
- ✓ Integration of microwave remoted sensing data with hyperspectral data will provide more accurate results related to age of the crop and respective water requirement.
- ✓ Arecanut crop irrigation scheduling can be effective forecastable by extending this study for past data sets.
- ✓ Field based experiments for calculating ET_0 for Arecanut crops adds more accuracy to the study.
- ✓ Comparing different methods of evaporation estimation models can improve study results.
- ✓ Usage of air borne hyperspectral data enables forecasting the crop water demand more accurately.
- ✓ Addition parameters such as leaf area index, greenness index. Canopy cover soil moisture can improve the results.

REFERENCES

- Anshu Miglani., Ray, S. S., Pandey, R.,and Parihar, J.S.,(2008). “Evolution of EO-1 Hyperion Data for Agricultural Applications”. *J. Indian Soc. Remote Sens.*(36)255–266.
- Apan, A., Held, A., Phinn, S., and Markley, J. (2003). “Formulation and assessment of narrow-band vegetation indices from EO-1 Hyperion imagery for discriminating sugarcane disease”, *Proceedings of the Spatial Sciences Institute Biennial Conference: Spatial Knowledge Without Boundaries (SSC2003)*, 1-13.
- Apan, A., Held, A., Phinn, S., and Markley, J. (2004). “Detecting sugarcane ‘orange rust’ disease using EO-1 Hyperion hyperspectral imagery”, *International Journal of Remote Sensing*, 25(2), 489-498.
- Arafat, S. M., Aboelghar, M. A., and Ahmed, E. F. (2013). “Crop Discrimination Using Field Hyper Spectral Remotely Sensed Data”. *Advances in remote sensing*, 2, 63-70.
- Arecanut Research and Development Foundation (ARDF) (2011). ARDF – About Arecanut. <<http://www.arecanut.org/arecanut.html>> (October. 31, 2012).
- Ashoori, H., Fahmnejad, H., Alimohammadi, A and Soofbaf, S.R. (2008). “Evaluation of the usefulness of texture measures for crop type classification by Hyperion data.” *The International Archives of the photogrammetry, Remote Sensing and Spatial Information Sciences.*, 37, 999-1006.
- Balasimha D., Abdul Khader B. and Bhat Ravi. (1996). “Gas exchange characteristics of cocoa grown under arecanut in response to drip

- irrigation”. *Proc. All India Seminar on Modern Irrigation Techniques*, pp 96-101.
- Balasimha D., Abdul Khader B. and Bhat Ravi. (1996). “Gas exchange characteristics of cocoa grown under arecanut in response to drip irrigation”. *Proc. All India Seminar on Modern Irrigation Techniques*, pp 96-101.
 - Bandyopadhyay K.K., S. Pradhan, R.N. Sahoo, Ravender Singh, V.K. Gupta, D.K. Joshi, A.K. and Sutradhar (2014). “Characterization of water stress and prediction of yield of wheat using spectral indices under varied water and nitrogen management practices”. *Agricultural Water Management* 146, 115–123.
 - Bijay Singh and Jimly Dowerah, (2010), “Hyperspectral Imaging: New Generation Remote Sensing”. *Journal of Geographic Information System, Open access e-Journal Earth Science India, Vol. 3 (III)*.
 - Boulesteix, A. L., and Strimmer, K. (2007). “Partial least squares: a versatile tool for the analysis of high-dimensional genomic data.” *Briefings in bioinformatics* 8,1.
 - CAMPCO (2010) About Arecanut, <http://campco.org/Webpages/Arecanut.aspx> (October. 31, 2012).
 - Carter G.A. (1994). “Ratios of leaf reflectances in narrow wavebands as indicators of plant stress”. *International Journal of Remote Sensing*, 15, 697–704.
 - Casa R., Rossi M., Sappa G. and Trotta, A. (2009). “Assessing crop water demand by remote sensing and GIS for the Pontina Plain, Central Italy”. *Water resources management*, 23(9), 1685-1712.
 - Chakravorty Somdatta., and Chakrabarti, S. (2011). “Preprocessing of Hyperspectral Data : A Case Study of Henry and Lothian Islands in Sunderban Region, West Bengal, India”. *International Journal of Geomatics and Geosciences*, (2), 2- 1

- Chávez, P., Zorogastúa, P., Chuquillanqui, C., Salazar, L. F., Mares, V., and Quiroz, R. (2009). "Assessing Potato Yellow Vein Virus (PYVV) infection using remotely sensed data". *International Journal of Pest Management*, 55(3), 251-256.
- Chemura, A., van Duren, I., and van Leeuwen, L. M. (2014). "Determination of the age of oil palm from crown projection area detected from WorldView-2 multispectral remote sensing data: The case of Ejisu-Juaben district", Ghana. *ISPRS Journal of Photogrammetry and Remote Sensing*.
- Chong, I. G., and Jun, C. H. (2005). "Performance of some variable selection methods when multicollinearity is present". *Chemometrics and Intelligent Laboratory Systems*, 78(1), 103-112.
- Congalton, R. G. (2001). "Accuracy assessment and validation of remotely sensed and other spatial information". *International Journal of Wildl and Fire*, 10(4), 321-328.
- Datt B. and Jupp D., (2004) "Hyperion Data Processing Workshop: Hands-on processing instructions", *CSIRO Office of Space Science and Applications Earth Observation Centre*.
- Dinesh Kumar E.V and Mukundan K. (1996) "Economics of arecanut cultivation in Kerala". *J.Platn.Crops*. 24:827-831
- Droogers P and Allen R. G. (2002) "Estimating reference evapotranspiration under inaccurate data conditions." *Irrigation and drainage systems*, 16(1), 33-45.
- Dutta, S., Bhattacharya, B.K., Rajak, D. R., Chattopadhyay, C., Patel, N. K., and Parihar, J. S. (2006). "Disease Detection In Mustard Crop Using EO-1 Hyperion Satellite Data", *Journal of the Indian Society of Remote Sensing*, 34 (3).

- Fahimnejad, H., Soofbaf, S. R., Alimohammadi, A., and ZOEJ, M. V. (2007). "Crop type classification by Hyperion data and unmixing algorithm". In *Hyderabad, India: GIS development, Map World Forum*.
- Franke, Jonas, Mewes, Thorsten, and Menz, Gunter (2008). "Airborne hyperspectral imaging for the detection of powdery mildew in wheat", *Imaging Spectrometry XIII, Proc. of SPIE 7086*, 708609-1.
- FuminWang., Jing Feng Huang., Qi Fa Zhou and Xiu-zhen Wang. (2008). "Optimal waveband identification for estimation of Leaf area index of paddy rice." *Journal of Zhejiang University.*, 9, 953-963.
- Galvao, L. S., Formaggio, A. R., and Tisot, D. A. (2005). "Discrimination of sugarcane varieties in Southeastern Brazil with EO-1 Hyperion data". *Remote Sensing of Environment*, 94(4), 523-534.
- Gaurav Agrawal., and Jyoti Sarup. (2011) "Comparison Comparison of QUAC and FLAASH Atmospheric Correction Modules on EO-1 Hyperion Data of Sanchi". *International journal of advanced engineering and technologies.*(4) 1, 178-186.
- George P. Petropoulos., Krishna Prasad Vadrevu and Chariton Kalaitzidis. (2012). "Spectral angle mapper and object based classification combined with hyperspectral remote sensing imagery for obtaining land use/cover mapping in a Mediterranean region." *Geocarto International.*, 1-16
- Gomez-Chova, L., Calpe, J., Camps-Valls, G., Martin, J. D., Soria, E., Vila, J., and Moreno, J. (2003). "Semi-supervised classification method for hyperspectral remote sensing images". In *international geoscience and remote sensing symposium 3*, 1776.
- Govender, M., Chetty, K., Naiken, V and Bulcock, H. (2008). "A comparison of satellite hyperspectral and multispectral remote sensing imagery for improved classification and mapping of vegetation." *Water SA.*, 34, 147-154.

- Gualtieri J. A. and Cromp R. F. (1998), "Support Vector Machine for Hyperspectral Remote Sensing Classification", *27th AIPR Workshop, Advances in Computer Assisted Recognition. Washington D.C. Proceedings of SPIE*, Vol. 3584.
- Hamid Muhammed, H., and Larsolle, A. (2003). "Feature vector based analysis of hyperspectral crop reflectance data for discrimination and quantification of fungal disease severity in wheat". *Biosystems engineering*, 86(2), 125-134.
- Hansen P. M., and J. K. Schjoerring. "Reflectance measurement of canopy biomass and nitrogen status in wheat crops using normalized difference vegetation indices and partial least squares regression." *Remote sensing of environment* 86, no. 4 (2003): 542-553.
- Hargreaves G. H. and Samani Z. A., (1982). "Estimating potential evapotranspiration". *Journal of the Irrigation and Drainage Division, ASCE* 108(3), 225-230.
- Hargreaves, G. H. (1994). "Defining and using reference evapotranspiration". *J. Irrig. Drain Eng, ASCE*, 1994.120:1132-1139.
- Herold, M., Roberts, D. A., Gardner, M. E., and Dennison, P. E. (2004). "Spectrometry for urban area remote sensing—Development and analysis of a spectral library from 350 to 2400 nm". *Remote Sensing of Environment*, 91(3), 304-319.
- Huang, C., Davis, L. S., and Townshend, J. R. G. (2002). "An assessment of support vector machines for land cover classification". *International Journal of Remote Sensing*, 23(4), 725-749.
- Huang, W., Lamb, D. W., Niu, Z., Zhang, Y., Liu, L., and Wang, J. (2007). "Identification of yellow rust in wheat using in-situ spectral reflectance measurements and airborne hyperspectral imaging". *Precision Agriculture*, 8(4-5), 187-197.

- Huang, Y., Yuan, L., Reddy, K. N., and Zhang, J. (2016). “In-situ plant hyperspectral sensing for early detection of soybean injury from dicamba”. *Biosystems Engineering*, 149, 51-59.
- Jabloun M. D. and Sahli A., (2008). “Evaluation of FAO-56 methodology for estimating reference evapotranspiration using limited climatic data: Application to Tunisia.” *Agricultural Water Management*, 95(6), 707-715.
- Jensen J. R. (2009). “Remote Sensing of the Environment: An Earth Resource Perspective”. *Pearson Education India*.
- Jensen, J. R. (1996). *Introductory digital image processing: a remote sensing perspective* (No. Ed. 2). Prentice-Hall Inc.
- Jing, L., Jinbao, J., Yunhao, C., Yuanyuan, W., Wei, S., and Wenjiang, H. (2007). “Using hyperspectral indices to estimate foliar chlorophyll a concentrations of winter wheat under yellow rust stress”. *New Zealand Journal of Agricultural Research*, 50(5), 1031-1036.
- Jovivek, V., Hemalatha, T and Soman, K.P. (2009). “Determining an efficient supervised classification method for hyperspectral image.” *IEEE International Conference on Advances in Recent Technologies in Communication and Computing.*, 384-386.
- Jones, C. D., Jones, J. B., and Lee, W. S. (2010). “Diagnosis of bacterial spot of tomato using Spectral signatures”, *Computers and Electronics in Agriculture* 74, 329–335.
- Joshi, N. V and Joshi, S.G (1949). "The ‘band’ disease of areca palm". *Indian Farming*.10:197-200.
- Kamble B., Kilic A. and Hubbard K, (2013). “Estimating crop coefficients using remote sensing-based vegetation index”. *Remote Sensing*, 5(4), 1588-1602.
- Khurshid K. S., K. Staenz L. Sun R. Neville H. P. White A., Bannari C. M. Champagne R. and Hitchcock, (2006) “Preprocessing of EO-1 Hyperion data” *Can. J. Remote Sensing*, Vol. 32, (2), pp. 84–97.

- Krishna, G., Sahoo, R. N., Pargal, S., Gupta, V. K., Sinha, P., Bhagat, S., and Chattopadhyay, C. (2014). “Assessing wheat yellow rust disease through hyperspectral remote sensing”. *The International Archives of Photogrammetry, Remote Sensing and Spatial Information Sciences*, 40(8), 1413.
- Kumar, J., Vashisth, A., Sehgal, V. K., and Gupta, V. K. (2013). “Assessment of Aphid Infestation in Mustard by Hyperspectral Remote Sensing”. *Journal of the Indian Society of Remote Sensing*, 1-8.
- Larsolle, A., and Muhammed, H. H. (2007). “Measuring crop status using multivariate analysis of hyperspectral field reflectance with application to disease severity and plant density”. *Precision Agriculture*, 8(1-2), 37-47.
- Laudien, R., Bareth, G., and Doluschitz, R., (2004) “Comparison of Remote Sensing Based Analysis of Crop Disease by Using High Resolution multispectral and Hyperspectral data. A case study; Rhizpctonia Solani in Sugar Beet”. *Int. Conf. On Geoinformatics-Geospatial Infoamtion Researc.Proc 12*.
- Laudien, R., Bareth, G., and Doluschitz, R. (2003). “Analysis of hyperspectral field data for detection of sugar beet diseases”. *EFITA 2003 Conference Debrecen, Hungary*, 375–381.
- Lenio Soares Galvao., Antonio Roberto Formaggio and Daniela Arnold Tisot. (2005). “Discrimination of sugarcane varieties in Southeastern Brazil with EO-1 Hyperion data.” *Remote Sensing of Environment.*, 94, 523–534.
- Lin C., Ma R., Zhu Q. and Li J. (2015). “Using hyper-spectral indices to detect soil phosphorus concentration for various land use patterns”. *Environmental monitoring and assessment*, 187(1), 1-10.
- Mahesha A., Khader K. A., and Ranganna G. (1990). “Consumptive use and irrigation requirement of arecanut palm (Areca catechu). *Indian Journal of Agricultural Sciences*”, 60(9), 609-611.

- Mahlein, A. K., Rumpf, T., Welke, P., Dehne, H. W., Plümer, L., Steiner, U., Oerke, E. C., (2013). "Development of spectral indices for detecting and identifying plant diseases". *Remote Sensing of Environment* 128, 21–30.
- Marshall, M., Thenkabail, P., Biggs, T., and Post, K. (2016). "Hyperspectral narrowband and multispectral broadband indices for remote sensing of crop evapotranspiration and its components (transpiration and soil evaporation)". *Agricultural and Forest Meteorology*, 218, 122-134.
- Miglani, Anshu, Ray, S. S., Pandey, R., and Parihar, J. S. (2008). "Evaluation of EO-1 Hyperion Data for Agricultural Applications". *Journal of Indian Society of Remote Sensing* 36,255–266.
- Mirik, M., Ansley, R. J., Michels, G. J., and Elliott, N. C. (2012). "Spectral vegetation indices selected for quantifying Russian wheat aphid (*Diuraphis noxia*) feeding damage in wheat (*Triticum aestivum* L.)". *Precision Agric* 13:501–516.
- Moshou, D., Bravo, C., Wahlen, S., West, J., McCartney, A., De Baerdemaeker, J., and Ramon, H. (2006). "Simultaneous identification of plant stresses and diseases in arable crops using proximal optical sensing and self-organising maps". *Precision Agriculture*, 7(3), 149-164.
- Mozaffar, Heidari, M., Valadan, Zoej, M. J., Sahebi, M. R., and Rezaei, Y. (2008). "Vegetation Endmember Extraction in Hyperion Images", *The International Archives of the Photogrammetry, Remote Sensing and Spatial Information Sciences*. 38, B7.
- Muhammed, H. H. (2005). "Hyperspectral crop reflectance data for characterising and estimating fungal disease severity in wheat". *Biosystems Engineering*, 91(1), 9-20.

- Nidamanuri, R. R., and Zbell, B. (2012). "Existence of characteristic spectral signatures for agricultural crops–potential for automated crop mapping by hyperspectral imaging". *Geocarto International*, 27(2), 103-118.
- Nielsen A. A. (2011), “Kernel Maximum Autocorrelation Factor and Minimum Noise Fraction Transformations”. *IEEE Transactions on Image Processing*, Vol. 20, (3).
- Panigada C., R. Colombo, M. Meroni, M. Rossini, S. Cogliati, L. Busetto, F. Fava , Picchi V., Migliavacca M., and Marchesi A. (2010) “Remote sensing of vegetation status using Hyperspectral data”. *4th International workshop on remote sensing of vegetation fluorescence* , 15-17 Nov. 2010, Nalencia (Spain)
- Patel,G. I. and Rao, K.S.N (1958). "Important diseases and pests of arecanut and their control". *Arecanut J.* 9:89-96.
- Pereira L. S., Raes D. and Smith M., (1998). “Crop evapotranspiration-Guidelines for computing crop water requirements-FAO Irrigation and drainage” *paper#56. FAO, Rome, 300, 6541.*
- Petropoulos G. P., Kalaitzidis C., and Vadrevu K. P. (2012). “Support vector machines and object-based classification for obtaining land-use/cover cartography from Hyperion hyperspectral imagery”. *Computers and Geosciences*, 41, 99-107.
- Prabhakar, M., Prasad, Y.G., Thirupathi, M., Sreedevi, G., Dharajothi, B., and Venkateswarlu, B. (2011). “Use of ground based hyperspectral remote sensing for detection of stress in cotton caused by leafhopper (Hemiptera: Cicadellidae)”. *Computers and Electronics in Agriculture* 79, 189–198.
- Prasad S. Thenkabail, John G. Lyon and Alfredo Huete, (2011) “Hyperspectral Remote Sensing of Vegetation”, *Taylor and Francis.*

- Prasannakumar N. R., Subhash Chander , R. N. Sahoo and V. K. Gupta (2013). “Assessment of Brown Planthopper, (*Nilaparvata lugens*) [Stål], damage in rice using hyperspectral remote sensing”, *International Journal of Pest Management*, 24(2).242-249
- Pu, R., Gong, P., Biging, G. S., and Larrieu, M. R. (2003). “Extraction of red edge optical parameters from Hyperion data for estimation of forest leaf area index”. *Geoscience and Remote Sensing, IEEE Transactions on*, 41(4), 916-921.
- Rajat Satpathy., Vivek K.S., Reshma P. and Jeyaseelan A.T. (2010), “Spectral Analysis of Hyperion Data for Mapping the Spatial Variation of AL+OH Minerals in a Part of Latehar and Gumla District, Jharkhand”. *Journal of Geographic Information System*, 210-214.
- Rama Rao Nidamanuria and Bernd Zbell. (2012). “Existence of characteristic spectral signatures for agricultural crops – potential for automated crop mapping by hyperspectral imaging.” *Geocarto International.*, 27, 103–118.
- Rama Rao, N., Garg, P.K. and Ghosh, S.K. (2007). “Development of an agricultural crops spectral library and classification of crops at cultivar level using hyperspectral data.” *Precision Agric.*, 8, 173–185.
- Ramappa B.T (2013). "Economics of Areca nut Cultivation in Karnataka, a Case Study of Shivamogga district". *Journal of Agriculture and Veterinary Science* 3, 1, 50-59.
- Rao, N. R., Garg, P. K., and Ghosh, S. K. (2007). "Development of an agricultural crops spectral library and classification of crops at cultivar level using hyperspectral data". *Precision Agriculture*, 8(4-5), 173-185.
- Ray S. S. and Dadhwal V. K., (2001). “Estimation of crop evapotranspiration of irrigation command area using remote sensing and GIS”, *Agricultural water management*, 49(3), 239-249.

- Ray, S. S., Jain, N., Arora, R. K., Chavan, S., and Panigrahy, S. (2011). “Utility of Hyperspectral Data for Potato Late Blight Disease Detection”. *Journal of the Indian Society of Remote Sensing*, 39(2), 161-169.
- Richard G. Allen (2000). Using the FAO-56 dual crop coefficient method over an irrigated region as part of an evapotranspiration intercomparison study. *Journal of Hydrology*, 229(1), 27-41.
- Richard G. Allen, Pereira, L.S., Raes, D. and Smith, M., (1998). “Crop evapotranspiration: guidelines for computing crop water requirements”. *FAO Irrigation and Drainage Paper #56, Rome, Italy*.
- Rumpf, T., Mahlein, A. K., Dörschlag, D.,and Plümer, L., (2009). “Identification of combined vegetation indices for the early detection of plant diseases”. *Proceedings of the SPIE Conference on Sensing for Agriculture, Ecosystems and Hydrology*. 7472.
- Rumpf, T., Mahlein, A. K., Steiner, U., Oerke, E. C., Dehne, H. W.,and Plümer, L. (2010). “Early detection and classification of plant diseases with Support Vector Machines based on hyperspectral reflectance”. *Computers and Electronics in Agriculture* 74, 91–99.
- Saad Gazala, R.N. Sahoo, Rakesh Pandey Bikash Mandal, V.K. Gupta, Rajendra Singh and P. Sinha (2013). “Spectral reflectance pattern in soybean for assessing yellow mosaic disease”. *Indian J. Virol* 24(2).242-249
- Sahoo R.N., S.S. Ray and K.R. Manjunath (2015) “Hyperspectral remote sensing of agriculture”. *CURRENT SCIENCE*. 108, 5, 848-859.
- Sai, Sesha, M. V. R., Ramana, K. V.,and Hebbar, R. (2010). “Remote Sensing Applications”. *National Remote Sensing Centre, Agriculture*, 1-20.

- Sankaran, Sindhuja, Mishra, Ashish, Ehsani, Reza, Davis, and Cristina (2010). "A review of advanced techniques for detecting plant diseases", *Computers and Electronics in Agriculture* 72, 1–13.
- Seelan, S. K., Laguette, S., Casady, G. M., and Seielstad, G. A. (2003). "Remote sensing applications for precision agriculture: A learning community approach". *Remote Sensing of Environment*, 88(1), 157-169.
- Shafri, H. Z., and Hamdan, N. (2009). "Hyperspectral Imagery for Mapping Disease Infection in Oil Palm Plantation Using Vegetation Indices and Red Edge Techniques". *American Journal of Applied Sciences*, 6(6), 1031.
- Shalei Song., Wei Gong., Bo Zhu and Xin Huang, (2011). "Wavelength selection and spectral discrimination for paddy rice, with laboratory measurements of hyperspectral leaf reflectance." *ISPRS Journal of Photogrammetry and Remote Sensing.*, 66, 672-682.
- Shankar, Shibendu, Ray, Jain, Namrata, Arora, R. K., Chavan, S., Panigrahy, and Sushma (2011). "Utility of hyperspectral data for potato late blight disease detection". *J Indian Soc Remote Sens* 39, 161-169.
- Shankar, Shibendu, Ray, Singh, J. P., Panigrahy, Sushma (2010). "Use of Hyperspectral Remote Sensing For Crop Stress Detection: Ground - Based Studies". *International Archives of the Photogrammetry, Remote Sensing and Spatial Information Science*, 38, 8.
- Sheshagiri K.S., Narayanaswamy H., and Shivanna, B. K. (2010). "Methods of Arecanut Cultivation". A report by *Arecanut Research Centre*, Agriculture College, Navile, Shimoga.
- Shwetank, J. K., and Bhatia, K. J. (2010). "Review of Rice Crop Identification and Classification using Hyper-Spectral Image Processing System". *International Journal of Computer Science & Communication*, 1(1), 253-258.

- Skowronek, S., Ewald, M., Isermann, M., Van De Kerchove, R., Lenoir, J., Aerts, R., and Rocchini, D. (2016). “Mapping an invasive bryophyte species using hyperspectral remote sensing data”. *Biological Invasions*, 1-16.
- Song, Shalei, Gong, Wei, Zhu, Bo, Huang, and Xin (2011). “Wavelength selection and spectral discrimination for paddy rice, with laboratory measurements of hyperspectral leaf reflectance”. *ISPRS Journal of Photogrammetry and Remote Sensing* 66, 672–682.
- Steddom, K., Bredehoeft, M. W., Khan, M., and Rush, C. M. (2005). “Comparison of visual and multispectral radiometric disease evaluations of Cercospora leaf spot of sugar beet”. *Plant Disease*, 89(2), 153-158.
- Stephanie Delalieux., Jan, A.N. Aardt., Pablo, J., Zarco-Tejada., Pieter Kempeneers., Willem, W. Verstraeten and Coppin., (2007). “Development of Robust Hyperspectral Indices for the Detection of Deviation of Normal Plant State”. *EARSel ePROCEEDINGS* 6.
- Thenkabail, P. S., Mariotto, I., Gumma, M. K., Middleton, E. M., Landis, D. R., and Huemmrich, K. F. (2013). “Selection of hyperspectral narrowbands (HNBs) and composition of hyperspectral twoband vegetation indices (HVIs) for biophysical characterization and discrimination of crop types using field reflectance and Hyperion/EO-1 data”. *IEEE Journal of Selected Topics in Applied Earth Observations and Remote Sensing*, 6(2), 427-439.
- Thenkabail, P. S., Smith, R. B., and De Pauw, E. (2000). “Hyperspectral vegetation indices and their relationships with agricultural crop characteristics”. *Remote sensing of Environment*, 71(2), 158-182.
- Thomas Lillesand, Ralph W. Kiefer and Jonathan Chipman, (2004), “Remote Sensing and Image Interpretation” *John Wiley and Sons*.

- Thomas Oommen., DebasmitaMisra., Navin, K.C. Twarakavi., Anupma Prakash., Bhaskar Sahoo and Sukumar Bandopadhyay. (2008). “An Objective Analysis of Support Vector Machine Based Classification for Remote Sensing.” *Math Geosci.*, 40, 409–424.
- Thorsten Mewes., Jonas Franke., and Gunter Menz (2008) “Multitemporal Spectroscopy for crop stress detection using band selection methods”. *Imaging Spectrometry XIII, Proc. of SPIE* Vol. 7086,
- Vigier, B. J., Pattey, E., and Strachan, I. B. (2004). “Narrowband vegetation indexes and detection of disease damage in soybeans”. *Geoscience and Remote Sensing Letters, IEEE*, 1(4), 255-259.
- Wang, Cuizhen, Zhou, Bo, Harlan, L.and Palm (2008). “Detecting Invasive Sericea Lespedeza (Lespedeza cuneata) in Mid-Missouri Pastureland Using Hyperspectral Imagery”, *Environmental Management* 41, 853–862.
- Wang, M., Li, Xin-ju, Yao, Qian-qian, and Liu, Yi (2012). “Extraction of Diseases and Insect Pests for Tobacco Based on Hyperspectral Remote Sensing”, *Geod.* 3, 209–216.
- West, J. S., Bravo, C., Oberti, R., Lemaire, D., Moshou, D., and McCartney, H. A., (2003). “The potential of optical canopy measurement for targeted control of field crop diseases”, *Annual Review of Phytopathology* 41, 593–614.
- Wilson, J. H., Zhang, C., and Kovacs, J. M. (2014). "Separating Crop Species in Northeastern Ontario Using Hyperspectral Data". *Remote Sensing*, 6(2), 925-945.
- Wold, S., Sjöström, M., and Eriksson, L. (2001). “PLS-regression: a basic tool of chemometrics”. *Chemometrics and intelligent laboratory systems*, 58(2), 109-130.

- Xu, L., and Xie, D. (2012). "Prediction for Available Nitrogen and Available Phosphorus by Using Hyperspectral Data". In *Remote Sensing, Environment and Transportation Engineering (RSETE), 2012 2nd International Conference on*. 1-4. IEEE.
- Yang, C. M. (2010). "Assessment of the severity of bacterial leaf blight in rice using canopy hyperspectral reflectance". *Precision Agriculture*, 11(1), 61-81.
- Yeniay, O., and Goktas, A. (2002). "A comparison of partial least squares regression with other prediction methods". *Hacettepe Journal of Mathematics and Statistics*, 31(99), 111.
- Younan, N. H., King, R. L., and Bennett Jr, H. H. (2004). "Classification of hyperspectral data: a comparative study". *Precision Agriculture*, 5(1), 41-53.
- Zhang H., Lan Y., Lacey R., Hoffmann W. C. and Huang Y. (2009). "Analysis of vegetation indices derived from aerial multispectral and ground hyperspectral data". *International Journal of Agricultural and Biological Engineering*.
- Zhang, J. C., Pu, R. L., Wang, J. H., Huang, W. J., Yuan, L., and Luo, J. H. (2012). "Detecting powdery mildew of winter wheat using leaf level hyperspectral measurements". *Computers and Electronics in Agriculture*, 85, 13-23.
- Zhang, J., Wu, J., and Zhou, L. (2010). "Estimation of vegetation Equivalent Water Thickness using hyperspectral data and partial least square regression". In *Geoinformatics, 2010 18th International Conference on* 1-6. IEEE.
- Zhang, M., Qin, Z., and Liu, X. (2005). "Remote sensed spectral imagery to detect late blight in field tomatoes". *Precision Agriculture*, 6(6), 489-508.

APPENDIX I: Calculation of Reference Crop Evapotranspiration

Daily reference crop evapotranspiration (ET_o in mm/day) is computed based on equation 3.12 presented by Hargreaves and Samani:

$$ET_o = 0.0135(KT) (R_a) (TD)^{1/2}(TC+17.8)$$

Where $TD = T_{max} - T_{min}$ ($^{\circ}C$), and TC is the average daily temperature ($^{\circ}C$).

$$TD = 30.40 \text{ }^{\circ}C - 16.31 \text{ }^{\circ}C = 14.09 \text{ }^{\circ}C$$

The relationship explicitly accounts for solar radiation and temperature. Although relative humidity is not explicitly contained in the equation, it is implicitly present in the difference in maximum and minimum temperature.

The temperature coefficient is then calculated using equation 4.4 as,

$$KT = 0.00185(TD)^2 - 0.0433 TD + 0.4023 = 0.159$$

Later extraterrestrial radiation (R_a) is calculated using FAO-56 methodology

$$R_a = (1440/\pi) (G_{sc}.d_r) [\psi_s \sin(\varphi) \sin(\delta) + \cos(\varphi) \cos(\delta) \sin(\psi_s)]$$

where;

$$G_{sc} = \text{Solar constant (0.0820 MJ/m}^2/\text{min)}$$

d_r = Inverse relative distance from earth to sun

$$d_r = 1 + 0.033 \cos \left[\frac{2\pi JD}{365} \right] = 1.03$$

JD = Julian day of the year = 21

ψ_s = Sunset hour angle (rad)

$$\psi_s = \arcsin [-\tan(\varphi) \tan(\delta)] = 1.48 \text{ Rad}$$

$$\delta = \text{Solar declination (rad)} = 0.409 \sin \left(\frac{2\pi JD}{365} \right) - 1.39 = -0.35 \text{ Rad}$$

φ = Latitude of location (rad) = 0.2426

TC = Daily mean temperature = 23.36 $^{\circ}C$

Therefore,

$$R_a = 30.45 \text{ MJ/m}^2/\text{d} = 12.53 \text{ mm/day}$$

Hence,

Reference crop evapotranspiration, $ET_o = 4.169 \text{ mm/day}$

Table 1.1 Soil nutrient statuses

Sl. No.	Latitude	Longitude	pH	EC dS/m	OC (%)
1	14°2'35"	75°56'58"	8.29	0.773	0.82
2	14°2'33"	75°56'59"	7.789	0.473	1.05
3	14°3'26"	76°0'9"	8.076	0.446	0.48
4	13°58'60"	75°57'35"	6.43	1.269	0.57
5	14°3'46"	75°59'30"	7.46	1.435	1.05
6	13°59'36"	75°57'52"	8.072	1.684	0.48
7	14°6'30"	75°58'41"	7.887	1.416	0.69
8	14°5'27"	75°58'5"	7.623	1.492	0.78
9	14°7'24"	76°0'4"	8.405	1.462	0.87
10	14°1'54"	76°0'10"	7.996	0.743	0.93
11	14°7'22"	76°0'19"	8.024	0.719	1.02
12	13°56'41"	75°58'11"	7.982	0.718	1.08
13	13°58'39"	75°58'0"	8.173	0.929	0.98
14	14°3'45"	75°56'59"	7.736	0.546	0.87
15	14°4'18"	75°59'8"	7.754	1.333	0.39
16	14°3'51"	75°59'58"	8.107	1.205	0.75
17	14°7'33"	75°59'10"	8.535	0.989	0.85
18	13°59'36"	75°57'52"	8.185	0.84	0.81
19	14°2'25"	76°0'5"	7.893	0.463	0.66
20	13°57'36"	75°57'23"	7.477	0.501	0.69
			Acidic-01	Safe- 09	Low-3
			Neutral-02 Critical -10	Med-05	
			Basic-17	Unsafe -01	High-12

Table 1.2 Soil nutrient statuses

Sl. No	Latitude	Longitude	Avg. N kg/ha	Avg. P ₂ O ₅ kg/ha	Avg. K ₂ O kg/ha	S kg/ha	Fe (ppm)	Mn (ppm)	Zn (ppm)	Cu (ppm)
1	14°2'35"	75°56'58'	257.15	104.28	539.40	23.71	12.19	54.44	0.51	5.02
2	14°2'33"	75°56'59'	263.42	40.90	292.68	24.97	17.49	66.16	0.44	4.91
3	14°3'26"	76°0'9"	219.42	40.15	284.40	22.81	8.45	28.52	0.23	2.56
4	13°58'60"	75°57'35'	244.60	45.82	539.40	18.50	16.83	48.84	0.76	5.25
5	14°3'46"	75°59'30'	257.15	90.78	501.36	33.95	10.26	25.43	1.02	3.52
6	13°59'36"	75°57'52'	244.60	80.01	539.40	18.14	14.42	45.81	1.00	4.87
7	14°6'30"	75°58'41'	244.60	92.46	539.40	18.86	10.19	33.55	0.36	3.87
8	14°5'27"	75°58'5"	213.24	107.23	261.96	22.81	9.85	24.21	0.39	2.19
9	14°7'24"	76°0'4"	257.15	27.63	206.04	20.66	21.87	42.25	0.90	5.77
10	14°1'54"	76°0'10"	238.33	102.89	539.40	21.20	20.35	46.82	0.78	5.56
11	14°7'22"	76°0'19"	225.79	32.85	255.00	14.01	7.25	22.47	0.58	2.11
12	13°56'41"	75°58'11'	232.06	80.70	489.36	15.63	23.24	47.07	1.06	5.92
13	13°58'39"	75°58'0"	206.97	17.79	419.52	20.48	11.32	27.62	0.36	4.46
14	14°3'45"	75°56'59'	232.06	23.46	482.28	20.66	22.97	46.97	0.94	2.08
15	14°4'18"	75°59'8"	219.52	92.00	297.48	27.48	15.62	37.55	0.83	2.53
16	14°3'51"	75°59'58'	269.34	93.74	418.92	19.76	15.67	28.35	0.52	3.35
17	14°7'33"	75°59'10'	257.15	22.30	537.72	19.22	10.22	34.95	0.30	3.13
18	13°59'36"	75°57'52'	244.60	89.62	539.40	55.15	16.38	47.60	0.98	4.89
19	14°2'25"	76°0'5"	225.79	123.05	507.72	19.76	15.18	26.37	0.72	3.77
20	13°57'36"	75°57'23'	206.97	40.03	76.92	20.84	30.91	68.70	0.35	7.35

Avg.	237.99	67.3847	413.388	22.930	15.53	40.18	0.651	4.154
Max	269.34	123.05	539.40	55.15	30.91	68.70	1.06	7.35
Min	206.97	17.79	76.92	14.01	7.25	22.47	0.23	2.08
	Low-20	Low-02	Low-01	Low-00	Low-00	Low-00	Low-10	Low-00
	Med-00	Med-07	Med-06	Med-08	High-20	High-20	High-10	High-20
	High-00	High-11	High-13	High-12				

Table 1.3 Prescribed range of soil nutrient status

pH	EC		OC	
<6.5 –Acidic	<0.8-Safe		<0.5-Low	
6.5-7.5- Neutral	0.8-1.6 –Critical		0.5-0.75- Med	
>7.5- Basic	>1.6 –Unsafe		>0.75- High	
Av. N	Av. P₂O₅	Av. K₂O		S
<280-Low	<22.9-Low	<141-Low		<10-Low
280-560-Med	22.9-56.6-Med	141-336-Med		10-20-Med
>560-High	>56.6-High	>336-High		>20 –High
Micro nutrients	Fe	Mn	Zn	Cu
Deficiency	<2.0	<2.0	>0.6	<2.0
Sufficiency	>2.0	>2.0	>0.6	>2.0

Table 1.4 Water Quality Analyses

Water sample					(Meq/l)		(meq/100g)		
Sl. No.	Latitude	Longitude	pH	EC (dS/m)	CO ₃	HCO ₃	Ca	Mg	Ca+Mg
1	14°7'33"	75°59'10"	7.31	0.235	NIL	11.40	0.8723	0.56	1.43
2	14°7'22"	76°0'19"	7.6	0.505	NIL	5.80	--	--	--
3	14°3'46"	75°59'30"	7.15	0.449	NIL	5.00	1.1098	0.68	1.79
4	14°4'18"	75°59'8"	7	0.977	NIL	2.20	1.4656	0.82	2.29
5	14°3'51"	75°59'58"	7.28	0.734	NIL	3.80	1.3797	0.81	2.19
6	14°3'26"	76°0'9"	6.89	0.663	NIL	11.20	0.8308	0.51	1.34
7	13°59'36"	75°57'52"	6.76	0.719	NIL	10.20	0.9954	0.58	1.58
8	14°2'35"	75°56'58"	6.74	0.437	NIL	9.20	0.8128	0.46	1.27
9	13°58'39"	75°58'0"	7.5	0.312	NIL	8.20	0.6955	0.37	1.07
10	14°5'27"	75°58'5"	7.08	0.467	NIL	3.60	0.6649	0.43	1.09
11	14°3'45"	75°56'59"	7.05	0.271	NIL	4.80	0.2852	0.17	0.46
12	14°6'30"	75°58'41"	6.81	0.69	NIL	7.00	0.5733	0.34	0.91
13	14°2'25"	76°0'5"	7.39	0.447	NIL	8.00	0.7296	0.41	1.14
14	13°56'41"	75°58'11"	7.51	0.325	NIL	6.80	0.416	0.23	0.65
15	14°7'24"	76°0'4"	7.48	0.589	NIL	10.80	0.520	0.28	0.80

pH	EC
<6.5- use with amendments	<0.25- Safe
6.5-7.5-Safe	0.25-0.75-Leaching required
>7.5-use after treatment	0.75-2.25-Not safe
	>2.25 –Not safe

Table 1.5 Soil Physical properties

Sl. No.	Bulk Density g/cm ³	Moisture (%)	Dry Density g/cm ³	Specific Gravity
1A	1.92	24.2	1.55	2.36
1B	1.73	26.0	1.37	2.48
1C	1.94	21.2	1.60	2.42
1D	2.01	18.2	1.70	2.42
2A	1.79	17.5	1.52	2.45
2B	1.75	20.7	1.45	2.37
2C	1.86	22.1	1.52	2.32
2D	1.87	20.7	1.55	2.29
3A	1.87	23.0	1.52	2.57
3B	1.73	19.6	1.44	2.34
3C	1.92	23.6	1.56	2.33
3D	1.92	23.1	1.56	2.32
4A	1.77	22.9	1.44	2.36
4B	1.71	20.9	1.42	2.36
4C	1.73	17.1	1.48	2.50
4D	1.90	16.3	1.64	2.38
5A	1.97	28.9	1.53	2.32
5B	2.12	28.7	1.65	2.37
5C	2.12	24.5	1.70	2.32
5D	2.12	24.2	1.71	2.36
Avg	1.89	22.2	1.55	2.38
Max	2.12	28.9	1.71	2.57
Min	1.71	16.3	1.37	2.29

MATLAB codes used in the study:

Sorting of samples

```
t=To_sort;
% permutation of 130 samples
k=randperm(130);
% Stores 60 samples to a data set and rest to another data set
mnew=t(k(1:85),:);
restm=t(k(86:end),:);
```

Partial Least Squares Regression

```
%Part 1- Choosing no. of PLS components
X =zscore(calibx);
y = caliby;
% Cross validation method to find optimum no. of components to be used in model
[Xl,Yl,Xs,Ys,beta1,pctVar,PLSmsep] = plsregress(X,y,10,'CV',10);
figure,plot(0:10,PLSmsep(2,:),'b-o');
xlabel('Number of components');
ylabel('Estimated Mean Squared Prediction Error');
% Plotting percentage variance explained to find optimum no. of components
```

```
[Xloading,Yloading,Xscore,Yscore,beta2,PLSpctvar] = plsregress(X,y,10);
figure,plot(1:10,cumsum(100*PLSpctvar(2,:)),'-bo');
xlabel('Number of PLS components');
ylabel('Percent Variance Explained in Y');
%Part 2- Finding weights of PLS components
[Xl,Yl,Xs,Ys,beta3,pctvar,mse,stats] = plsregress(X,y,6);
plot(1:124,stats.W,'-');
xlabel('Variable');
ylabel('PLS Weight');
```

%Part 3- Calibration

```
[Xloadings,Yloadings,Xscores,Yscores,beta] = plsregress(X,y,6);
y_modelled = [ones(62,1) X]*beta;
SST = sum((y-mean(y)).^2);
SSR= sum((y- y_modelled).^2);
rsquared_c = 1 - SSR/SST;
rmse = sqrt(sum((y(:)- y_modelled (:)).^2)/numel(y))
display(rsquared_c)
```

%Part-4 Validation

```
z = zscore(validx);
c = validy;
y_predicted = [ones(26,1) z]*beta;
SST= sum((c-mean(c)).^2);
SSR = sum((c- y_predicted).^2);
rsquared_v= 1 - SSR/SST;
rmse = sqrt(sum((c(:)-y_predicted (:)).^2)/numel(c))
display(rsquared_v)
```

Outlier identification

```
xsuby = xdata-ydata; % xdata is actual value, ydata is predicted value
mean=mean(xsuby);
```

```

std=std(xsuby);
outlier =(xsuby-mean) > std;
data2=xsuby;
data2(outlier)=NaN;
outlier1=(xsuby-mean) < (-1*std);
data3=data2;
data3(outlier1)=NaN;
VIP score estimation
X=X; % X is calibx, y is caliby
Y=y;
A=6;
varX=sum(sum(X.^2));
varY=sum(sum(Y.^2));
for i=1:A
error=1;
u=Y(:,1);
niter=0;
while (error>1e-8 &&niter<1000) % for convergence test
64
w=X'*u/(u'*u);
w=w/norm(w);
t=X*w;
q=Y*t/(t'*t); % regress Y against t;
u1=Y*q/(q'*q);
error=norm(u1-u)/norm(u);
u=u1;
niter=niter+1;
end
p=X'*t/(t'*t);
X=X-t*p';
Y=Y-t*q';
%+++ store
W(:,i)=w;
T(:,i)=t;
P(:,i)=p;
Q(:,i)=q;
end
%+++ calculate explained variance
R2X=diag(T'*T*P'*P)/varX;
R2Y=diag(T'*T*Q'*Q)/varY;

Wstar=W*(P'*W)^(-1);
B=Wstar*Q'; % b coefficient
Q=Q';
%+++
s=diag(T'*T*Q*Q');
[m,p]=size(X);
[m,h]=size(T);
%+++ calculate VIP;
VIP=[];

```

```
for i=1:p
weight=[];
for j=1:h
weight(j,1)= (W(i,j)/norm(W(:,j)))^2;
end
q=s'*weight; % explained variance by variable i
VIP(i)=sqrt(p*q/sum(s));
end
%+++
SMLR regression
A= stepwise (X, y);
```


PUBLICATIONS

INTERNATIONAL JOURNAL PAPER

Bhojaraja B E., Amba Shetty, M K. Nagaraj and P. Manju (2015). “Age based classification of Arecanut crops: a case study of Channagiri, Karnataka, India”, *Geocarto International*, DOI: 10.1080/10106049.2015.1094528.

(Publisher: Taylor & Francis, Journal: Geocarto International. Impact Factor 1.37)

INTERNATIONAL CONFERENCES PAPER

Bhojaraja B E., Amba Shetty, Nagaraj M K (2014). "An Integrated Approach for Arecanut Crop Health Monitoring" 19th International Conference on Hydraulics, Water Resources and River Engineering, ISH - HYDRO 2014 INTERNATIONAL

Bhojaraja B. E., Gaurav Hegde, Pruthviraj U., Amba Shetty, Nagaraj M. K. (2015) " Mapping Agewise Discrimination of Arecanut Crop Water Requirement using Hyperspectral Remote Sensing" *International Conference on Water Resources, Coastal and Ocean Engineering ICWRCOE 2015*. <http://dx.doi.org/10.1016/j.aqpro.2015.02.186>

Bhojaraja B. E., Amba Shetty, M. K. Nagaraj (2015). “Assessment of Arecanut crop water requirement using hyperspectral data and PLSR model”, 20th *International Conference on Hydraulics, Water Resources and River Engineering*, ISH - HYDRO 2015 INTERNATIONAL.

Bhojaraja B. E., Amba Shetty, M. K. Nagaraj (2016). “Agewise Arecanut Crop Water Requirement Model Using SMLR and Hyperspectral Data”, 21st *International Conference on Hydraulics, Water Resources and River Engineering*, ISH - HYDRO 2016 INTERNATIONAL.

RESUME

Name: Bhojaraja Benkipura Eshwarappa

Date of Birth: 23/06/1986

Address: Opposite to Ganaprabha Vidya Smsthe,
Kumbara Street, Shivamogga PIN 577202, Karnataka, India.



Contact Details

Mobile: 09886814626

E-mail: be.bhojaraj@gmail.com

Professional Education:

M.Tech (RS&GIS)

NITK-Surathkal (2009-2011).

B.E. (Civil)

Siddaganga Institute of Technology, Tumakuru (2005-2009).

Publications

- International Journal: **01**
- International Conference: **05**
- National Conference: **01**